Progress in Materials Science 112 (2020) 100668

Contents lists available at ScienceDirect

Progress in Materials Science

journal homepage: www.elsevier.com/locate/pmatsci

Cellulose nanocrystal based multifunctional nanohybrids

Erlantz Lizundia[a,b,*], Debora Puglia[c], Thanh-Dinh Nguyen[d], Ilaria Armentano[e,*]

[a] Department of Graphic Design and Engineering Projects, Faculty of Engineering in Bilbao, University of the Basque Country (UPV/EHU), Bilbao 48013, Spain
[b] BCMaterials, Basque Center for Materials, Applications and Nanostructures, UPV/EHU Science Park, 48940 Leioa, Spain
[c] University of Perugia, Civil and Environmental Engineering Department, UdR INSTM, Strada di Pentima 4, 05100 Terni, Italy
[d] Department of Chemistry, University of British Columbia, 2036 Main Mall, Vancouver, British Columbia V6T 1Z1, Canada
[e] Department of Economics, Engineering, Society and Business Organization (DEIM), University of Tuscia, Largo dell'Università snc, 01100 Viterbo, Italy

ARTICLE INFO

Keywords:
Cellulose nanocrystals
Hybrid materials
Multifunctional materials
Applications
Environmental impact

ABSTRACT

Cellulose nanocrystals (CNC) based nanohybrids are emerging as multifunctional materials and alternative to traditional petroleum-based plastics. The growth in academic and industrial interest in this field is highlighted by the increasing number of works published in the last decade. While several reviews have been focused on the synthesis of these materials, little has been done to catalogue the properties and potential applications of CNC based multifunctional nanohybrids. In this review, we establish an up-to-date state-of-the-art in this field, with a special emphasis on processing, functional properties and application area. The review leads to the combination of cellulose nanocrystals with different types of organic or inorganic nanoparticles, in order to study and analyze the important scientific and industrial uses of the multifunctional nanohybrids and open new horizons in materials science. In particular, engineering and biomedical applications are analyzed, including supercapacitors, solar cells and batteries, separation technologies and wastewater treatment, catalytic, sensing, tissue enegineering, wound dressing, drug delivery and cancer therapy. Nanotoxicity aspects and environmental impact are also discussed.

1. Introduction

Cellulose nanocrystals (CNC) are bio-based and renewable nanosized materials that can be derived from plants or bacteria and in general from a variety of highly available and renewable cellulose-rich sources of the most abundant natural polymers [1,2]. Cellulose nanocrystals represent a new category of renewable and innovative nanoparticles, that incorporated and combined with other micro- or nano-materials can permit to develop efficient and sustainable multifunctional devices [3–8].

Scientific research on CNC may take the development of a wide range of products ranging from scaffolds for biomedical applications [9] or supercapacitors [10], porous separator films for batteries [11], films for electronics [12] and anti-counterfeiting applications [13], for sensing purposes [14], for free-standing catalytic films [15], or water purification applications [16]. According to the Web of Science database, there are more than 5000 publications on nanocellulose (1994–2019) [17], with a significant increase in interest in the last decade. Patents granted during the same period, according to Google Patents database [18], reached

* Corresponding authors at: Department of Graphic Design and Engineering Projects, Faculty of Engineering in Bilbao, University of the Basque Country (UPV/EHU), Bilbao 48013, Spain (E. Lizundia). Department of Economics, Engineering, Society and Business Organization (DEIM), University of Tuscia, Largo dell'Università snc, 01100 Viterbo, Italy (I. Armentano).
E-mail addresses: erlantz.liizundia@ehu.eus (E. Lizundia), ilaria.armentano@unitus.it (I. Armentano).

https://doi.org/10.1016/j.pmatsci.2020.100668
Received 7 May 2019; Received in revised form 7 March 2020; Accepted 16 March 2020
Available online 19 March 2020
0079-6425/

more than 500.

In order to shift from a laboratory and academic interest to commercial and industrial applications, researchers must perform transition from CNC extracted on the bench scale to material produced on an industrial scale [19]. There are a lot of companies that are able to produce kilogram to ton per day quantities of nanocellulose, by using different purification procedures; so now the characterization of these materials becomes a critical point, since CNC stability and behaviour are highly dependent on the surface chemistry, surface charge density, and particle size [20]. Hence key and standard test methods that should be employed to characterize these properties to ensure a "known" starting material and consistent performance, are necessary. Overall, the current industrial production level of cellulose nanocrystals is encouraging, suggesting a good progression to commercial-scale applications [19].

FPInnovations, that is known to be a catalyst in developing and innovation core for the forest area including industry, governments, universities, research centres, suppliers and the innovation capacity, evaluated that the nanocellulose market would be around 250 million USD (United States dollar) in North America by 2020 [21], while Future Markets estimated the market to 2024 [22]; according to Stratistics Market Research Consulting, the Global Nanocrystalline Cellulose Market is accounted for 22.2 million USD in 2017 and is expected to reach 227.2 million USD by 2026 growing at a compound annual growth rate (CAGR) of 29.5% during the forecast period. Some of the factors, such as increasing demand for green materials in developing countries, growth demands for renewable and biodegradable natural materials and progressions in the personal care industry are leading to market growth, while the high quantities of low cost substitute products may negatively affect the growth. An increased require for technological improvement in end-user industries as paper, paperboard and plastics, textiles, food packaging, cosmetic and personal hygiene, pharmaceutical, biomedical, paints and coatings is driving the nanocellulose market [22]. The companies referred to in the market research report include Nippon Paper Group Inc. (Japan), Melodea Ltd. (Israel), Kruger Inc. (Canada), Innventia AB (Sweden), Daicel FineChem Ltd. (Japan), Sappi Ltd., CelluForce Inc. (Canada), American Process Inc. (U.S.A.), J. Rettenmaire & Sohne GmBH (Germany), Borregard ASA (Norway), Asahi Kasei Corporation (Japan), and Stora Enso (Finland), however Asia-Pacific acquired the largest market share during the forecast period, due to enhance in automotive industries in Japan is supposed to develop new growth promise for nanocrystalline cellulose market [23]. Most of the companies are focusing on high volume production for nanocomposites, packaging and paper industries. However, new and innovative opportunities are in 3D printing technology, textiles and biomedical applications. Up to date the production capacity far exceeds the market demand, although probably this situation will modify, since prices of the nanocellulose drop in the next futures [24].

The cost per gram of the CNC can vary from 3 to 25 USD, according to the preparation method and companies [25], which is is similar to that for carbon nanotubes. Considering that cellulose is the most abundant organic polymer and that the developing processing technology to extract cellulose from a variety of sources in comparison with the chemical synthetic approaches used for carbon nanotubes, CNC cost may be significantly reduced in the near future. Furthermore, another factor to be considered in order to increase the use of CNC in the different applications is the method of extraction. CNC are currently extracted from hydrolysis of cellulose by using different acid treatments. New and environmentally benign methods have to be developed in order to obtain sustainable bio-based nanomaterials [1,26].

The main contribution of this review is to discuss the effect of CNC on nanohybrid materials, defined as materials composed of two or more organic or inorganic constituents at the nanometre or molecular level. Commonly one of these compounds is inorganic and the other one organic. Nanohybrid processing methods, properties and applications were mainly considered. The advantages and disadvantages of the main processing technologies used to obtain CNC-based nanohybrid materials are mainly discussed. At first, a brief introduction on CNC properties are presented and discussed. Important issues related to the fabrication of CNC-based nanohybrids, processing issues and dispersion are addressed in the following sections. The fundamental knowledge of the effect of CNC on the nanohybrid properties is covered. The addition of CNC as a strategy to develop nanohybrid materials with improved performance, with emphasis in engineering and biomedical applications, is analyzed. The environmental impact associated with the use of CNC nanohybrids is also summarized. Finally, conclusions and future perspectives are presented and discussed.

2. Nanohybrid fabrication technologies

CNC based nanohybrids having different morphologies and shapes have been fabricated through different fabrication techniques. Accordingly, this section describes the most popular fabrication technologies for CNC nanohybrid processing.

2.1. Solution casting

Solution casting has been the most common fabrication technology to obtain either pure or nanohybrid CNC materials. This method is simple yet effective, as it allows obtaining free-standing films with controllable thickness by simply dispersing CNC and the reinforcing nanoparticles into a liquid (typically water) and then casting the dispersion onto a Petri-dish to allow solvent evaporation (usually around 2 days). After room temperature drying, a film can be peeled off from the substrate. Obtaining a homogeneous dispersability of nanohybrid counterparts into the liquid solution becomes an essential prerequisite to obtain well-dispersed CNC and homogenous films. In this sense, sulphated CNC are preferred as the electrostatic repulsive forces between adjacent nanoparticles keep them well-dispersed in aqueous solutions.

During the last decade, solution casting technique has been an alluring approach to exploit the fascinating lyotropic liquid crystalline (LLC) behaviour of CNC derived from sulphuric acid hydrolysis, firstly reported by Marchessault et al. in 1959 [27]. In this sense, Revol et al. showed in the early 90s that water-dispersed CNC could form a chiral nematic (or cholesteric) phase when their

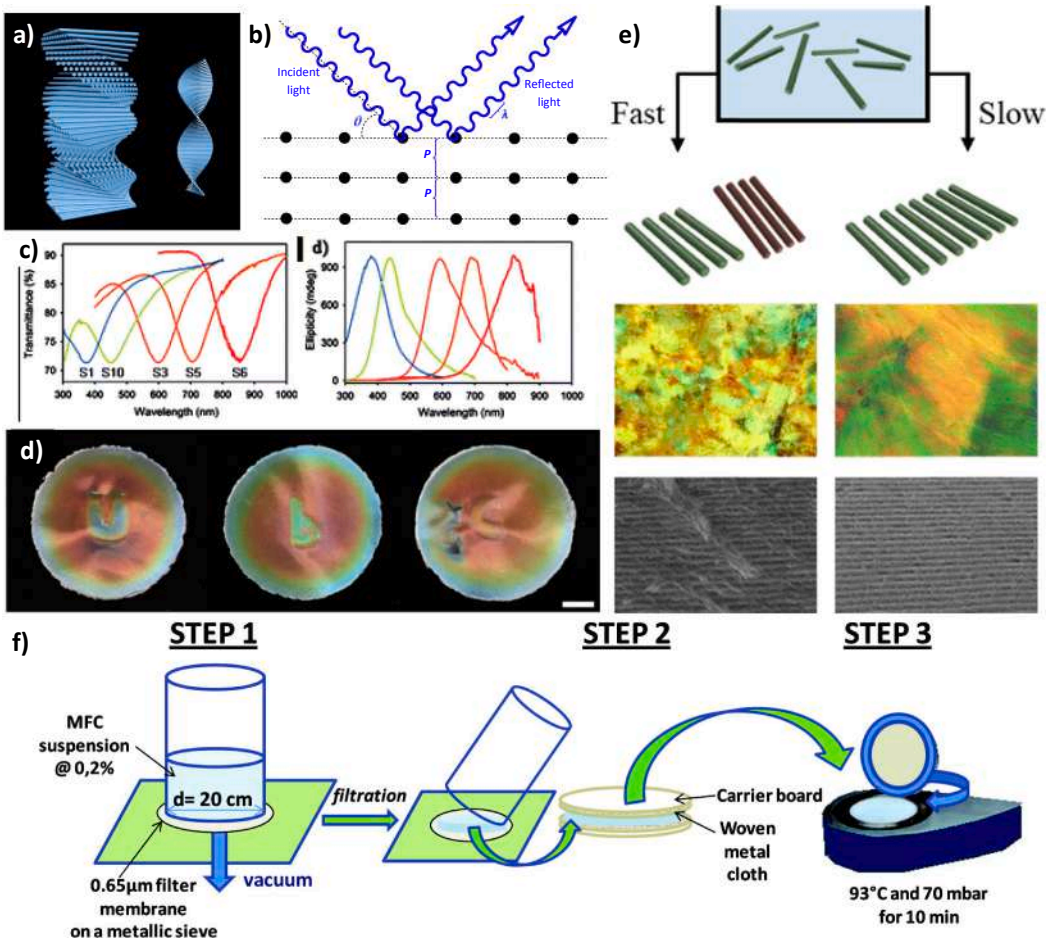

Fig. 1. (a) Scheme displaying the twisted layered chiral nematic structure formed upon EISA of CNC, where each rod represents a single CNC. (b) Relationship between the helical pitch P and the λ_{max} of the reflected light as determined in Eq. (1). (c) Transmittance mode UV–Vis and CD spectra of chiral nematic CNC films. Reproduced from Ref. [33] with permission from The Royal Society of Chemistry. (d) Patterning of CNC films using cellulose acetate masks (the scale bar represents 1 cm). Reproduced with permission of ACS Publications from Ref. [44]. (e) The extension of "tactoid annealing" intermediate stage (tune through fast and slow drying processes) improves CNC layer ordering, leading to homogeneous photonic properties through the film. Reproduced with permission of ACS Publications from Ref. [48]. (f) Fabrication of a cellulosic film following the filtering process. Reproduced with permission of ACS Publications from Ref. [56].

content remains around 3 wt% [28], which contrasts with the concentration that need other cellulosic derivatives, such as hydroxypropylcellulose, to form a lyotropic chiral nematic behaviour (50–75 wt%) [29]. Gray and co-workers showed then an intriguing ability of CNC to self-assembly into a chiral nematic liquid crystal when dispersed in water, giving access to the fabrication of solid films which can retain the long-range helicoidal chiral nematic order [30]. This was achieved upon solvent evaporation, where CNC undergo through a process called evaporation induced self-assembly (EISA) to form films with a chiral nematic structure (Fig. 1a). Such helicoidal ordering induces vibrant colours similarly to what is observed in certain plants and animals, a phenomenon called structural colour. This colour originates as result of the interaction of the incident light with the hierarchical organisation of layered structures [31], and can be determined in terms of Braggś diffraction. Since the distance between successive layers in CNC films is known as the helical pitch or *P* (the repeating distance for a full 360° turn of CNC), Bragg's law can be simplified as:

$$\lambda_{max} = n_{avg} P sin\theta \tag{1}$$

where λ_{max} is the wavelength of the selectively reflected light, n_{avg} is the refractive index of the CNC (1.55) and θ is the angle of the incident light (Fig. 1b) [30]. Thus, visible iridescence colours are achieved when the helical pitch is similar to the wavelength of the visible light between 400 and 700 nm. Moreover, this colour (λ_{max}) can be modified by tuning the repeating distance between successive CNC layers, yielding interesting stimuli responsive properties to the CNC films. These stacked CNC layers rotate in a counter-clockwise fashion similarly to what is found in nature as Bouligand-type organization [32], resulting in films which selectively reflect circularly polarized left-handed light. As depicted in Fig. 1c, the ultraviolet–visible (UV–Vis) reflectance peak (left) of a given film matches with its circular dichroism (CD) signal (right), where a characteristic positive ellipticity is observed as a result of the left-handed ordering of CNC films [33].

Many works have been reported on the understanding and control of the photonic properties of CNC films. Schültz et al. found that as the CNC concentration increases from 2.5 to 6 vol% during EISA, the pitch varies from 15 to 2 μm (corresponding to an average distance between neighbouring CNC of 39 and 25 nm respectively), while the twist angle between adjacent CNC increases from about 1° up to 4° [34]. Thanks to the negative diamagnetic anisotropy character of CNC, Kimura et al. oriented chiral nematic CNC films under an external magnetic field of 1 T as CNC align perpendicularly to applied magnetic field (the helix is aligned along the magnetic field) [35]. Similarly, Habibi et al. were able to uniformly align CNC during their EISA by applying alternating electric fields of 2000 V cm^{-1} (10^4–10^6 Hz) [36].

Reflected light can be tuned from the ultraviolet to infrared over the visible spectrum by increasing the ionic strength of the medium (high ionic strengths reduce CNC electrostatic repulsion forces, resulting in a blue shift in the iridescence) [37], by increasing the drying temperature (blue shift) [38], upon ultrasonic treatment before EISA (red shift) [39], upon the incorporation of different counterions to the surface sulphate ester groups (increased van der Waals radii in the $H^+ < Na^+ < K^+ < Cs^+$ order red-shifts the colour) [40], or by changing the casting substrate [33]. However, it should be noted that the occurrence of structural colour can be only achieved under specific experimental conditions, as the LLC phase can be disturbed by changes in pH, ionic strength, CNC desulfation, CNC concentration within the dispersion [41,42]. This ability to tune the photonic properties of CNC films could be used to produce patterned coatings with spatial control by methods, such as differential heating [43], or by applying cellulose acetate masks to tune water evaporation kinetics (Fig. 1d) [44].

Nowadays, the fabrication of homogeneous and high-quality photonic CNC films remains as one of the main concerns in the field, as many iridescent films reported consist on multidomain mosaic patterns where the uniformity of the helical pitch and helix orientation is far from ideal. In this context, Hyun Park et al. proved that the film uniformity could be dramatically improved by increasing the CNC concentration in the initial suspension to the fully LC range, as this promotes a homogeneous helix orientation within the film [45]. A weak circular shear-flow during EISA could be also applied in order to significantly improve film homogeneity, aligning CNC parallel to the shear-flow direction [46]. CNC fractionation according to their L/d ratio (length-to-diametre or aspect ratio) has also been proven as an efficient method to obtain dispersions consisting on a 100% LC phase with no gelation [47]. As shown in Fig. 1e, film homogeneity can be improved by extending the evaporation time just after the onset of liquid crystallinity [48]. The extension of the stage called “tactoid annealing”, found between phase separation and gel vitrification, was critical for the improvement of film homogeneity. During this intermediate stage, the mobile tactoids fuse to reduce the interfacial tension between anisotropic/isotropic layers, leading to extended undisturbed domains of several millimetres.

Novel chiral materials with upgraded functional properties arise when CNC hosts nanoparticles. Usually, nanoparticles are mixed together with the CNC in water, and after a sonication step to properly disperse CNC and nanoparticles, they are cast onto a substrate to allow their EISA, yielding solid nanohybrid films. Some relevant examples include plasmonic gold nanorods [49], quantum dots [13], carbon nanotubes [50], carbon dots [51], or rare-earth compounds [52]. This method offers the advantage of yielding uniform structures thanks to the fact that individual nanohybrid components are homogeneously distributed in solution (usually aqueous) at the molecular level [53]. However, the incorporation of such nanoparticles is usually limited to low loading (around 1–1.5 wt%) as their presence often results in the disruption of the chiral nematic long-range order of CNC [54,55]. Increasing the particle loading results essential towards the fabrication of multifunctional materials as such the larger the presence of responsive nanoparticles, the larger their response to external stimuli would be. In this context, the development of nanoparticles with suitable surface functional groups that make them compatible with hydrophilic CNC remains as one of the main challenges in this field. Hydrophobic nanoparticles could be therefore surface-modified with amphiphilic stabilizers [52], or with moieties such as carbonyl, hydroxyl and carboxylate groups [51].

2.2. Filtering process

Taking the advantage of traditional papermaking processes, aqueous CNC suspensions can be quickly transformed into films by simple filtering processes, which involve obtaining a wet gel (known as gel/cake) and then allow time for water evaporation (Fig. 1f) [56–58]. As the water in the gel/cake continuously evaporates, the formed capillary forces bring the CNC close enough to yield secondary attraction forces, resulting in all-cellulose films with Young’s modulus in the range of 5–10 GPa and tensile strengths up to 70 MPa [59,60]. Although wet cakes could be eventually naturally dried under ambient conditions [61], several attempts have been made in order to decrease the time required for film fabrication, including the vacuum filtration of CNC suspension, peeling off from the filter and subsequent oven drying or hot pressing at high pressures [56,57]. Unfortunately, although filtering results interesting from the industrial point of view, these procedures fail to take advantage of the intriguing ability of CNC to self-assemble into very characteristic structures.

2.3. Layer by layer deposition

Layer-by-layer (LbL) assembly technique, firstly introduced by Iler in 1966 [62], is a convenient route to obtain nanostructured multilayered thin films having two or more species, provided that they exhibit mutual attractive interactions. Although initially intended for polyelectrolytes having opposite charges, this concept has been expanded to other systems including CNC. In this line, positively charged gibbsite nanoplatelets and negatively charged CNC multilayer films were obtained by Martin et al. [63]. Results show that layer thickness can be controlled from 13 to 70 nm by varying the ionic strength (upon monovalent salt incorporation) of the CNC suspension. Iridescent materials can also be obtained following the LbL assembly. For instance, combining colloidal SiO_2 and CNC, layers with alternating low and high refractive index were fabricated, obtaining films reflecting at 550 nm (green colour) [64].

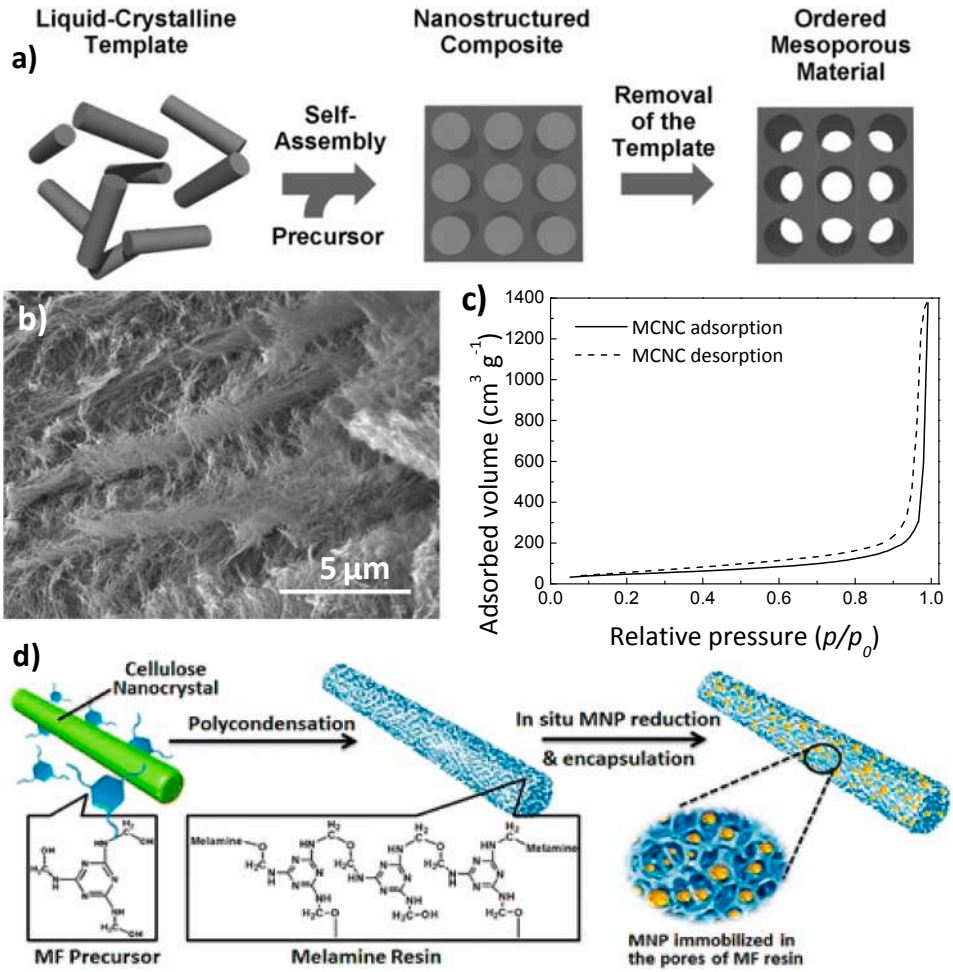

Fig. 2. (a) Templating procedure followed for the synthesis of mesoporous materials using CNC. Reproduced with permission of John Wiley & Sons Ltd from Ref. [69]. (b) FE-SEM images of a mesoporous CNC film. Reproduced from Ref. [8] with permission from The Royal Society of Chemistry. (c) N_2 adsorption-desorption isotherms showing the typical type IV isotherm with hysteresis obtained in mesoporous cellulose nanocrystal (MCNC) films. Reproduced from Ref. [8] with permission from The Royal Society of Chemistry. (d) Schematic of the preparation of tiny metal nanoparticles onto CNC. Reproduced with permission of ACS Publications from Ref. [75].

Using a spin assisted layer-by-layer (SA-LbL) assembly technique, a high strength and high toughness graphene oxide/CNC nanohybrid having a laminated morphology (7–15 nm per bilayer) similar to the natural nacre was obtained [65]. SA-LbL has also been extended to other nanohybrid systems including multi-walled carbon nanotube (MWCNT)/CNC [66], alumino-silicate imogolite nanotube/CNC [67], or zinc oxide/silver (ZnO/Ag) [6]. As the stability of these multilayered nanohybrids which rely on the electrostatic interactions as the driving force can be somewhat low in harsh conditions, the interaction between bilayers can be enhanced introducing different functional groups onto CNC surfaces to yield longer lasting materials [67].

2.4. Soft and hard templating

The template synthesis based on the self-assembly of CNC as a model LLC has been exploited to synthesize mesoporous solids (pores in the range of 2–50 nm) with large specific surface areas and periodic porosity [68]. As schematically shown in Fig. 2a, a CNC dispersion is mixed with a compatible precursor, which is allowed to self-assemble to yield a nanostructured hybrid material [69]. Then, one of the phases is selectively removed from to obtain the porous material. Following this approach, a controlled mesoporosity can be introduced into ordered periodic CNC structures, making CNC nanohybrids advantageous for applications such as catalyst supports, enantioselective sensors, capacitor materials or anodes for batteries [70]. The use of CNC as a template offers the advantage of being a soft-templating method, which results a particularly interesting fabrication method over the hard-templating approach, as it offers a good control over the morphology, requires fewer fabrication steps and could be done in an economical fashion [71].

Although the first example showing the use of CNC as soft templates was reported back in 2003 [72], it was not until 2010 when MacLachlan and his co-workers reported a successful replication of the chiral nematic CNC using silica as a model material [73]. Later, Giese et al. fabricated a new form of mesoporous photonic cellulose (MPC) materials derived from CNC following the approach

shown in Fig. 2a, which upon supramolecular cotemplating can combine the adjustable photonic properties of CNC with a unique mesoporosity [74]. To that end, urea-formaldehyde resin comprising CNC was fabricated by the self-assembly of lyotropic CNC in the presence of a water-soluble urea-formaldehyde precursor, subsequent overnight drying and heat curing at 120 °C to complete polymerization. After a controlled alkaline treatment of the films with 15% aqueous potassium hydroxide solution at 70 °C, the urea-formaldehyde was removed, yielding a chiral nematic mesoporous cellulosic film. Mesoporous MPC films having a specific surface area (S_{BET}) of 252 $m^2\ g^{-1}$ were stable in boiling water, while CNC films rapidly disperse in water. Interestingly, their colour was reversibly modified upon applying different liquids and external stress, making them useful as humidity and pressure sensing materials.

In an attempt to improve the control over the porosity and helical pitch of the final material, Schlesinger et al. prepared free-standing chiral nematic mesoporous cellulose films by a concomitant assembly of CNC with a silica precursor, its condensation and its subsequent removal [76]. A sol-gel precursor that does not perturb the self-assembly process of CNC during EISA was selected. Adding tetramethyl orthosilicate (TMOS, $Si(OMe)_4$) at a ratio of 1.8–3 μL mg^{-1} CNC, chiral nematic CNC-silica films were obtained. TMOS is compatible with CNC self-assembly as generated silica does not perturb EISA process, the isoelectric point of silica matches with the pH of CNC dispersion and silica polymerization is limited to the last stage of EISA [73,77]. Alkali hydroxides such as lithium hydroxide (LiOH), sodium hydroxide (NaOH) and potassium hydroxide (KOH) at 1.8 M can be used for silica removal, retaining the long-range left-handed chiral nematic order and the crystalline character of original CNC (see Fig. 2b) [8]. A good control over the optical properties and mesoporosity was obtained by either modifying the CNC-silica ratio or the substrate used for EISA. As depicted in Fig. 2c, nitrogen adsorption measurements show a type IV isotherm with hysteresis characteristic of mesoporous structures, yielding Brunauer-Joyner-Halenda (BJT) pore size distributions in the range of 6–15 nm and maximum S_{BET} of 314 $m^2\ g^{-1}$. To avoid network collapse during silica removal, wet chiral nematic CNC films are dried under supercritical carbon dioxide (sc-CO_2) (during air-drying a S_{BET} of 44 $m^2\ g^{-1}$ is achieved) [74]. The severe cracking suffered by capillarity pressures gradients generated during the EISA of CNC/TMOS (tetramethyl orthosilicate) dispersions was solved upon simple sugar (glucose, sucrose) addition during the mixing of CNC with TMOS. Resulting solid films remain mechanically flexible and could be bent, folded or cut with scissors without breakage [78], allowing the fabrication of large free-standing films.

The functional properties of mesoporous cellulosic materials could be further upgraded upon the encapsulation of guests such as metal nanoparticles within the channels to obtain chiroptical activities with surface plasmon resonance (SPR) [76], or by coating them with conducting polymers such as polypyrrole (PPy) to obtain materials for energy storage applications [8]. The mesoporous chiral nematic order obtained in CNC films can also be transferred to many other materials by hard templating methods given the compatibility of the fast CNC self-assembly with inorganic precursors during sol-gel reactions [71]. For instance, using water-dispersed CNC as a chiral nematic phase, Shopsowitz et al. synthesized free-standing chiral nematic mesoporous carbon films with specific areas as high as 1465 $m^2\ g^{-1}$ [71], representing the first example of mesoporous carbon with chiral order (EISA of CNC with TMOS followed by pyrolysis at 900 °C under nitrogen atmosphere and subsequent silica etching by NaOH was carried out). Similarly, chiral nematic CNC/silica film can be calcined at 540 °C under air to leave a high surface area silica film [73]. The mesoporous chirality of CNC can also be transferred to further materials in the form of free-standing mesoporous films based on silica, organosilica, metals/metal oxides or fluorescent conjugated polymers [79].

2.5. Nanoparticle growth onto CNC

The trend of nanoparticles to aggregate upon mixing due to their high surface energy can be overcome by directly growing inorganic nanoparticles onto CNC surfaces. Using CNC as solid templates, nanoparticles can grow through hydrothermal or reduction methods [80]. For example, ZnO nanoparticles were grown onto water-dispersed CNC which were coated by a thin layer of melamine-formaldehyde. Hydrothermal dehydration at 100 °C of an aqueous zinc acetate dehydrate and NaOH together with CNC yielded spherical ZnO nanoparticles of 20–25 nm [81]. CNC/Au nanohybrids were synthesized by heating an aqueous mixture of CNC, polyethylene glycol and chloroauric acid ($HAuCl_4$) at 80 °C for 1 h. Upon the reduction of the gold ions onto CNC surfaces and the formation of primary nanoclusters, nanoparticles having below 25 nm in diametre were formed onto CNC surfaces [82]. As schematized in Fig. 2d, tiny platinum and palladium nanoparticles having 1–2 nm in size were chemically reduced onto melamine-formaldehyde coated CNC using ethylene glycol as dispersant and a reducing agent (chloroplatinic acid hexahydrate and potassium tetrachloropalladate as precursors) [75]. Interestingly, taking advantage of the high density of hydroxyl groups onto CNC surfaces, Eisa et al. reported a solvent free reduction process where silver and gold nanoparticles of ~100 nm can grow onto CNC using metal precursors and ascorbic acid [83]. Using sodium borohydride as a reducing agent for silver nanoparticles, Lokanathan et al. found that the amount of sulphate groups onto CNC notably affects nanoparticle nucleation and growth [84].

2.6. Sol-gel process

Sol–gel process involves the conversion of a “sol”, a colloidal solution, into a “gel”-like system having both a solid and a liquid phase. The morphologies of both phases can range from discrete particles to continuous polymeric networks. When water is used as the liquid phase, the most common case for CNC, the sol-gel process leads to hydrogels, which are three-dimensional highly porous hydrophilic networks capable of entrapping large amounts of water that keep the network structure integrity [85]. Taking the advantage of the long-range chiral nematic ordering of CNC, stimuli-responsive photonic hydrogels which show large colour changes in response to pH, solvent or temperature changes were developed in 2013 [86]. The chiral nematic phase was retained by mixing CNC with non-ionic hydrogel precursors (acrylamide, acrylic acid, 2-hydroxyethylmethacrylate, polyethylene glycol methacrylate or

N-isopropylacrylamide as monomers). Upon UV irradiation, the self-assembled structure was locked in. Additionally, ionic-strength and pressure sensing CNC hydrogels were fabricated by Hiratani et al. using a mechanical shearing process in order to obtain anisotropic structures with marked birefringence [14].

In a pioneering work, Cranston and co-workers developed for the first time an injectable *in-situ* forming hydrogel based on aldehyde-functionalized CNC, carboxymethyl cellulose and dextran [87]. Interestingly, gelation took place within few seconds as hydrogel components were mixed upon extruding through a syringe, opening the path towards the design of CNC-based hydrogels with potential long-term drug delivery and tissue engineering applications. This was achieved thanks to the cross-linking effect of aldehyde-functionalized CNC, which yield covalent hydrazone bonds when physically mixed with adipic acid dihydrazine-modified carboxymethyl cellulose and aldehyde-functionalized dextran. This approach has been followed to develop further CNC-based hydrogels using different soft components such as gelatin (aldehyde CNC react with gelatine to form imine cross-links) [88], quaternized cellulose (QC) using a β-glycerophosphate cross-linking agent [89]. The ability of modified CNC to act as multifunctional cross-links was used to obtain self-healing and self-recoverable hydrogels by a reversible Diels-Alder (DA) click-reaction using PEG as a matrix [90]. Although it has been mainly applied to develop polymer-based hydrogels, this approach could eventually be used to develop hydrogel nanohybrids where CNC act as the soft-matrix phase. In this line, Khabibullin et al. synthesized fluorescent cross-linked hydrogels based on CNC and graphene quantum dots (GQD) thanks to the formation of hydrogen bonds between the –OH groups of CNC and the –COOH groups of GQDs (GQDs as a cross-links) [91].

Despite to these examples which require CNC to induce a gelation of a polymer, notably fewer works have been dealing with the development of pure CNC-hydrogels (no presence of a polymeric phase, only CNC and water). The fabrication of pure CNC hydrogels has been accomplished in several ways. The most simple approach is the increase of CNC concentration within the dispersion at content above 14 vol% to yield a continuous network of entangled rods that spans from the nanoscale up to the macroscopic scale [92]. A low power ultrasound treatment also yields a gelled 3D network of CNC as hydrogen bond interactions between neighbouring CNC are created [93]. A more elegant method to obtain hydrogels results the controlled reduction of the electrostatic repulsive forces between adjacent CNC, which may collapse the charge-stabilized dispersions. Accordingly, salt incorporation screens the electric double layer of CNC [94], increasing their zeta-potential and thus reducing the electrostatic repulsive forces between CNC [37]. Upon salt addition, the attractive forces become dominant, yielding a CNC aggregation and subsequent hydrogel.

Chau et al. found that salts with increased charge number and ionic radius ($Na^+ < Mg^{2+} < Al^{3+}$) were more efficient for gelation [95]. Similarly, divalent cations were more effective than monovalent cations to induce gelation [96]. For instance, 10 mM NaCl are enough to induce gel formation for a 4 wt% CNC aqueous suspension, while further addition of salt resulted in increased G′ storage modulus values, indicating the formation of further intermolecular interactions through decreased electrostatic repulsion (see Fig. 3a). A green, straightforward and effective approach for CNC hydrogel fabrication has been recently reported using a hydrothermal treatment to induce CNC surface desulfation, decreasing their dispersability and finally favouring their attraction to form a hydrogel (Fig. 3b) [42]. It was shown that tuneable mechanical properties could be obtained controlling hydrothermal temperature, reaction time, CNC concentration and pH. The same group also reported on the fabrication of CO_2-switchable CNC hydrogels, where gelation took place due to the increase on the ionic strength caused by the protonation of imidazole and the formation of bicarbonate in solution upon CO_2 sparging (reversible process via N_2-sparging) [97].

2.7. Oven-drying, freeze-drying and supercritical-drying

The liquid phase of hydrogels can be removed through different approaches to obtain highly porous (99%) and ultra low-density (4–500 mg cm^{-3}) nanostructured solid materials with large specific surface areas (100–1000 $m^2\ g^{-1}$). Such porous structures, known as aerogels and firstly reported in 1931 by Kistler [99], can be obtained following different drying techniques, where freeze-drying and supercritical drying remain as the preferred ones. Till the date, a wide variety of aerogels composed of carbon, silica, alumina and tin oxide have been reported so far [100,101]. Fabricating highly porous CNC structures may open new opportunities towards the development of materials with selective sorption properties, thermally and electrically insulating properties, acoustic damping ability, and as templates/supports for other materials. Interestingly, using cellulose has been proposed as a plausible solution to face the inherent fragility of aerogels, as natural polymers are generally mechanically flexible [102 103].

Solvent removal step has a dramatic impact on the morphology and properties of resulting aerogels and remains as the main challenge in their production. Indeed, liquid evaporation from the porous framework yields to capillary pressure-induced stresses, leading to pore-deformation, aerogel shrinkage or even structure collapse and cracking [104]. Techniques such as liquid evaporation using an oven drying, freeze-drying or supercritical drying preceded by a solvent-exchange step are the most commonly used techniques. Practically, liquid evaporation using an oven is not recommended due to the marked capillary pressure-induced stresses, which collapse the structure and lead to shrinkage values higher than 90% (xerogel). Freeze-drying, also referred as lyophilisation, is a common technique for aerogel fabrication and involves converting the liquid phase within the hydrogel into an ice-phase to form a cryogel, that latter is sublimated at low temperature and pressure (-55 °C, < 0.02 mbar) [105]. Ice sublimation avoids the formation of a liquid/vapour interface, limiting the presence of capillary pressures that collapse the structure. The rapid freezing of the solvent by immersion in liquid nitrogen, for example, can keep the original hydrogel structure, while slow freezing is typically applied as a mean of patterning the structure. In this technique, known as ice templating (IT) [106], the dispersed phase segregates as a result of the growing ice crystals. The structure of ice crystals can be controlled by a directional thermal gradient to produce honeycomb 2D shapes that are aligned parallel to the freezing direction, offering interesting anisotropic mechanical properties [106,107]. Supercritical drying, on the contrary, involves the substitution of the hydrogeĺs solvent by a supercritical fluid in order to prevent the formation of a liquid/vapour interface, avoiding the risk of capillarity pressures. Typically, carbon dioxide is used for supercritical

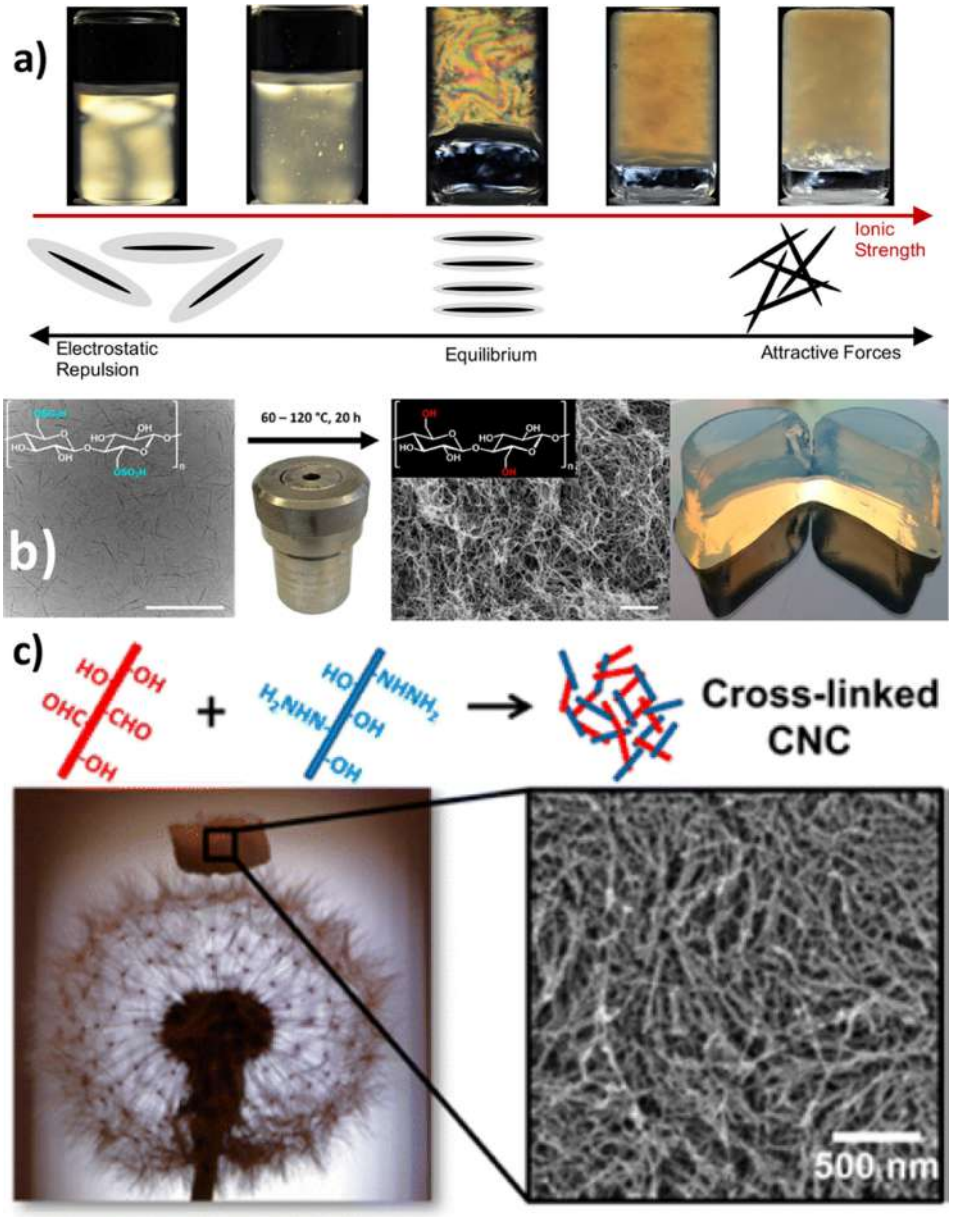

Fig. 3. (a) 4 wt% CNC dispersions with increasing salt concentrations photographed between cross-polarizers together with a sketch depicting CNC aggregation (black lines correspond to CNC, gray regions to their electric double layer). Reproduced with permission of ACS Publications from Ref. [96]. (b) Hydrothermal gelation process in CNC dispersions [42]. (c) Hydrazone cross-linked CNC aerogels are lightweight and show a highly porous structure. Reproduced with permission of ACS Publications from Ref. [98].

drying (sc-CO_2), as its critical point is found at 31.3 °C and 72.9 atm. Due to the immiscibility of supercritical CO_2 with water, a solvent-exchange procedure to intermediate solvent is required. Ethanol is commonly used as this intermediate solvent, leading to the formation of an alcogel (the liquid phase is an alcohol instead of water). Pressures of about 100 bar are employed for sc-CO_2 drying of gels, where slow depressurization rates (5 bar min^{-1}) up to ambient conditions yield structures with low shrinkage [93]. Although very high specific surface areas could be obtained, its multi-step character and high cost limit its industrial implementation.

Following the above-mentioned approaches, in 2010, Heath et al. prepared for the first time pure-CNC aerogels by solvent exchanging a CNC hydrogel with anhydrous ethanol and sc-CO_2 drying, yielding specific surface areas (SSAs) of 605 m^2 g^{-1} and densities as low as 7.8 mg cm^{-3} [93]. As CNC concentration within the initial hydrogel increases, a linear increase in the aerogel density together with a decrease in porosity was obtained. CNC aerogels with controllable pore-size (> 5 μm) have been prepared by directional freeze-drying [108]. Mueller et al. found that the shrinkage suffered by the aerogel upon liquid removal by freeze-drying can be reduced using high aspect ratio CNC, leading to aerogels with lower densities and thus, larger SSAs [109]. Importantly, most of

reported CNC aerogels are obtained through weak cellulose-cellulose interactions, leading to poor mechanical response and to a re-dispersion process when immersed in aqueous environments. This structure loss can be upgraded by covalently binding CNC [98,110–112], where the formed linkages between adjacent CNC are able to hold the structure upon their immersion in different solvent media. In this regard, Cranston and co-workers synthesized chemically cross-linked CNC aerogels with shape-recovery and superabsorbent properties upon the surface modification of water-dispersed CNC with hydrazide and aldehyde groups (Fig. 3c) [98]. Hydrazone cross-link bonds between $NHNH_2$-CNC and CHO-CNC are formed when orthogonally modified CNC come into contact, displaying enhanced mechanical properties over physically cross-linked CNC aerogels.

The combination of CNC with inorganic nanoparticles may lead to lightweight free-standing aerogels with upgraded functionalities. In this sense, functional nanoparticles were *in-situ* incorporated into CNC networks during their assembly process, allowing the fabrication of high mass ratio of active material into CNC support structure in a single step [10]. Manganese dioxide nanoparticles and polypyrrole nanofibres at high loading were incorporated during aerogel formation. This procedure could be also extended to other CNC-hybrid aerogels, such as carbon nanotubes, to develop supercapacitors with high compression stabilities [113], red mud to fabricate aerogels with good flame retardancy, thermal/sound insulation and oil absorbance properties [114], or to develop CNC aerogels with high loadings (up to 50 wt%) of metal-organic framework (MOF) particles [115]. Very recently, Nguyen et al. reported a promising novel synthetic approach for imparting a chiral helicoidal arrangement and hierarchical organization of CNC aerogels using phase-separated lyotropic chiral nematic CNC [116], or after the incorporation of gelatin during the templating process [117].

2.8. Electrospinning

Electrospinning technique is gaining an increasing interest for functional material fabrication as it serves to fabricate 1D nano and micro-fibers in a continuous fashion [118]. A solution containing a given material (dissolved, dispersed or molten) is discharged from a spinneret upon the application of an electric field, and assisted by electrostatic interactions, it is then deposited onto a collector to yield electrospun fibrous mats. Parameters such as solution concentration, solvent selection, applied voltage, distance between the needle tip and the collector and relative humidity markedly affect the morphology of resulting materials [119]. During electrospinning, rod-like CNC are aligned parallel to the main fibre axis, allowing obtaining materials with tailored anisotropic properties. Unfortunately, due to the difficulties shown by CNC to form a continuous phase, so far CNC have been mostly used as a reinforcing phase into polymeric fibrous mats [120,121], and no work has reported the development of pure CNC electrospun fibres. However, taking into account the excellent dispersability of CNC in water, we believe that electrospinning holds a great potential to develop novel CNC-nanohybrids with fibrous morphologies.

2.9. Printing techniques

Three-dimensional (3D) printing is a bottom-up manufacturing technology which allows the layer-by-layer deposition of a given material in specifically designed three-dimensional shapes [122]. This fabrication method provides a unique opportunity for the development of novel geometric designs as it allows obtaining complex macroscopic shapes with controlled microstructures (and properties), from the nano to macro scale [123–125]. Thanks to their special rheological properties, CNC result especial interesting for the development of 3D printing inks. Indeed, liquid-dispersed CNC present a strong non-Newtonian shear-thinning behaviour, enabling an easy flow through nozzles at low pressures (during printing) while quickly recovering the solid-like response after extrusion, ensuring a good dimensional stability and shape fidelity once printed. The specific requirements for a proper printing process include apparent viscosities of 10^4 Pa s^{-1} and few Pa at low (0.001 s^{-1}) and high (50 s^{-1}) shear rates, respectively [126].

Although CNC have been used in many technological applications, their use as an ink formulation for 3D printing is still in its infancy. Most of the published works are focused on the design of inks based on long and flexible cellulose nanofibrils (CNFs) gels [127,128]. A significant breakthrough in the field was carried out by the group led by Prof. Jennifer A. Lewis, who inspired by botanical systems was able to fabricate CNF-based hydrogel architectures showing a controlled shape-change upon immersion in water [129]. Although most of the works dealing with 3D printing of CNC have been focused on their use as a reinforcing phase for a polymeric host such as sodium alginate and gelatine [126], several examples can be found in the literature dealing with inks composed solely by CNC. In this context, pure CNC aerogels having a dual pore size distribution with customizable 3D structure were produced by direct ink write (DIW) technique without any support material [130]. Aqueous CNC gels in the range of 2–30 wt% were used as inks to produce complex geometries (see Fig. 4a) with porosities up to 92.1% and macropore sizes of 20–800 μm by using nozzle tip diameters ranging from 200 to 500 μm. Such high concentration of CNC could be achieved given their relatively low aspect ratio, as the pressure needed to extrude particles having larger aspect ratio reaches prohibitive values due to the increase in ink viscosity [127,131]. Taking advantage of the tailored rheological properties by simple changing CNC concentration, the shape of CNC structures could be easily designed and rapidly manufactured in comparison with traditional aerogel fabrication technologies, providing architectures which suffer minimal shrinkage or damage during freeze drying.

Although it is well-known that anisotropic nanoparticles tend to be aligned during 3D printing owing to generated shear stresses [129,132], scarce efforts have been made to carefully study this effect in CNC-filled inks. In this context, the dynamics of CNC orientation in highly concentrated inks have been very recently studied by Hausmann et al. combining shear-induced polarized light imaging and steady-state rheological experiments [133]. Their results indicate that CNC are continuously aligned as a result of a velocity profile arising from the shear stress imposed on the ink itself during the extrusion process (see Fig. 4b). They concluded that the time period needed for CNC orientation directly scales with CNC concentration and inversely scales with applied shear rate at the nozzle. This work represents a step forward in the rational design of rheological properties of CNC-inks, nozzle geometries and

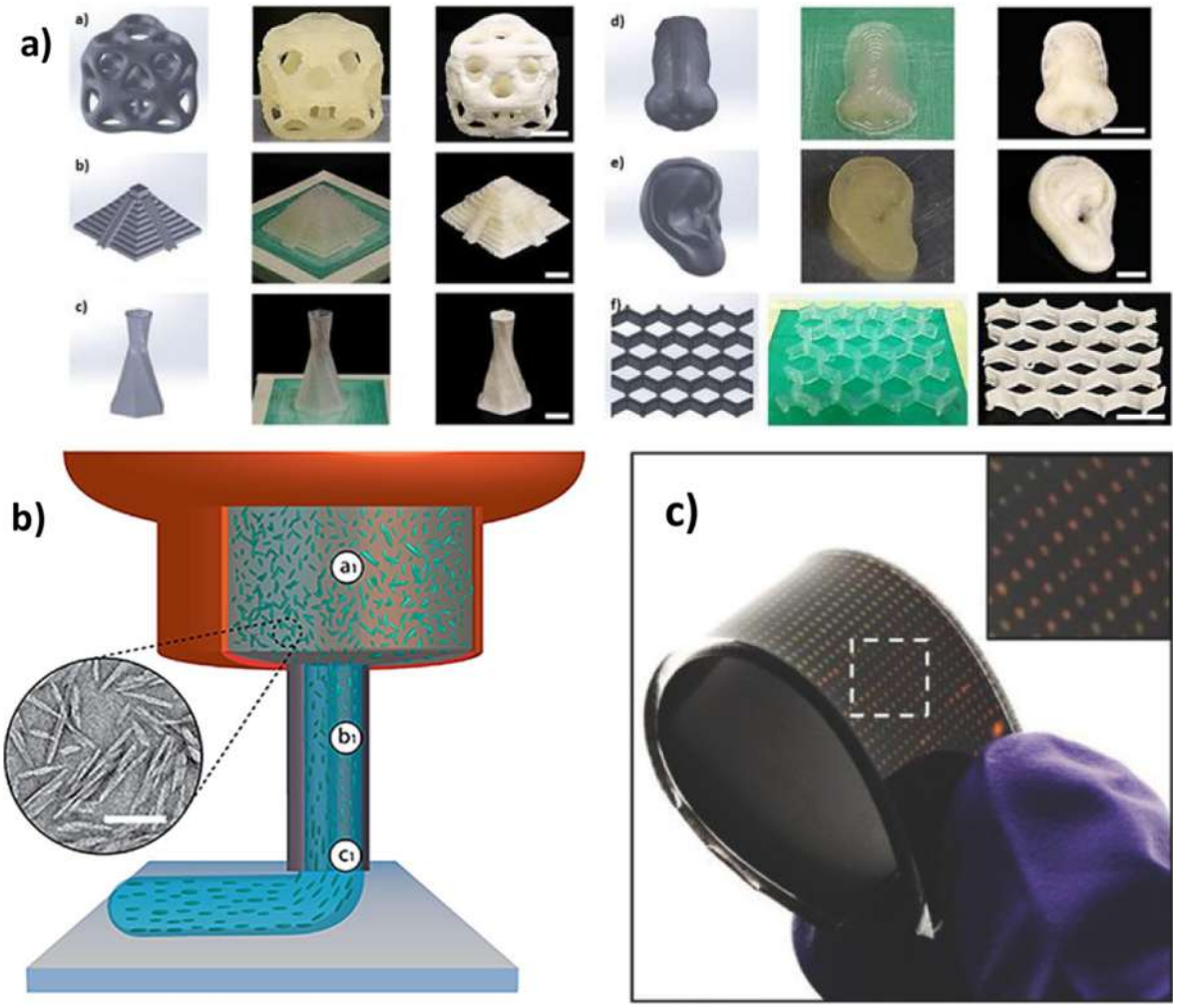

Fig. 4. (a) DIW 3D printed pure CNC structures (octet cube, pyramid, hexagonally twisting vase, nose model, ear model, and honeycomb). Scale bars are 1 cm. Reproduced with permission of Nature Publishing Group from Ref. [130]. (b) Scheme depicting the CNC alignment upon 3D printing, where three regions are distinguished: randomly organized cellulose nanocrystals in the cartridge (a_1), shear-induced alignment during extrusion through the nozzle (b_1) and the final oriented CNC (c_1). TEM scale bar is 100 nm. Reproduced with permission of ACS Publications from Ref. [133]. (c) Photograph of a CNC microfilm array prepared on a flexible PDMS substrate. Reproduced with permission of John Wiley & Sons Ltd from Ref. [136].

printing conditions [134]. Recently, Siqueira et al. printed inks formed by CNC to obtain materials with enhanced stiffness along the printing direction after shear-induced alignment, mimicking the microreinforcing effect occurring in plant cell walls [135]. Obtained pure CNC architectures display enhanced load transfer through shear stresses at the matrix-reinforcing elements interface, opening new paths for the fabrication of lightweight structures with tuneable mechanical performance.

Printing techniques can also be used to fabricate interactive photonic CNC microfilm arrays [136]. Inspired by the offset printing technique, CNC-based microfilm arrays having uniform and intense predefined colours were fabricated *via* spatially-defined nanoliter sessile droplet method. These arrays were obtained onto a variety of substrates including glass or polydimethylsiloxane (PDMS) (see Fig. 4c), allowing the development of structurally colored CNC films capable of withstanding large deformations with no cracking, which is in marked contrast with many brittle photonic CNC films [137,138]. In order to obtain uniform colours within a microfilm, the “coffee-ring” effect was solved by slowly drying the aqueous CNC droplets under an immiscible layer of hexadecane oil, slowing down the evaporation process. Obtained monochromatic CNC microfilms (diameters of 600–1000 μm) display a dramatic real-time colourimetric response to changes in relative humidity. For instance, upon exposure to humid breath, these arrays change from blue to infrared (passing through green and red) in only 4 s, while they are able to recover their original colour after 4 s of stopping exposure to humidity.

3. Nanohybrid types

3.1. CNC structural, chemical and physical properties

When accounting for the chemical and physical properties of CNC, one should take into account that their properties strongly depend on the method used for their isolation. CNC are extracted through a controlled hydrolysis of cellulose, where the less organized (amorphous) regions suffer a cleavage of their glycosidic bonds, leaving behind the more resistant highly crystalline regions. Although Filson et al. reported in 2009 an enzymatic hydrolysis process to obtain CNC [139], their production is mostly accomplished following a strong acid-assisted hydrolysis. Typically, cellulose is immersed into an aqueous sulphuric acid (H_2SO_4) solution (64 wt%) at 45 °C for 30 min under constant stirring [8,26,60], although other acids including phosphoric, nitric, hydrobromic or hydrochloric can be also used. Upon further mechanical treatment using sonication, water-dispersed CNC are obtained. As sulphuric acid-assisted hydrolysis this is the most commonly followed approach, in this section the structural, chemical and physical properties of CNC extracted through this acid will be shown.

CNC are needle-like shaped crystalline nanoparticles composed by β-1,4-linked anhydro-D-gluycose units whose diameters can be in the range of 3 to 20 nm, while their length can vary from 150 to 2000 nm depending on the cellulose source and synthetic conditions, although usually values of 100–250 nm are obtained [140,141]. CNC usually present a degree of polymerization (DS, or number of glucose units) of 500 to 15.000, and thanks to their anisotropic character, their specific surface area is found in between 150–250 $m^2\ g^{-1}$. Cellulosic chains are packed into a monoclinic structure with two chains per unit cell following the cellulose I_β structure (unit cell parameters at 20 °C of a = 7.784 Å; b = 8.201 Å; c = 10.380 Å; α = 90.0°; β = 90.0°; γ = 96.5°) [142]. The crystallinity index (X_c) of CNC can be extracted from X-ray diffraction analysis according to Segal equation [143], or alternatively following the Ruland–Rietveld approach [144]. Overall, crystallinities above 85% are obtained, with crystalline dimensions of ~6.8, ~5.3 and ~6.6 nm for (*2 0 0*), (*1 1 0*) and (*1 1 0*) planes respectively according to the Scherrer equation.

As a result of the sulphuric acid hydrolysis, CNC surfaces are decorated with anionic sulphate ester groups ($–OSO_3^-$), yielding nanoparticles with zeta-potential values of nearly −40 mV. Usually, CNC extracted through sulphuric acid route present 0.6–0.8, ~42 and ~51% of elemental sulphur, carbon and oxygen by weight, respectively, yielding a degree of substitution (DS) for $–OSO_3^-$ of about 13.5% for standard synthesis conditions, although DS values as high as 48% have been reported (0.08 to 350 mmol g^{-1}) [20,145]. The negatively charged electrostatic layer that covers the surface of CNC renders them highly dispersible and stable in polar solvents such as water, being able to remain well-dispersed for months when stored in water at concentrations below 2 wt% (CNC formed by enzymatic hydrolysis are not negatively charged, decreasing the suspension stability). On the contrary, CNC are not compatible with many organic solvents or polymers such as polyolefins. The numerous surface hydroxyl groups, estimated to be in the range of 0.96–2.65 mmol g^{-1} [143], can be readily functionalized with plethora of molecules, allowing an easy tailoring of their surface properties through different post-functionalization approaches [146].

Upon temperature increase, the glycosyl units within CNC begin to depolymerise, dehydrate and decompose, yielding to weight loss events at temperatures above 150 °C [7]. Unfortunately and as a result of the sulphate groups, the thermal stability of CNC is lower than that of native cellulose. Exchanging the acidic protons on the sulfate groups for other cations renders CNC with enhanced thermal stability, delaying thermodegradation events by up to 100 °C. Similarly, CNC extracted from enzymatic hydrolysis present higher thermal stability [139]. CNC present impressive mechanical properties: the axial elastic modulus (Young's modulus, *E*) of native CNC ranges from 110 to 220 GPa, and the tensile strength ranges from 7.5 to 7.7 GPa, which are comparable, and within the range of other reinforcement nanomaterials, such as carbon nanotubes, metallic nanoparticles and nanoclays. Interestingly, taking into account that their density is as low as 1.61 g cm^{-3} (for pure crystalline cellulose I_β) [142], the specific *E* of CNC (elastic modulus to weight ratio) can reach up to 85 J g^{-1} in comparison with the 25 J g^{-1} for steel [26]. Moreover, CNC presents a remarkably low coefficient of thermal expansion (CTE) of ~0.1 ppm $°C^{-1}$, which is notably lower than the CTE of many metals and plastics (13 ppm $°C^{-1}$ for steel or 20 ppm $°C^{-1}$ for Kapton®) [147]. Although CNC are an electrically insulating material, with conductivities in the range of 10^{-12} S cm^{-1} [148], using molecular dynamics (MD), Diaz et al. concluded that the thermal conductivity (*k*) of the cellulose I_β form of CNC depends on the crystalline direction, where *k* varied from 5.7 ± 0.9 W mK^{-1} in the chain direction to 0.72 ± 0.12 W mK^{-1} in the transverse direction (for comparison, thermoplastic materials typically show a *k* of 0.15–0.24 W mK^{-1}) [149,150]. Such differences were ascribed to the intrinsic crystalline anisotropy of the CNC, where weaker intermolecular interactions (hydrogen bonding) are present in the transverse directions in comparison with the covalent forces in the axial direction. In this line, this asymmetric crystalline structure also gives the CNC piezoelectric properties (change of electrical polarization upon mechanical stresses), achieving effective shear piezoelectric constant (d_{25}) values of 2.1 Å V^{-1}, which results even larger than the d33 values of 1.3 Å V^{-1} measured for a reference piezoelectric ZnO film [151].

The spectacular ability of CNC to form a lyotropic chiral nematic liquid crystalline (LC) phase when dispersed in water (typically comprising pH values of 2.1–2.8) [152], which was firstly reported by Revol and co-workers in 1992 [28], deserves an especial mention. From the pioneering work of Marchessault et al. in 1959, who reported the birefringence (optical anisotropy) of CNC [27], the curious periodicity of the helical modulation in aqueous CNC dispersion above a certain concentration (nearly 4.5 wt%, while lower CNC concentrations result in the formation of an isotropic phase [28], has been exploited by many authors to obtain solid-state left-handed chiral nematic materials with tuneable helical pitch (*P*). Rheological properties of CNC strongly depend on the cellulose source, synthetic conditions for their extraction, applied shear rate and solution concentration. Generally, water-dispersed CNC display a strong shear-thinning behaviour at low concentrations (highly viscous at low shear forces but rather fluid at high shear forces), while an elastic gel-like behaviour is observed at intermediate and high concentrations [133]. Zero shear viscosity values of 63 and 127 mPa s for CNC extracted from cotton and wood respectively (H_2SO_4 hydrolysis 64 wt%, 45 °C, 60 min; concentration of

3.5 wt%) have been reported [152].

3.2. CNC/metal and CNC/metal oxide nanohybrids

Polysaccharides present a vast window of opportunities when combined with different metallic nanoparticles (mNPs) [153]. Currently, it is observed an increasing interest not only in the use of plant cellulose and its derivatives, but also their nanometric systems, for a combination to give hybrid materials [154]. The high number of publications in this area confirms the potentiality of cellulose-based hybrid materials: numerous reviews in this field can be found, in which more detailed information on this type of materials has been provided [153–163]. For example, the review by Pinto et al. describes hybrid materials based in plant and bacterial cellulose [155]; most recent examples of cellulose/mNPs hybrid materials are represented by gold (Au), silver (Ag), copper (Cu), palladium (Pd) and platinum (Pt) based cellulose nanohybrids, mainly obtained by using *in situ* reduction or by impregnation methods, that found applications in several different sectors, such as thermal/electrical conductivity, catalysis, sensing, biomedical and water remediation.

In the case of Au, it is recognized that cellulose nanocrystals and metal nanoparticles have stimulating features and their combination creates functional materials with distinctive properties. This subject was recently reviewed by Van Rie and Thielemans with emphasis on materials having specific catalytic, antimicrobial, sensing and antioxidant performances [156]. Examples for CNC can be found in the work of Majoinem et al. [157], where the authors used CNC as templates for the preparation of nanostructures having a pronounced chiral right-handed plasmonic response, taking into consideration that sizes of both CNC and AuNPs need to match to provide the signal. Chu et al. obtained a series of rational engineered photonic–plasmonic coupled hybrid materials by self-co-assembly of renewable liquid-crystalline CNC and plasmonic silver and gold nanorods [158,159]: these materials combine metallic and dielectric components into morphologically well-defined hybrid structures, that mix the intrinsic merits of plasmonic and photonic materials through synergistic electromagnetic interactions. The highly impressive optical performances, together with the stacked layer structure, the abundance of initial raw materials, and the cost-efficient “bottom-up” self-assembly method, make these hybrid devices suitable for application in integrated optophotonics (Fig. 5a–d).

Previously, Campbell et al. [160,161], demonstrated scalable fabrication of thin mesoporous films, achieving arrangement of ordered nanoscale organic CNC-based films, beside the long-range oriented metal nanostructures, that are of great importance for renewable energy, optical, catalytic and anti-counterfeiting technologies (Fig. 5e). In parallel, Semenikhin et al. converted CNC into individual gold nanoshell-bearing particles with tuneable surface plasmon resonance bands. By using cellulose functionalization methods, stable suspensions of positively charged CNC have been generated [162]. In the paper of Herreros-López [163], azide-functionalized cellulose nanocrystals have been linked to alkynyl-dendrons of the PAMAM family, used as templates for the realization of stable and monodispersed gold nanoparticles in aqueous media and their catalytic capabilities studied in a model reaction. The results indicated that those promising catalysts are also amenable to be scaled-up in production, as well as recyclable by filtration or centrifugation procedures.

The coassembly of CNC and shape isotropic AuNPs, with different dimensions and surface charges and at different number densities of AuNPs, into macroscopic free-standing films, was studied by Lukach and co-workers [164], proving that nanohybrid films preserved the birefringence, iridescence, and chiroptical activity of the CNC matrix, open the possibility of realizing functional materials with coupled optical properties. From the same group [165], it was shown that nanorods-CNC films have strong plasmonic chiroptical characteristics, which are beneficial for fundamental studies of collective plasmonic chiroptical activity properties and their potential applications.

Rojas et al. recently investigated, with success, the formation of silver and gold nanoparticles, respectively of hexagonal and spherical shape, on CNC surface, by demonstrating their green and potential scalable synthesis for application in heterogeneous catalysis [83]. Hybrids of Au nanoparticles monodispersed onto multifunctional CNC–graphene sheets were studied by Wang et al. [166], in details an efficient synthesis method has been developed for deposition without the use of additional reducing and capping agents, showing a strong catalytic activity, described to the synergistic effect resulting from the coexistence of CNC and graphene. In recent times, even Zhang et al. prepared, by ATRP, P4VP-g-CNC (poly(4-vinylpyridine) (P4VP) grafted cellulose nanocrystal nanohybrids for the stabilization of gold nanoparticles and they found that, distinctive from Au@CNC, the Au@P4VP-g-CNC material could be conveniently recovered by flocculation at pH $>$ 5, while the recycled catalyst still displayed a relatively high activity [167].

CNC can be decorated by silver by using different methods (UV reduction, electrostatic assembly, microwave-assisted preparation, surface pre-modification) [168,169], and they can be applied not only for catalysis, but even for antibacterial activity and as DNA biosensor [170].

Metal oxide nanoparticles (NPs), such as titanium dioxide (TiO_2), zinc oxide (ZnO), copper oxides (CuO and Cu_2O), silica (SiO_2) and iron oxides (Fe_2O_3 and Fe_3O_4), are requested for their multifunctional, modulated and versatile properties [171], essential for several high-tech applications, including catalysts, absorbent materials, optoelectronic materials, magnetic nanocomposites, luminescent materials, drug delivery systems, sensors, antimicrobial materials, imaging. Boury and Plumejeau revised the association of metal oxides and polysaccharides, highlighting on the different methods to combine them, on the controlled hydrolysis/polycondensation and nucleation growth process [172]. Goikuria et al. incorporated ZnO, SiO_2, TiO_2, Al_2O_3 or Fe_2O_3 nanoparticles into CNC films and studied the thermodegradation behaviour of obtained materials [173]. Results showed that the thermodegradation process of CNC films could be delayed by 75 °C after the incorporation of both ZnO and Fe_2O_3, while in the case of CNC loaded with TiO_2 and SiO_2 nanoparticles the increase of thermal stability was not so evident.

The combination of cellulose nanocrystals and TiO_2 NPs is one of the most studied strategies to fabricate bio-based materials for photocatalytic properties [177,178]. Xue et al. prepared CNC iridescent films with retained helicoidal chiral nematic order and

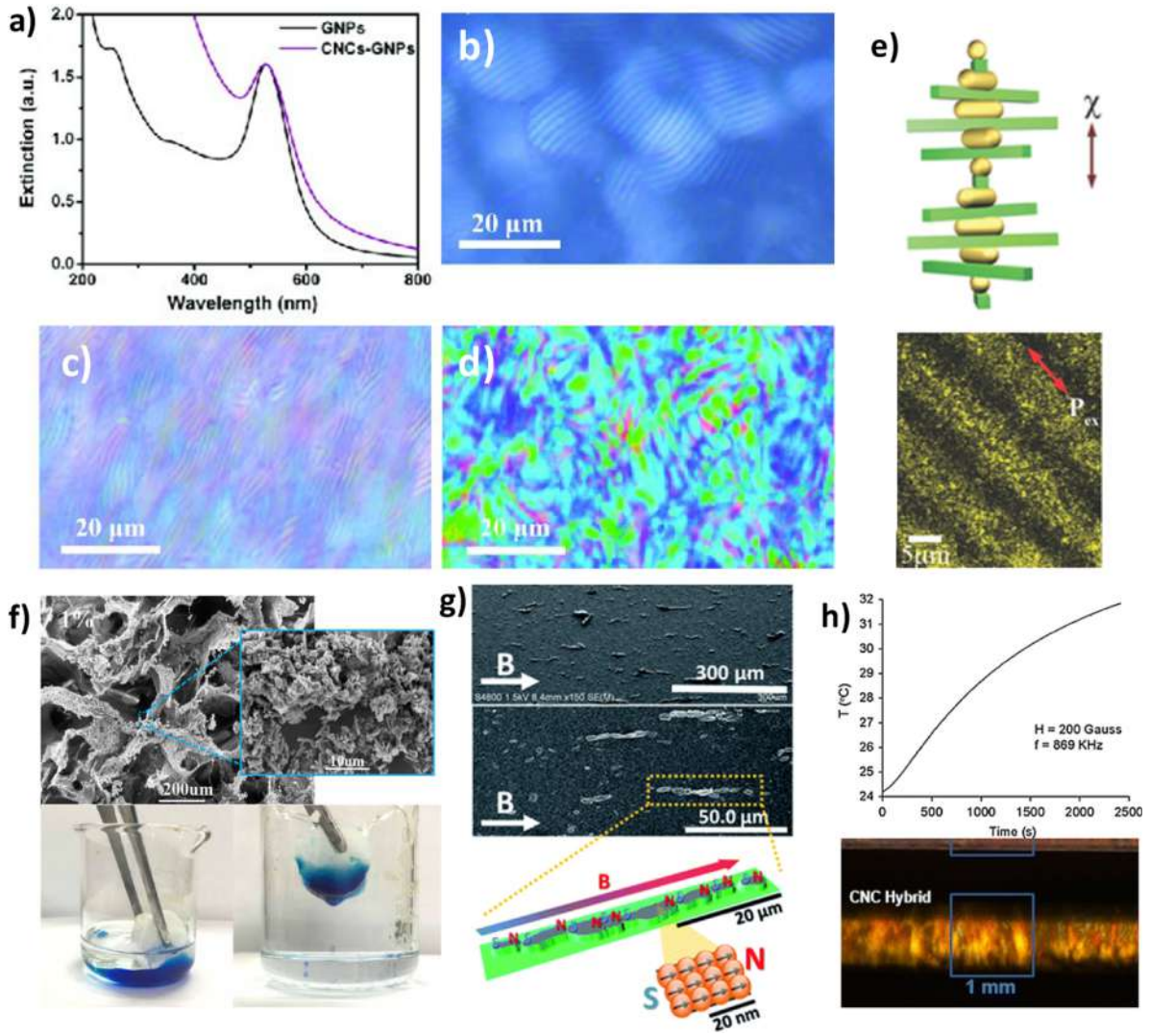

Fig. 5. (a) Steady-state UV-Vis spectra of the GNPs (Gold Nano Particles) suspension and CNC/GNPs mixed suspension, respectively. (b) POM image of the CNC/GNPs mixture during evaporation, showing fingerprint textures. (c) POM image of the liquid crystalline CNC/GNPs mixture with the evaporation continued, exhibiting a compressibility effect in helical pitch (d) POM image of the dried CNC/GNPs nanohybrids with characteristic marble-like texture, indicating the reservation of the chiral nematic architecture. All the images were taken with the polarizers in a crossed arrangement. Reproduced with permission of ACS Publications from Ref. [159]; (e) Schematic of helicoidal assembly of Gold Nano Rods (GNRs) in a cholesteric dispersion of CNC and two-photon luminescence image of the helicoidal assembly of GNRs in CNC Reproduced with permission of John Wiley & Sons Ltd from Ref. [161]; (f) FE-SEM images of cryogels-ZnO-1% and photos of the removal of methylene blue (200 mg L^{-1}) below silicone oil with the cryogels-ZnO-1%; Reproduced with permission of ACS Publications from Ref. [174]; (g) FESEM images of unidirectionally linear magnetic self-assembled CAHMCs (cellulose akaganeite hybrid magnetic nanocrystals) under a magnetic field intensity of 4 T at different magnifications and schematic illustration of the magnetically self-assembled CAHMCs. Reproduced from Ref. [175] with permission from The Royal Society of Chemistry; (h) temperature profile of a CNC-inorganic aqueous dispersion exposed to an alternating magnetic field (200 Gauss, 869 Hz) and neat CNC and CNC-inorganic dispersion (ca. 8.5 wt%) observed under crossed polarizers. Reproduced with permission from Springer Nature from Ref. [176]. (For interpretation of the references to colour in this figure legend, the reader is referred to the web version of this article.)

layered structure, providing skeleton for the formation of mesoporous TiO_2 and modulating visible light catalytic activity of TiO_2 by inserting carbon quantum dot [179]: because of the formation of linear O-C-O units in TiO_2/C-dot nanohybrids, they demonstrated that such a green preparation strategy and results are beneficial for the construction of functional materials with desirable morphologies and high performance. Nanohybrid systems containing CNC and TiO_2 nanoparticles were prepared and studied by Martakov et al. In a structure similar to core-shell, promising their successful application in the field of catalysis, optics, electronic devices and as anisotropic filler in nanocomposites of biocompatible materials [180].

In the later years, a huge number of cellulose/ZnO hybrids have also been described in literature [60]. Recently, as shown in Fig. 5f, Wang et al. studied the behaviour of CNC/ZnO nanohybrids with modulated morphology [174], dual pH/temperature

responsiveness to modulate water swelling ability, while the effect of ZnO on melamine formaldehyde-coated cellulose nanocrystals (MFCNC) was evaluated [81]. These ZnO@MFCNC hybrid nanostructures were evaluated for their *in vitro* sun protection factor performance and photocatalytic activity under simulated UV and solar radiation and the system displayed smart UV-absorption and photocatalytic characteristics, contributing to the adaptation of this renewable and sustainable technology to intelligent cosmetic formulations.

Because of the well-recognized magnetic properties of some oxides and ferrites, in the last years, the combination of cellulose and iron oxide or cobalt ferrite NPs have been also essentially investigated to produce magnetic materials for application in water purification, drug delivery, sensing [181]. Compared with cellulose nanofibres, limited studies have been conducted on CNC/magnetic NP hybrids. This is due to the fact that well-dispersed CNC aqueous suspensions undergo phase separation once metal cations are introduced: electrostatic interactions between sulphate ester groups and metal cations induce the irreversible aggregation of CNC. While the aggregation issue changes the nanoscale nature of CNC and hinders the applications of CNC/magnetic NP hybrids as nanodevices, it does not affect their applications in magnetic assisted separation processes.

In Mahmoud et al. [182], CNC@Fe_3O_4 nanohybrids were obtained through the *in situ* co-precipitation of Fe^{2+} and Fe^{3+} by ammonium hydroxide, and Au NPs were later embedded to immobilize papain enzyme. Although Fe_3O_4 NPs and Au NPs were well-dispersed on the CNC surface, the aggregation and crosslinking of CNC occurred due to electrostatic attraction resulting in the formation of a micron-sized network. Despite the aggregation, the nanohybrids showed a significantly high loading. Guo et al. presented an efficient and scalable approach for selective protein separation from a complex mixture via magnetically responsive Fe_3O_4@CNC hybrids [183].

Cellulose akaganeite hybrid nanocrystals (CAHNCs) were synthesized *in situ* from a ferrous chloride aqueous solution in the presence of pre-oxidized cellulose nanocrystals as a reducing agent for the reduction of dissolved ferrous ions under heat treatment and neutral gas flow [175] (see Fig. 5g). Although the authors focused on fabricating a cellulose core magnetic shell nano-heterostructure that efficiently responds to considerably weaker modulated external magnetic fields with a positive magnetic susceptibility, the explained method will provide novel concepts for obtaining novel 1D organic–inorganic core–shell hybrid nanostructures that consist of cellulose nanocrystals and a huge range of functional metal oxides with distinctive and exceptional properties that can be used in modern high-tech industries and medicine. The group of Rojas fabricated self-standing films of cellulose nanocrystals and electrospun nanocomposite fibres with CNC and polyvinyl alcohol both with magnetic properties arising from cobalt iron oxide nanoparticles (see Fig. 5h) in the CNC matrix: the authors demonstrated that these materials can have potential applications in packaging, magnetic shielding and separation applications, other than drug delivery and cell treatment [176].

3.3. CNC/carbonaceous nanomaterials

Carbon nanostructures can be classified according to their aspect ratio and the nanometre dimension in 1D as nanotubes or nanofibres, 2D as graphene nanoplatelet or graphene oxide, and 3D as fullerene or carbon black nanoparticles [184]. Carbon nanotubes (CNTs) are formed by rolling-up graphene sheets in a cylindrical way. They are classified in single-walled CNTs (SWCNTs), double-walled CNTs (DWCNTs) and multi-walled CNTs (MWCNTs) by the difference in the number of layers, obtaining tubes with different diameter dimension, while the length can be from some hundred nanometre until millimetre, by changing the process and parameters. Furthermore CNTs can be metallic or semiconductive according to the chiral vector [185,186].

Graphene is a two dimensional carbon material made of a single sheet of graphite, with a single layer of carbon atoms arranged in a hexagonal lattice, hence theoretically has the thickness of 0.35 nm. Andre Geim and Kostya Novoselov were awarded the 2010 Nobel Prize in Physics for “groundbreaking experiments regarding the two-dimensional material graphene” [187,188]. It shows high electrical conductivity and strength and has a Young's modulus of 1 TPa, with an ultimate strength of 130 GPa. It is a material with extraordinary mechanical properties even when compared to CNTs. Fullerene is another allotrope form of carbon, with spherical shape. It was the first nanometre form of carbon discovered and it was manufactured by Richard Smalley at Rice University [189].

All carbon nanostructures have very unusual electrical properties and they were used in combination with other nanomaterials, in order to transfer this effect in the insulator materials. Carbon nanostructures permit to develop high conductive sheets from carbon-CNC nanohybrids. Most of conductive hybrid materials feature the use of carbon nanotubes or graphene, two relatively new materials with astounding properties. Carbon black (CB) are also used, since they have intrinsic conductivity with large surface areas.

Functional hybrid materials with nanocellulose have, for example, adjustable conductivity by introducing carbon nanotubes [190,191], or graphene [192]. In particular, carbon naomaterials are applied in combination with cellulose nanocrystals in order to transfer the electrical transport properties to CNC that are known to be insulator nanomaterials. However, the major challenge in preparing materials that take advantage of the properties of carbon nanomaterials is obtaining stable dispersions of these nanoparticles, because they tend to aggregate due to the van der Waals interactions [186].

Cellulose nanocrystals and carbon nanostructures are combined in order to develop conductive and flexible papers with enhanced properties by using different CNT content and weight fractions and study potential synergistic effects between the CNTs and the CNC in hybrid networks. The nanohybrid films show superior tensile and improved electrical properties by comparison with the neat CNC film [193].

One of the critical merits of high performance nanohybrid materials with reinforcing nanoscale components, as CNTs, is the ability to maximize stress transfer across interfaces in order to promote material strength with high toughness [194]. However, poor dispersion of reinforcing carbon nanostructures at the nanoscale, and weak interfacial interactions, may lead to failure at small deformations, resulting in brittle material with limited strength and toughness [195]. Different studies were performed on the formation of CNT/cellulose conductive hybrid paper [196–199]. Different studies report the analysis of the electrical properties of the

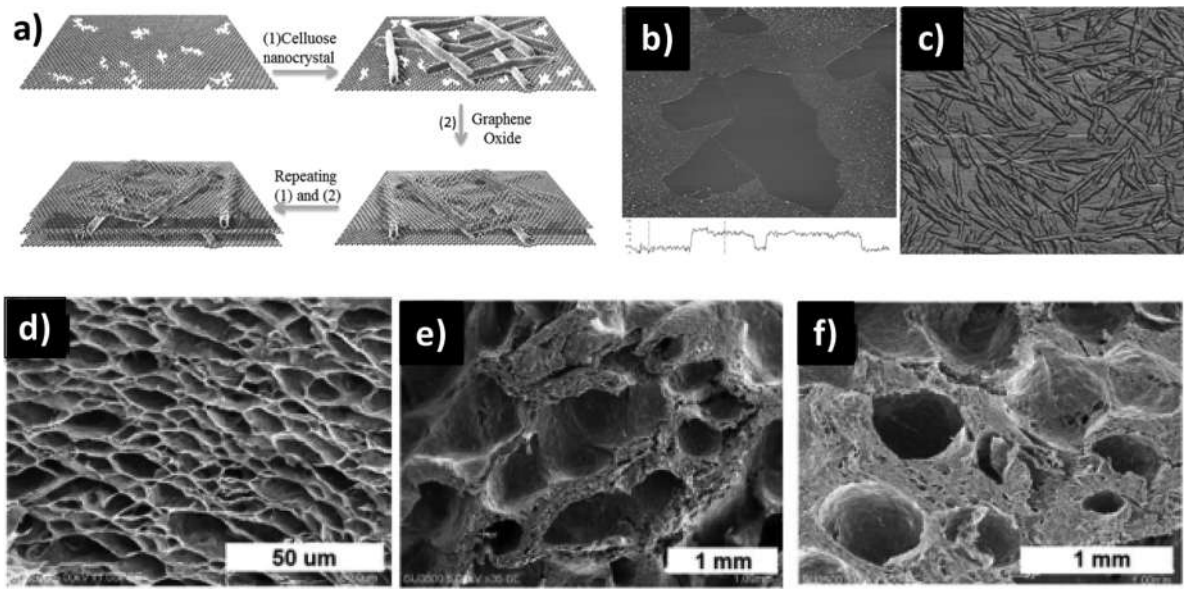

Fig. 6. Design strategy of the cellulose nanocrystal-graphene oxide nanomaterials: (a) fabrication of the laminated cellulose nanocrystals/graphene oxide nanomembranes. (b) The AFM phase image of graphene oxide, and (c) cellulose nanocrystals on graphene oxide. Reproduced with permission of John Wiley & Sons Ltd from Ref. [65]. SEM micrographs of the cryo-fractured surfaces of vitamin C graphene oxide sponge with a mass ratio of 1:150 (d) and the same systems with CNC at GO:CNC mass ratio of (4:1) and (1:2) respectively (e,f). The evolution of the pore structure and morphology was studied. Reproduced from Ref. [203] with permission from The Royal Society of Chemistry.

cellulose/carbon nanostructure based materials, however, systematic analysis of the electrical properties of these innovative materials is required in order to elucidate their electromagnetic interference (EMI) shielding properties and to design an EMI shielding material. CNT addition enhanced film performance, which are worthwhile for investigation, because of expected properties from both nanomaterials in the electronic field, such as electromagnetic interference shielding and electronic circuit [200].

As shown in Fig. 6a, b and c, Xiong et al. developed ultrarobust, highly optical transparent and electrical conductive cellulose nanocrystals-graphene membranes by combining two different classical reinforcing nanocomponents: 2D strong flexible graphene oxide sheet and 1D cellulose nanocrystals rigid reinforcing nanostructures that are able to promote high mechanical strength along with excellent toughness. The nanomembranes, 60 nm thick, have an overall uniform surface with root-mean-square roughness, which is much smoother than other graphene oxide (GO)-based nanohybrids fabricated by common drop-casting or vacuum-assisted filtration methods [201]. The results were synergetic properties that cannot be achieved in previously reported graphene-based polymer nanocomposites [65]. Zhang et al. developed an electrochemical chiral sensor based on CNC and MWCNTs, for discrimination of tryptophan enantiomer. On the basis on the natural right-handed chirality of CNC and high conductivity induced by the presence of MWCNTs, they developed a device with different advantages as rapid recognition, high sensitivity and stability, and respect to previous reports, the sensor showed high enantiospecificity [202].

Yousefi et al. exploited the capacity of self-assembly of graphene oxide nanosheets vitamin C (VC), and cellulose nanocrystals with the aim to develop an ultrastrong and a 3D porous scaffold for the adsorption of water contaminants, as dyes, heavy metals, and pharmaceuticals from water (Fig. 6d, e and f) [203]. The VC works as the reducing agent, and its concentration represents a critical part in tailoring the pore architecture of the sponges [203].

3.4. CNC/luminescent nanoparticles

The concomitant integration of light emitting materials and iridescence has been sought as an attractive way for the design of novel optical devices. Quantum dots (QDs) are tiny semiconductors which show a quantum confinement induced tuneable and narrow light emission spectrum that results especially useful for sensing and optical switching [204,205]. Accordingly, Nguyen et al. prepared water-soluble polyacrylic acid/mercaptopropionic acid-stabilized cadmium sulfide (CdS) QDs in order to obtain free-standing iridescent films with photoluminescent properties [55]. QDs were passivated with appropriate amphiphilic stabilizers to avoid their aggregation and ensure the formation of the chiral nematic phase. The photoluminescence (PL) emission intensity of the films was proportional to the QD loading, exhibiting a green to red-coloured luminescence (emission at 490–680 nm) when irradiated with UV light. Fabricated materials underwent a strong luminescence quenching when exposed to trinitrotoluene (TNT) solutions or vapour, making them suitable candidates as optical sensors. Unfortunately, they are potentially toxic and require complex functionalization steps to achieve a homogeneous dispersion within their host matrix [55], making desirable the development of further environmentally safer alternatives.

Carbon dots (CDs) are metal-free photoluminescent nanomaterials that are witnessing an increasing interest thanks to their low

cost, stable PL and inherent physicochemical properties [206]. In contrast to that usually found in many semiconducting nanoparticles, the photoluminescence of CDs strongly depends on the precursor materials used for their synthesis, making them attractive to develop materials for sensing, catalysis or patterning. Interestingly, the carbonyl and hydroxyl surface functional groups of CDs make them highly compatible with hydrophilic materials such as CNC [207]. In this framework, Lizundia et al. reported a green, simple, scalable and fast hydrothermal approach to fabricate CDs that were then introduced by EISA within a film that retains the chiral nematic long-range ordering of CNC [51]. CDs were doped with nitrogen through the incorporation of D-glucose and melamine during the hydrothermal process to endow improved photophysical properties. Obtained films presented photoluminescent properties, emitting at nearly 505 nm when films were excited (λ_{ex}) under a light of 365 nm. Such materials can be prospectively used for advanced photonics applications with potential chemosensing capacity towards Fe^{3+} and Zn^{2+} ions.

Very recently, Zhang et al. prepared dual-emitting fluorescent materials from CNC-assisted CDs which where grafted with $SrAl_2O_4$, Eu^{2+}, Dy^{3+} (SAO) phosphors [208]. CDs-coated SAO phosphors were surface-modified with (3-aminopropyl) trimethoxysilane in order to modify the surface activity of the phosphors and improve the interfacial properties. Obtained materials showed an optical dual-emitting spectrum under exposure to 365 nm light with a high sensitivity to surrounding temperature in the 243 to 383 K.

Bovine serum albumin-protected gold nanoclusters (Au@BSA NCs) were incorporated into CNC-based hydrogel beads to obtain materials that could simultaneously sense and scavenge heavy metal ions [209]. The used clusters are known as aspicules, which are quantum clusters of noble metals with good photostability, high quantum yield and ease of functionalization [210]. Fabricated materials were particularly efficient with Hg^{2+} ions in water, where concentrations as low as 1 ppm were enough to markedly quench the deep red emission (660 nm) when excited under 365 nm light.

Despite to the efforts made on the development of photoluminescent CNC-based materials, little efforts have been paid to fabricate CNC hybrids with up-converting properties. Up-converting (UC) materials have the ability of absorbing two or more photons of near infrared (NIR) light and emit within the visible spectrum via the “photon upconversion” process [211]. In this sense, Nguyen et al. provided the first evidence of producing up-converting photonic films with chiral nematic ordering using CNC as a hosting matrix for the incorporation of polyvinyl alcohol-stabilized $NaYF_4$:Yb,Er hexagonal nanorods [52]. $NaYF_4$:Yb,Er hexagonal nanorods were selected as up-converting nanoparticles thanks to their good quantum yield, intense up-conversion luminescence and relatively high half-maximal effective concentration (EC_{50}) after grafting [212]. Obtained free-standing films emitted light within the optical range when irradiated with lower energy infrared light. Following these efforts, Fedorov et al. prepared up-converting hybrid films based on CNC together with SrF_2:Ho nanoparticles by simply mixing the components in water and subsequent EISA [213]. Mechanically flexible and optically translucent hybrid films with an intense red luminescence upon excitation with a 1912 nm laser radiation were obtained. Fabricated films can be used as probes for near-IR laser radiation visualization in areas such as biomedicine or as a luminescent labelling for covert security papers.

3.5. CNC/nanoclays

Several approaches have recently been considered for self-assembled biomimetic films, aiming to combine high toughness, strength, and stiffness [214]. However, it remains a challenge to succeed high toughness using simple processes, especially for bulk materials. It was demonstrated, as an examples, that cationic native nanofibrillated cellulose (C-NFC) and anionic nanoclay, i.e., montmorillonite (MTM), permit local self-assemblies by a simple centrifugation process to achieve 3D bulk materials and the obtained tough bulk nanocomposites have potential in applications for sustainable and environmentally friendly materials in construction and transportation [215]. Okamoto et al. prepared stimuli-responsive colloidal nanohybrid hydrogels, by exploiting noncovalent interactions between anionic cellulose nanocrystals and polycationic aminopropyl-functionalized magnesium phyllosilicate clays (Fig. 7a), offering an excellent opportunity to fabricate new stimuli-responsive hydrogels that are bioactive and biocompatible, and of possible use in applications such as wound dressing and consumer care products [216].

Recently, Li et al. used imogolite to fabricate thin films with polyelectrolytes via layer by layer (LBL) assembly [67], by considering phosphate (P) modification of CNC for increasing interaction, while Sheikhi developed a brick-and-mortar-like ultrasoft nanohybrid metallogel formed by crosslinking CNC with ammonium zirconium carbonate (AZC) to trap and reconfigure dextran, a model biomacromolecule: this work will endeavour the development of molecularly imprinted hybrid metallogels for conformation engineering and smart delivery [217].

Nanoclay has been used from many years as nanostructured additive in polymers to increase the thermal shielding. In this sense, Carosio et al. developed multilayered thin films based on nanocellulose and aligned nanoclay to obtain materials with improved thermal resistance. Indeed, clay nanoplatelets are responsible for high through-thickness interface density and thermal shielding properties, while nanocellulose expands to realize thermally stable carbonaceous residue connecting clay platelets [218]. Although a cellulose nanofibre matrix has been used to obtain materials which resist at the penetration of a flame torch (temperature $\approx$ 900 °C) with a temperature drop larger than 600 °C on the unexposed side, the same approach could be prospectively used to improve the thermal performance of CNC-based materials.

3.6. CNC/biobased hybrids

Nature’s design of functional materials relies on smart combinations of simple components to achieve desired properties: chitosan and silk are clever examples from nature that combined with cellulose, that possesses unparalleled strength and stiffness among natural materials, will give place to reply to hybrid materials with distinctive properties.

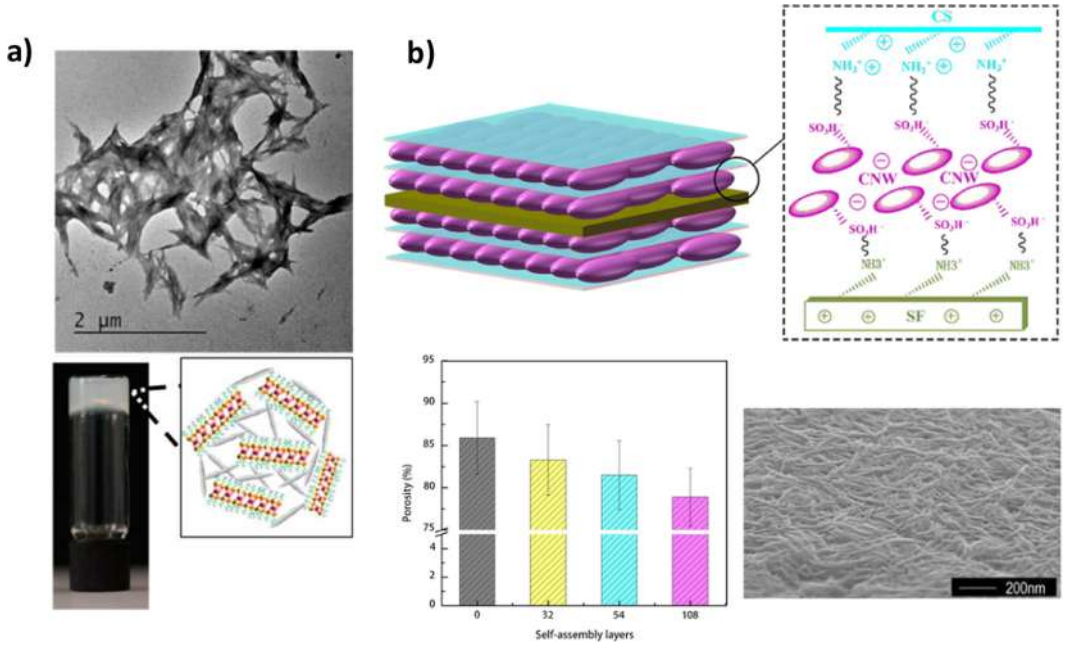

Fig. 7. (a) Unstained TEM image of cellulose nanocrystal (CNC)-organoclay hydrogel and photograph showing self-supported CNC:organoclay (1:0.13) colloidal nanocomposite hydrogel (inset, schematic illustration of cross-linked network formed by non-covalent interactions between CNC (grey) and exfoliated organoclay sheets). Reproduced with permission from MDPI AG [216]. (b) Schematic diagram of layer-by-layer self-assembly of CNW and CS onto SF substrate, porosity percentage of SF/CNW–CS scaffolds with different assembly layers and FE-SEM image of assembling CNW onto SF substrate. Reproduced with permission from Springer Nature from Ref. [219].

Wang and co-workers examined the effects of pH and salt concentration on the development of chitosan–cellulose nanocrystal (CNC) polyelectrolyte–macroion complexes (PMCs) [220,221], in particular the objectives of their study was the realization of PMCs from chitosan and CNC at different CNC concentrations and mixing sequences and to determine the properties of the resulting PMC particles with regard to their potential application as a multiparticulate oral drug delivery system. Chitosan was furthermore considered in the case of hybrid nanopapers based on cellulose nanofibres, that were prepared and physically cross-linked to expand the high mechanical properties of transparent CNF-based materials to the wet-state, as demanded in advanced applications [222]. Cellulose nanocrystal grafted with chitosan oligosaccharide (CNC-CSOS) were also used to encapsulate vitamin C (VC) and prepare CNC/VC complexes using tripolyphosphate via ionic complexation [223]. Other interesting applications of the same combined elements (oxidized cellulose nanocrystal (CNC) with chitosan oligosaccharide (CSOS)), can be found in Parinaz Akhlaghi et al. [224], where it was demonstrated how this original drug delivery system can be used as biocompatible and biodegradable drug carrier for transdermal delivery applications. Chitosan solutions and cellulose nanocrystal suspensions were even used to realize highly stable aqueous dispersions of multi-walled carbon nanotubes. The different MWCNT dispersions, having positive and negative charges, were considered for the preparation of multilayered hybrid thin films through electrostatic LBL self-assembly: the results presented in that work demonstrated the feasibility of the LBL technique for the deposition of active materials using the biopolymer pair chitosan/CNC. The obtained films can be employed for the design of transparent and biocompatible carbon nanostructured based electrodes [66].

In the case of collagen, De Mesquita et al. proposed the LBL assembly technique to combine crystalline rod-like nanoparticles with collagen, and the approach used in this work clearly represents a potential strategy to mimic the characteristics of natural extracellular matrix (ECM) [225].

Inspired by the ordered β-sheet crystalline structure and molecular orientation of natural silkworm silk, biomimetic silk fibres with advanced crystalline structure were produced incorporating cellulose nanocrystals into silk fibroin (SF) matrix to mimic the β-sheet crystallites in natural silk via wet-spinning assembly technology [226]: this study provides a new promising strategy to design high performance biomimic silk as well as expand the potential use of such artificial animal silk. Porous silk fibroin/CNC-chitosan nanohybrid scaffolds were also prepared with excellent mechanical properties and biological compatibility by LBL assembly. The hierarchical lamellar structure was formed by assembly of CNC and chitosan onto the silk fibroin lamella. The porous silk fibroin/CNC-CS nanohybrid would be a promising tissue engineering scaffold for bone generation and implantation [219,227].

4. Applications of CNC nanohybrids

Due to their outstanding properties such as relatively low cost and abundant supply, cellulose nanocrystal based nanohybrids are witnessing a continuously increasing interest to be applied at the interface of engineering, chemistry, biology and physics. Research on CNC–inorganic/organic nanohybrids is a fast growing interdisciplinary field in materials science and engineering offering

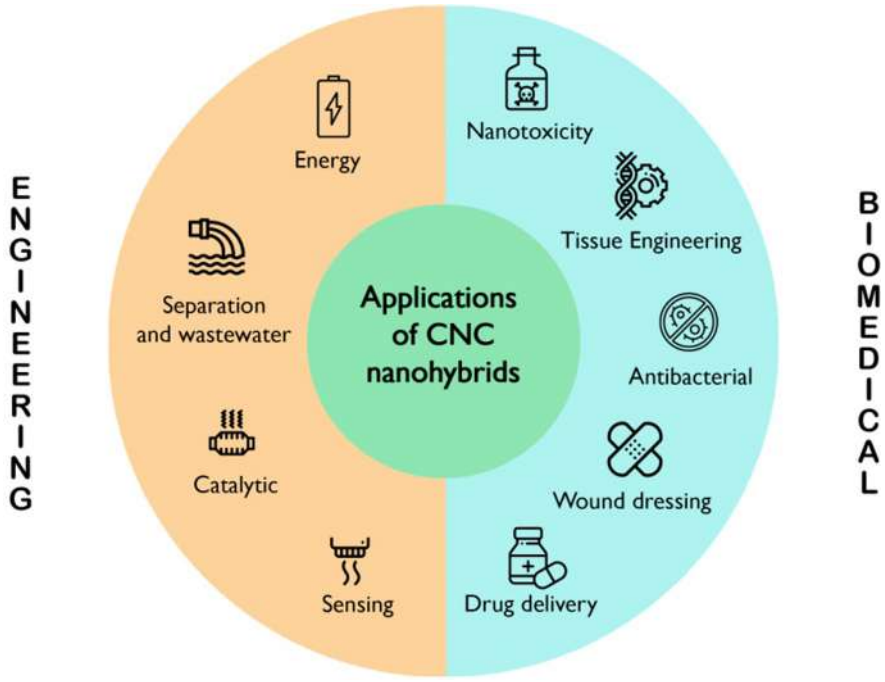

Fig. 8. Scheme displaying the engineering and biomedical applications of cellulose nanocrystal-nanohybrid based materials.Icons made by Prettycons and Freepik from www.flaticon.com.

beneficial properties of both components, not evident when used alone. In this sense, there are several patents, innovations and commercial products. Cellulose nanocrystals have been studied and evaluated for a plethora of applications notably in paper, polymer, plastics, chiral templating, flocculants, aerogels, hydrogels, drug delivery, sensing, catalytic, energetic and biomedical. As summarized in Fig. 8, such applications have been here classified into two main areas; those related to engineering field and those related to the biomedical field [168]. These two main areas are also divided into different sub-sections, as will be shown in Sections 4.1 and 4.2.

4.1. Engineering applications

4.1.1. Energy applications: supercapacitors, solar cells and batteries

Cellulose nanocrystals offer the advantages of high strength and flexibility for many advanced applications to produce more sustainable capacitor devices with higher power density and faster charging abilities compared to rechargeable batteries [10,199]. Fast-charging devices allow for significant energy saving, because they can accumulate energy during braking and release it during acceleration [228]. While conventional supercapacitors pose significant environmental hazards during its manufacture and disposal, cellulose-based electroactive nanohybrids can be fine-tuned to have more flexible structure at nanoscale [229].

CNC can be employed as: (i) a lightweight mechanical substrate that imparts flexibility and strength to electrochemically and electrically active materials (Fig. 9a); (ii) a natural template to be coated with other electrochemically active electrode materials or to be transformed into other carbon species through pyrolytic processes; (iii) a separator membrane between supercapacitor electrodes; and (iv) a material that facilitates the absorption of electrolytes acting as an electrolyte reservoir or even as a part of the electrolyte itself. Since most of the works carried out in this field have been focused on the use of cellulose nanofibres or bacterial cellulose, CNC offers a huge range of possibilities to develop novel materials and devices for energy storage applications. For instance, Borghei et al. studied several types of nanocelluloses [230], as electrolyte carriers for ultra-thin quantum dot-sensitized solar cells. Owing to its rich surface functional group on the fibrillar structure, a robust network was formed which allow very efficient electrolyte filling without interference (Fig. 9b). CNC can be also considered as an optically transparent substrate [231], and these cells can be easily separated and recycled into their major components using low-energy processes at room temperature, opening the door for a truly recyclable solar cell technology [232].

Cellulose also results a suitable material to develop environmentally benign batteries. In this sense, cellulose-derived separators emerge as a plausible green solution to the disposal issues associated with traditional microporous polymer membranes. Primarily, cellulose-derived membranes have been used for alkaline batteries thanks to their inherent wettability, porosity and low density [233]. Unfortunately, the hygroscopic nature of cellulose has limited the use of cellulosic membranes in lithium ion batteries (LIBs), due to the fact that water contents lower than 20–50 ppm are needed in order to avoid lithium hexafluorophosphate ($LiPF_6$) hydrolysis and hydrofluoric acid formation [234]. Membranes obtained from the self-assembly of fibrilliform cellulosic fibres with diameters from 0.5 to 5.0 μm soaked in an aprotic solvent showed a complex impedance lower than conventional polyolefin

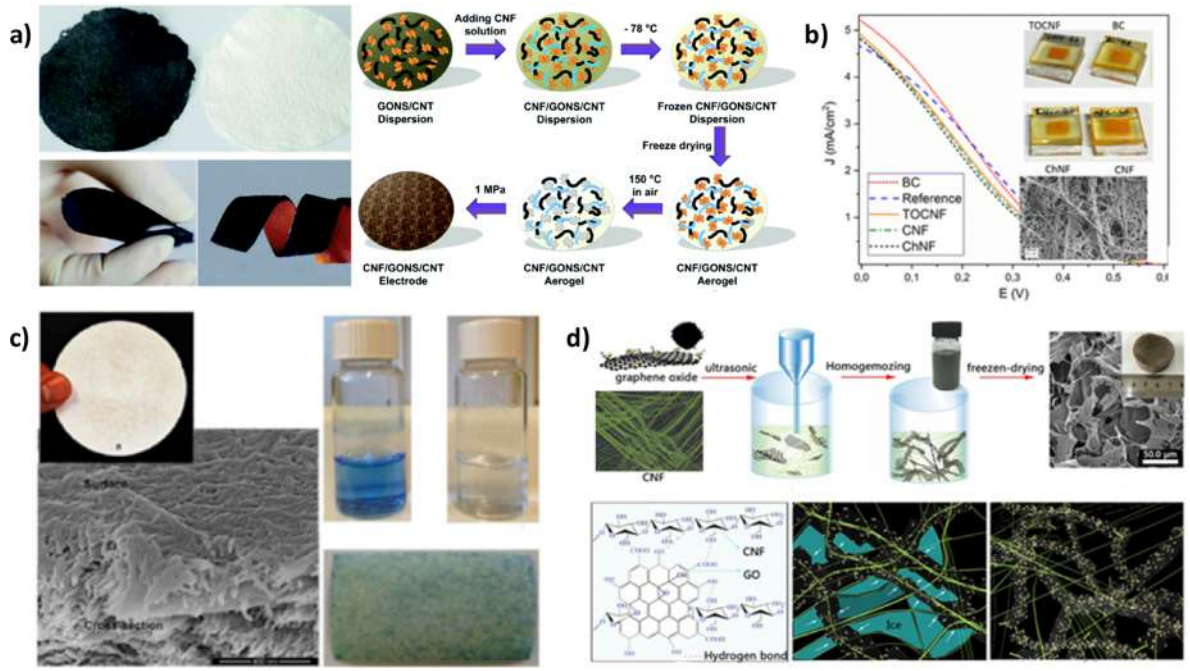

Fig. 9. (a) Photographs of the GNS/cellulose hybrid paper (black) and a pure cellulose paper (white) as a comparison (top); the bent hybrid paper, showing the flexibility of the paper (bottom left); a flexible supercapacitor made with a hybrid paper adhered to a copper foil as the electrical conductor (bottom right) and schematic diagram of the fabrication process of CNF/RGO/MWCNT electrodes. Reproduced from Ref. [228] with permission from The Royal Society of Chemistry. (b) J–V curves of CdS-sensitized QDSCs with embedded biobased aerogels compared to the reference cell with liquid polysulfide electrolyte, under 1 Sun illumination and (inset) SEM micrograph of CNF aerogel obtained after solvent exchange of hydrogel membranes with ethanol and tert-butanol followed by freeze drying. Reproduced with permission from Springer Nature from Ref. [230]. (c) Visual appearance of freeze-dried chitosan membranes and SEM images showing the CNC on the surface and bulk of the membrane. The membranes adsorbed 98% of Victoria blue 2B from water. Reproduced with permission from MDPI AG [242]. (d) Schematic showing the synthetic steps of the CNF/GO aerogel together with the CNF combined with GO through hydrogel bond, a schematic formation of the 3D structure and the 3D structure of CNF/GO. Reproduced with permission of Nature Publishing Group from Ref. [248]. (For interpretation of the references to colour in this figure legend, the reader is referred to the web version of this article.)

separators at the same time that were “pinhole-free” and kept proper mechanical properties [235]. Several works have shown that membranes composed of cellulose nanofibres display improved shrinkage resistance, thermal and mechanical performance and better cycling and rate capability in comparison with Celgard® membranes [236–238]. Recently, mesoporous membranes based of CNC have been used to develop LIB separators. Obtained three-dimensional mesoporous membranes composed of loosely packed CNC showed high ionic conductivities and specific surface areas up to 172 $m^2\ g^{-1}$, providing efficient paths for Li^+ ion migration. Furthermore, results proved that such membranes could be used together with ionic liquids (ILs) as feasible electrolytes for the development of environmentally friendly separator-electrolyte systems [239]. CNC ionomer electrolyte membranes could be obtained upon lithiation of the -OSO_3H groups on the surface of the CNC to yield solid electrolyte separators with a Li^+ transference number ($t_{Li}{}^+$) of 0.93, enabling a remarkable stable and homogenous plating/stripping of lithium [240]. Additionally, CNC-membranes have also been used for energy storage devices not-based on lithium in order to seek for more sustainable alternatives. In this framework, Glatz et al. used developed aqueous zinc batteries (AZBs) and studied the use of a CNC membrane to suppress the diffusion of the novel active organic cathode, 1,4 bis(diphenylamino)benzene (BDB), into the electrolyte [11]. Results showed that the negative surface charge of CNC acts as an “electrostatic filter” retaining positively charged BDB cations on the cathode side, enabling a long-term cyclability. Overall, the use of such inexpensive and safe aqueous electrolytes makes this system a potential candidate to develop large-scale energy storage applications.

4.1.2. Separation technologies and wastewater treatment

Cellulose-based functional materials are usually applied in separation field, especially in water treatment. Biopolymers including chitosan, chitin, and lignin are known to adsorb heavy metal ions from aqueous solutions. Cellulose-based functional materials offer good adsorption capacity for the applications in water treatment fields (Fig. 9c) [227,241,242].

Nanotechnologies have been considered as having great potential for limiting costs and lightening efficiency in pollution prevention, treatment and cleanup. Two applications for cellulose nanostructures in this area that have generated interest are as active sorbent materials for contaminants and as stabilizers for other active particles [243].

Bovine serum albumin-protected gold nanoclusters (Au@BSA NCs) incorporated into CNC-based hydrogel beads are emerged as an ideal solution for the *in situ* monitoring and purification of contaminated water, and their low detection limit makes them readily

implementable [209,244].

Cellulose nanomaterials, with their easily functionalizable surface, allows for the integration of chemical moieties that may increase the binding efficiency of pollutants to the nanocellulose. Carboxylation is the most studied methodology for enhancing their sorptive capacity. Yu et al. found that the incorporation of succinic acid groups onto CNC significantly increased the binding efficiency to Pb^{2+} and Cd^{2+} from aqueous solutions [245]. The sorption of organic contaminants has also been demonstrated with modified matrices [246]. In addition, membrane studies have demonstrated that hydrophobic surfaces improve protein adsorption, which often leads to biofouling and membrane inactivation. In hybrid systems, Zhu et al. exploited the potential of the nanoscale morphology [247], impressive adsorption capability and network formation of (TEMPO)-mediated oxidized cellulose nanofibres (TOCNF), and the functionality of graphene oxide (GO) to develop new materials for water purification, validating the potential use of the biohybrid as freestanding membranes for water purification.

A similar approach was considered by Yao et al. [248], that demonstrated how cellulose nanofibril/graphene oxide hybrid (CNF/GO) aerogel, fabricated via a one-step ultrasonication method, could show removal percentages (R%) for antibiotics up to 69%. Furthermore, the regenerated aerogels still could be repeatedly used after ten cycles without obvious degradation of adsorption performance (Fig. 9d).

Yang and Cranston prepared chemically cross-linked CNC aerogels based on cross-linking of hydrazide and aldehyde-functionalized CNC [98]. The resulting aerogels were ultra-lightweight (5.6 mg cm^{-1}) and highly porous (99.6%) with a bimodal pore distribution (mesopores $<$ 50 nm and macropores $>$ 1 μm). The cross-linked CNC aerogels showed enhanced mechanical properties and shape recovery ability, specifically the aerogel shape recovered more than 85% after 80% compression, even after 20 compress and release cycles. The results confirmed how CNC aerogels can be used as superabsorbents and for oil/water separations and they may also find application as insulating or shock-absorbing materials. Recently, Rafieian et al. indicated that ultra-light, hydrophobic and superabsorbent materials based on silane modified cellulosic aerogels have high oil adsorption capacity, and they represent a viable alternative to commonly used absorbents in the removal of oil spills from oily waste water [249].

4.1.3. Catalytic properties

Catalysis plays a crucial role in both industry and science as it provides efficient platforms to trigger a wide variety of chemical reactions. For example, catalysis could be used either to produce materials such as polymers or to serve for environmental remediation purposes by degrading pollutant molecules. The decomposition of organic pollutants from water provides means for the reduction of the extensive pollutant accumulation (i.e. antibiotics, pesticides…) in water reservoirs [250,251], which represents a global challenge for the 21st century.

As catalytic reactions usually take place on the surface of noble metal/non-noble metal materials, nanoscale particles are preferred as they offer larger specific surface areas with increased number reactive sites per mass unit. Unfortunately, many catalytic reactions took place using nanoparticles are dispersed in liquid media, which reduces their accessible specific surface area and difficult the recovery of catalyst particles once their function has been accomplished [252]. To address such challenge, catalytic nanoparticles can be immobilized onto different supporting materials such as cellulose [80], where surface hydroxyl groups enable a good adhesion between particles and the nanocellulose [253]. As only recently this field has gained attention, heterogeneous catalysis using CNC as supporting material is opened to novel findings.

Several CNC-supported metal nanoparticles have been synthesized so far for catalytic applications. While most of the works have been focused on the use of water-dispersed CNC [75,83], few reports exist on the use of solid CNC substrates as a template. Wu et al. showed in 2013 an interesting novel approach to synthesize catalytically-active palladium nanoparticles with size ranging from 10 to 40 nm *via* a “reagentless approach” [254]. The reported one-step environmental-friendly synthesis lies on the fact that CNC can act as both supporting matrix and reducing agents as the electron-rich nature of the hydroxyl group makes it suitable for the reduction of $PdCl_4^{2-}$. Interestingly, CNC-supported palladium nanoparticles showed an enhanced catalytic activity towards the reduction of methylene blue and 4- nitrophenol than the unsupported nanoparticles. Three years later, platinum and palladium nanoparticles (~1–2 nm) were uniformly immobilized onto melamine-formaldehyde (MF) coated CNC through MF precursor polycondensation followed by *in situ* nanoparticle reduction (see Fig. 10a) [75]. Materials having a specific surface areas up to 213 $m^2\ g^{-1}$ and mean pore diameter of 1.34 nm were obtained. A critical role of melamine-formaldehyde coating on the generation of uniform and size-controlled nanoparticles was found. Obtained materials were tested against 4-nitrophenol reduction, yielding remarkable turnover frequencies as high as 3168 h^{-1}. Very recently, Lizundia et al. showed a method for the electroless plating of platinum nanoparticles onto mesoporous cellulosic structures to obtain free-standing hybrid materials suitable for 4-nitrophenol reduction and hydrosilylation of styrene with triethylsilane [15]. Thanks to their large specific surface area, catalysis was particularly efficient using mesoporous cellulose nanocrystal films as supports. Similarly, Eisa et al. used CNC as solid supports for the nucleation and subsequent growth of silver and gold nanoparticles (6–35 and 18–25 nm respectively) using dry milling, yet solvent-free conditions [83]. The hydroxyl groups onto CNC surfaces enabled the formation of strong hydrogen bonds between cellulose and metallic nanoparticles. Hybrids were also proven efficient for 4-nitrophenol reduction, representing a step forward in the development of eco-friendly catalysts though scalable processes. Other works have also showed the ability of CNC/silver and CNC/gold for the reduction of 4-nitrophenol [82,255].

In other work, CNC/$MnFe_2O_4$ nanohybrids prepared through anchoring magnetic nanoparticles onto CNC supports through a hydrothermal approach proved efficient towards the degradation or organic dyes such as methylene blue, which is an extremely hazardous dye used in textile industry [256]. The combination of large specific surface area up to ~160 $m^2\ g^{-1}$ and low band gap of 1.64 eV contributes to the formation of a large number of hydroxyl radicals for H_2O_2, which in turn resulted in an increased catalytic activity of 60% in comparison with bare $MnFe_2O_4$. The obtained excellent recycling capacity proves those materials useful for

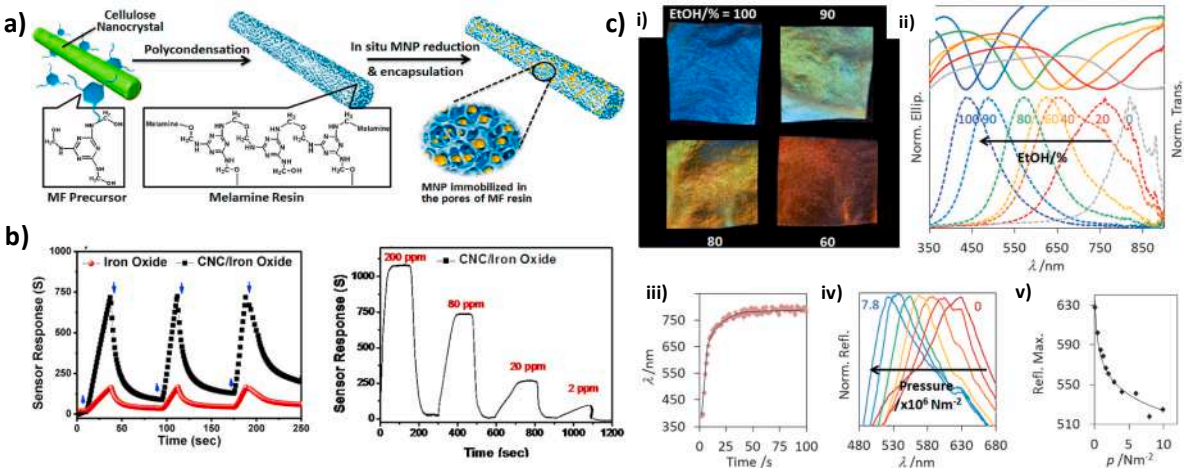

Fig. 10. (a) Scheme displaying the synthesis of CNC-supported metal nanoparticles with catalytic activity. Reproduced with permission of ACS Publications from Ref. [75]. (b) Relative resistance change upon the application of NO_2 gas at 1000 ppm on CNC/iron oxide hybrid together with the quantitative analysis for different concentrations. Reproduced with permission of Elsevier from Ref. [262]. (c) Sensing of mesoporous cellulose films displaying: (i) Photographs; (ii) UV–Vis (solid lines) and CD spectra (dashed lines) of films soaked in ethanol/water at different ratios; (iii) Swelling kinetics in water of films and the corresponding wavelengths change. (iv) Response of mesoporous films at applied pressures of 0, 0.4, 0.8, 1.6, 2.7, 5.9, and 7.8 × 10^6 N m^2 and (v) Plot of peak reflection wavelength versus pressure. Reproduced with permission of John Wiley & Sons Ltd from Ref. [74].

wastewater remediation, where natural sunlight exposure is only required.

Very recently Lizundia et al. reported the use of mesoporous CNC membrane as a substrate for metallic nanoparticle reduction in order to provide additional surface for the reduction of platinum nanoparticles [15]. Such highly porous cellulose framework coated with catalytically active platinum nanoparticles was proven effective to decompose organic pollutants from water (4-nitrophenol reduction) and hydrosilylation reactions. The combination of the high hydrophilicity, structural stability and high specific surface area provided by the cellulosic network together with the effective catalytic activity of platinum nanoparticles gives a hybrid material with remarkable turnover frequencies (TOF) and styrene conversion degrees up to 99%. Therefore, such nanohybrid materials result suitable for the fabrication of multifunctional nanomaterials to satisfy requirements for practical applications.

The potential of cellulose to act as chiral inducer in enantioselective catalysis was reported by Kaushik et al. in 2015 [257]. Highly crystalline CNC were used as 2D chiral inducers as ketone reagents simultaneously interact with CNC surfaces to be preferentially oriented as a function of their prochiral properties and palladium patches successfully hydrogenate the ketones. Unprecedented high enantiomeric excess (ee) during the hydrogenation of prochiral ketones in water at room temperature and 4 bar of H_2 were obtained for palladium patches deposited onto CNC. In fact, CNC/Pd hybrids showed an ee of 65% with conversions of 100%. Obtained enantioselective catalysis has a great potential for the synthesis of pure chiral molecules in the pharmaceutical field for example.

CNC-based hybrids could also serve as substrates to covalently immobilize enzymes. In this sense, Mahmoud et al. conjugated cyclodextrin glycosyl transferase (CGTase) and alcohol oxidase onto CNC/Au hybrids with recovered specific activities of 70% (300 U mg^{-1}) and 95% (37 U mg^{-1}) respectively, proving an efficient approach to immobilize enzymes that could be later used for diverse biocatalytic reactions [258].

4.1.4. Sensing applications

Despite to the fact that CNC-derived materials and devices are readily widespread, they are commonly used in low-tech applications. Therefore, there is an increasing interest in the development of CNC-based products for advanced technologies such as sensing [259]. In this sense, CNC/GO hybrids were fabricated by simply blending the materials followed by oven drying and their application as humidity sensors was explored [260]. Thanks to the many hydrophilic functional groups in the material (hydroxyl, ether, carboxyl and carbonyl of the GO), the material provided a fast and linear capacitance change (in log scale) within the relative humidity in the 25 to 90% range. Moreover, the sensitivity was independent on the environmental temperature. Similarly, TiO_2 and MWCNTs were incorporated into a CNC matrix to develop room temperature ammonia gas sensors [261]. The hybrid material displayed a large response when the gas concentration was within 50–500 ppm, being the response and recovery times of 100 and 50 s respectively. Such result was obtained thanks to a combined effect of the modulation of the depletion layers at the TiO_2 surfaces and the interface between TiO_2 and MWCNTs by the p–n junctions of MWCNTs and TiO_2. Sadasivuni et al. reported sensitivities as good as 2 ppm of nitrogen dioxide (NO_2) gas upon the fabrication of CNC/iron oxide hybrids fabricated by hydrothermal method [262]. As shown in Fig. 10b, the relative resistance change between initial resistance and the maximum value at the end of sensing cycle (identified as the sensor response) is markedly improved with the presence of CNC in comparison with bare iron oxide. Such fast and efficient response (50 s for response and 30 s for recovery) was obtained thanks to the formation of localized depletion regions acting as charge scattering sites at the CNC-iron oxide interfaces. Moreover, the sensor response was nearly linear with respect to the

NO_2 concentration. CNC/reduced graphene oxide hybrids have also been fabricated to develop proximity sensors without physical contact through a layer-by-layer spraying method [263]. Graphene oxide was reduced onto isophorone diisocyanate (IPDI) modified CNC and the obtained capacitance changes upon the presence of a human finger interface were analyzed. The constructed optically transparent optoelectronic sensing device showed a fast response and high sensitivity, detecting human finger within distance of 6 mm. The presence of a finger interface disturbs the fringe electric field as a result of the presence of a tiny electric charge transfer from the finger, yielding to a fluctuation in the capacitance signal. Obtained materials can be applied as touch/non-touch screens in mobile phones or as human skin with low energy consumption, overruling the visible IR proximity detectors currently used. Overall, the obtained good sensitivities and repeatability together with the cost-effective character of developed materials make CNC-based hybrids good candidates to develop low power consumption and environmentally safer sensing devices.

The chelation behaviour of different metal ions has been used to develop many colourimetric/fluorescent sensors based on CNC. For example, a real-time colourimetric ammonia gas sensor based on CNC/Cu(II) was constructed by simple EISA at varying Cu(II) ion loading of 0, 25, 75, 125, 175, 225, 275 and 375 mmol g^{-1} [51]. A concomitant chelation between copper ions and negatively charged CNC and an increase of the helical pitch within the CNC (leading to a 56 nm red-shift of reflective wavelength) structure was observed in presence of ammonia gas. In this line, the photoluminescence quenching effect suffered by luminescent materials such as CDs and QDs has been exploited to develop multifunctional materials with sensing capacity. Zhang et al. fabricated CNC/CDs grafted $SrAl_2O_4$, Eu_{2+}, Dy_{3+} hybrids as effective temperature sensing materials [208]. An increase on the surrounding temperature linearly decreased the photoluminescence of the hybrid material and blue-shifts emitted light (from green to blue) due to a heat-induced quenching effect. Nguyen et al. fabricated CNC/CdS QD hybrids as optical sensors for nitroaromatic explosive 2,4,6-trinitrotoluene (TNT) [55]. It was shown that the presence of TNT solution or vapour reversibly quenches the photoluminescence of the hybrid film as a result of the occurring electron transfer mechanism from the QD donors to electron-deficient aromatic rings of TNT acceptors. In an other work, Lizundia et al. obtained free-standing luminescent CNC/CD films able to sense Fe^{3+} and Zn^{2+} ions (a luminescence increase was observed upon Zn^{2+} addition, while iron quenches their light emission) [51]. This behaviour was ascribed to the interaction of surface hydroxyl and carboxyl groups with Fe^{3+} ions, which allows a non-radiative electron transfer from the excited CDs to the *d*-orbitals of Fe^{3+} [264].

Taking into account the bioavailability of cellulose as a raw material, enabling a shift from the idea of using CNC as a mere substrate for the functional component to making it the active material becomes one of the challenges that need to be faced towards sustainability. Taking advantage of the structural colouration arising from the chiral nematic CNC, Giese et al. developed mesoporous tuneable photonic cellulose films through a new supramolecular cotemplating method for humidity and pressure sensing [74]. Mesoporous photonic cellulose (MPC) films with specific surface areas up to 252 m^2 g^{-1} were obtained via the self-assembly of lyotropic CNC in the presence of a urea formaldehyde (UF) precursor followed by alkaline treatment of the films with 15% aqueous KOH at 70 °C. Desulfation was observed as a key step as it leads to films that are not dispersible in water. Fabricated mesoporous photonic cellulose films underwent a rapid and reversible colour change upon swelling in different solvents (see Fig. 10c). MPC films displayed a rapid red shift of their reflection peak from 330 nm for the dry film to 820 nm when immersed in polar solvents, making the colour change easily observable by the naked eye. Such swelling degree was very sensitive to the solvent as the colours could be tuned from 430 nm in pure ethanol to 840 nm in pure water. Furthermore, the potential of MFC for sensing pressure was also explored. Results revealed that the macroscopically applied pressure could be transferred to the nanoscale level, leading to compression of the layers which reduces the helical pitch of the chiral nematic structure. A reversible blue shift from 630 to 520 nm on the reflected light was achieved as upon stress removal the material relaxes and returns to its initial colourless state. The structural colouration of CNC has also exploited by Zhao et al., who reported on the spin coated CNC multilayers as real-time colourimetric sensing receptors for H_2O, $NH_3{\cdot}H_2O$, acetic acid (HAc) and hydrochloric acid (HCl) vapours [265]. Overall, the reflective wavelength of CNC coatings was red-shifted due to the enlargement of CNC inter-layer distance as a result of the occurring hydrogen bonding, charge repulsion and ionic affinity interactions at the CNC-layer interface upon the exposure of vapours. In this sense, HAc vapour showed the largest sensing transition of wavelength (nearly 120 nm shift), which was ascribed to the synergetic effects of steric space and repulsion between anionic acetate and the negatively charged CNC. The obtained naked-eyed qualitative detectability of vapours by CNC could open new avenues on the development of naked-eye chemical sensors based on renewable materials.

Although is not within the scope of this review, fluorescent labelling of CNC with dyes is a growing area of research useful in areas as varied as bioimaging or metal ion detection worthy of mention. In this field, Nielsen et al. modified CNC with via a thiol-ene click reaction in order to obtain pH-sensing materials. Succinimidyl ester dyes were grafted onto CNC and their photoluminescence in the pH range of 2.6–8.5 was measured [266]. A straightforward synthetic method for the covalent attachment of a pH-sensitive dye onto CNC was reported by Chauhan et al. who using a one-step procedure attached a Remazol dyes after the reaction with the hydroxyl group onto CNC surface through a vinylsulfone reactive linker [267]. The colour of the biosensors changed from yellow to pink depending on the environment pH. Wu et al. obtained fluorescent CNC through the conjugation of a 1,8-naphtalimide dye onto TEMPO-oxidized CNC [268]. Interestingly, the CNC/dye hybrid showed increased fluorescence sensitivity to solvent polarity and ion concentration in comparison with pure dye. Overall, the light emission of CNC/dye hybrid is markedly increased when reducing solvent permittivity or increasing ionic strength. Obtained hybrid materials showed good responsiveness to solvent polarity and ionic strength, making them potential candidates for nanosensor applications.

4.2. Biomedical applications

Specially and innovative designed biomaterials that control environmental conditions and modulate cell functions through cell adhesion, proliferation, migration and differentiation control, represent the future of the regenerative medicine [269–271]. The

engineering of an adequate interactive biomaterial surface for cell-contact is one of the most critical part in the development of new material for biomedical applications. The interface is the main part in the regulation of both *in vitro* and in vivo performance of biomaterials developed for the different biomedical applications.

The fate of all biomedical applications are governed by the specific cellular responses to the biomaterial characteristics; cell/biomaterial interactions are firstly correlated to the material's surface properties, such as wettability, topography, chemistry, surface charge and the presence of hydrophobic and hydrophilic character [272], that also contributes to the biocompatibility and mechanical properties of the biomedical device. According to their properties CNC are ideal candidate to engineer and develop new biomaterials for the biomedical fields [5,9,273,274].

An extensive number of scientific literature deals in this field, but there is a substantial amount of work that still remains to be done before realizing the full therapeutic potential of CNC and CNC based nanohybrids. Until now the scientists have not well correlated the material results with the biological mechanism. Studies should be focused on detailed *in vitro* and *in vivo* analysis of modified CNC constructs in order to better understand the integration of CNC and CNC based nanohybrids in the biological entities.

Cellulose in the form of sponges or fabrics have been previously investigated as a potential scaffold material for tissue engineering as it is biocompatible and it has tuneable chemical and mechanical properties [275–278]. Nowadays, additive manufacturing technologies of CNC combined with other biomedical materials is being studied and performed as an important viable and important route to future regenerative therapy [279].

With regard to *in vivo* applications, it is worth reminding that nanocellulose is a biodurable material; cells are not able to synthesize cellulases, hence they cannot induce a resorption of CNC. [276]. However, the chemical/physical modification and/or crosslinking of water-soluble cellulosics with bioresorbable moieties can modify this properties, and permit to develop resorbable nanocellulose-based devices [280,281]. Modulesky et al. demonstrated that the mammalian cell lines were able to proliferate and remain viable in the 3D cellulose scaffold *in vitro*, achieving cell densities similar to other synthetic and natural biomaterials [275].

4.2.1. Nanotoxicity

Before describing and analyzing the specific biomedical applications of the cellulose nanocrystals hybrid systems, a brief discussion of the biological and toxicity properties of CNC and CNC nanohybrids both *in vitro* and *in vivo* have to be presented. The CNC developing methods are correlated to the resulting nanotoxicity from the cellular to organism level. A common concern among researchers is the oral, pulmonary and dermal toxicity of CNC. Roman reviewed extensively this topic and apparently, no toxicity was demonstrated upon dermal and oral administration of CNC [282]. However, inconsistent results were reported for CNC pulmonary administration, since the conclusion was that further studies needed to evaluate the possible side effects upon ingestion or skin contact with CNC. Another important point is the quantification of the toxic dose for human exposure, in particular by skin and inhalation routes. Different aspects are considered to influence the toxicity of CNC, as: (i) diameter, length and morphology, (ii) crystallinity degree, (iii) surface chemistry, and (iv) colloidal stability. Furthermore, new and standardized protocols are fundamental, in order to establish facile and reliable evaluation of the size and surface chemistry of the nanoparticles, with the aim to provide a realistic comparison between different studies. *In vitro* cytotoxicity studies of CNC were tested by using different cell lines, the results were correlated to the concentration, showing no cytotoxic effects at a low concentration range (50 mg mL^{-1}), whereas CNC induced cell death and changes in the gene expression of mammalian cells at concentrations higher than 100 mg mL^{-1}) [87,283].

Size- and dose-dependent toxicity of cellulose nanocrystals on human fibroblasts and colon adenocarcinoma were studied by Hanif et al [284]. They synthesized four cellulose nanocrystals with different mean sizes (from 108 to 1174 nm) and shapes through acid hydrolysis of microcrystalline cellulose and investigated the toxicity effects of size and concentration against two different cell lines: NIH3T3 murine embryo-fibroblasts and HCT116 colon adeno-carcinoma. Biological results showed that none of the four CNC of varying size presented any substantial cytotoxicity against either cell line at various concentrations, ranging from 10 μg mL^{-1} to 250 μg mL^{-1}.

As the surface charge of CNC plays an important role in cellular uptake and cytotoxicity, the surface functionalization of the CNC was also investigated. Two fluorescent cellulose nanocrystals, CNC-rhodamine B isothiocyanate (RBITC) and CNC-fluorescein isothiocyanate (FITC), were investigated analyzing their ability to penetrate the membrane of two different cell lines. Covalent conjugation, as opposed to physical encapsulation, obviates the possibility of fluorophores being leached out from the nanoparticles in physiological milieu. Results showed that functionalized CNC have the ability to penetrate cells, with no indication of cytotoxicity. The surface charge of CNC could be modulated in order to favour the penetration inside the cell without causing cellular damage. In particolar CNC-RBITC was uptaken by human embryonic kidney 293 (HEK 293) and Spodoptera frugiperda (Sf9) cells without sign of the cell membrane damages, while no significant internalization of CNC-FITC was observed [285]. Another important aspect to be considered of the CNC is their genotoxic potential in human bronchial epithelial cells, since CNC may be inhaled in an aerosolized form during various stages of their life-cycle. Catalane et al. investigated whether exposure to CNC has genotoxic effects and results were compared with a commercially available non-nanoscale microcrystalline cellulose. Neither CNC (nanoscale) nor MCC (non-nanoscale) exhibited primary genotoxicity in human bronchial epithelial cells under the conditions tested [286].

In vivo studies were also performed and a comparison of pulmonary outcomes caused by exposure of specific pathogen-free adult female C57BL/6 mice to two different processed forms of CNC derived from wood was performed, in order to evaluate whether differently processed forms of CNC (solid flake/powder, liquid, gel) derived from the same source could cause distinct pulmonary toxicity in mice. The data clearly show that CNC, derived from wood pulp, elicit dose-dependent oxidative stress, tissue damage, and robust inflammatory responses in the lungs. However these responses varied significantly depending on the type of CNC material investigated: suspension (CNC) *vs.* freeze-dried powder form (CNCP). Compared to CNCP, greater increases in oxidative stress

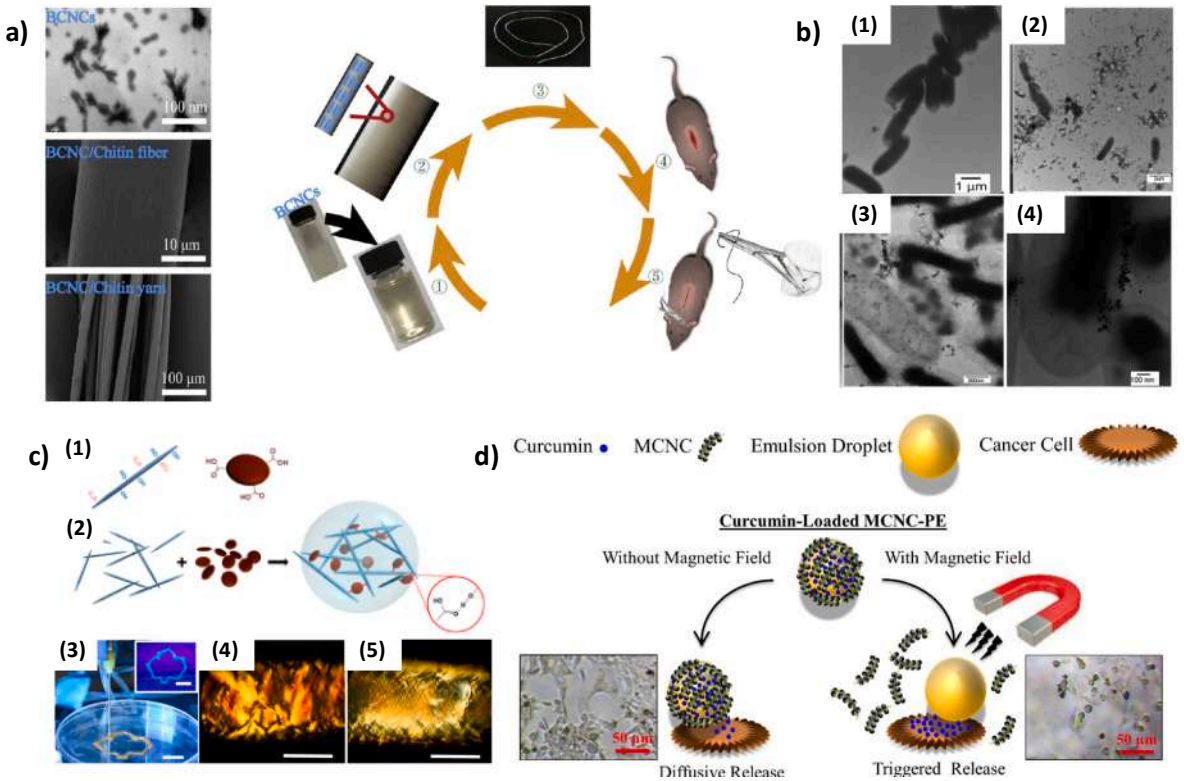

Fig. 11. Examples of biomedical applications of CNC nanonybrid systems. (a) Sutures: TEM image of BCNC, SEM images of BCNC/chitin fibre, SEM images of BCNC/chitin and analysis of the process of suture preparation and wound closure: (1) BCNC/Chitin solution, (2) BCNC/regenerated chitin filament, (3) Yarns made form filaments, (4) Mouse with an incisional dorsal skin wound and (5) Wound closed with sutures. Reproduced with permission of Elsevier from Ref. [319]. (b) Antibacterial properties: TEM images of (1) E. coli, (2) E. coli mixed with the AgNPs after 24 h, (3) E. coli mixed with the AgNPs-PD-CNC after 24 h and (4) AgNPs attached on the surface of E. coli at high magnification. Reproduced from Ref. [308] with permission from The Royal Society of Chemistry. (c) Hydrogels: Scheme showing the formation of the CNC-GQD hydrogel: (1) Building blocks of the hydrogel showing a CNC carrying surface hydroxyl and half-ester sulfate groups (left) and a GQD carrying surface edge carboxylic groups (right), (2) hydrogel formation upon mixing of the suspension of CNC and GQDs. The inset shows the formation of the hydrogen bond between the carboxyl groups of GQDs and the hydroxyl groups of CNC, (3) 3D printing of the CNC-GQD hydrogel (scale bar is 1 cm). Inset: Optical fluorescence microscopy image of the hydrogel thread at λ_{exc} = 365 nm. The scale bar is 1 cm. (4) Polarized optical microscopy image of the hydrogel thread (scale bar 1 mm) and (5) the dry thread (scale bar 1 mm). Reproduced with permission of ACS Publications from Ref. [91]. (d) Drug delivery: scheme showing the curcumin loaded magnetic cellulose nanocrystal stabilized Pickering emulsions and of the role of the external magnetic field application. Reproduced with permission of Elsevier from Ref. [323].

markers and inflammatory mediators were found in mice exposed to CNC. Finally, even slight modifications in the production of CNC materials can result in distinct respiratory responses [287].

CNC nanohybrids combined with different kind of organic or inorganic nanoparticles could integrate their individual advantages for multifunctional applications in biomedical field. However the toxicological aspects of these new and innovative biomaterials have to be elucidated, and they can be correlated to many different factors: chemical properties of individual nanomaterials, physical and chemical properties of the obtained nanohybrids and process technology. In the case of CNC/nanostructured carbon, negligible cytotoxicity was observed in the case of fullerene [288], graphene or CNTs based CNC nanohybrids [289,290]. A low cytotoxicity was detected also in the case of developed nanohybrids combined with gold nanoparticles. The cell viability of the selected complexes was evaluated in human embryonic kidney 293 (HEK 293) and rat glioma (C6) cells employing MTT assay, with a decrease in cell viability with the weight content, with a dose dependent behaviour [291].

In the following sections a detailed analysis of the recent developments in the use of unmodified and modified CNC as versatile nanoplatforms in developing nanohybrid materials, for emerging biomedical applications such as antimicrobial activity, wound dressing, sutures, drug delivery and cancer therapy systems, injectable materials, tissue engineering, and *in vivo* and *in vitro* results, are highlighted [274,292,293] (Fig. 11).

4.2.2. Tissue engineering

The designing and fabrication of a suitable scaffolding system able to comply with the composition and micro/nanostructure of the native selected tissues is very important for proper guiding of cell adhesion, proliferation, and differentiation for the regeneration of new tissues. Another important area of innovative and exciting potential for nanocellulose material use is tissue engineering

[274,294]. Thanks to the unique 3D network formed by cellulose and its mechanical properties and potential biocompatibility, cellulose is an ideal material candidate for a variety of tissue engineering applications. This model requires scaffolds with the ability to temporary substitute real tissue, and balance mechanical performance, mass transport, and encourages tissue regeneration.

One of the main problems related to the use of CNC in combination with other nanomaterials is their high hydrophilicity and strong tendency to form aggregates in hydrophobic media. Chemical modification may be employed to alter surface chemistry, allowing cell attachment [295]. Scaffolds developed from cellulose can range from hard materials blended with hydroxyapatite [296], to soft hydrogels [297], as well as variably crosslinked materials [298]. The main idea is that changes in the elastic modulus of the scaffolds can affect how cells respond and spread on the surface through mechanotransduction mechanism [299].

The scientific biomedical community has begun to exploit the hydrophilic qualities of cellulose in the development of hydrogels. They are appealing for the design of smart devices, and in particular they are widely explored as promising biomaterial candidates for cell scaffolds and drug delivery vehicles due to their high water content, tuneable porosity, good biocompatibility in a range of biological environments, and generally facile chemical tailorability [219,227,276,280,281,300].

Kumar et al. have effectively synthesized cellulose nanocrystals-reinforced double-network system through quaternary-interaction based on polyacrylamide/sodium alginate/silica glass hybrid, that showed good compressive stiffness, high porosity and an interconnected pore structure [301]. CNC have been used in the hydrogel scaffolds, in order to improve their mechanical performance, since hydrogel or injectable hydrogels applications are often limited by a relatively low elastic modulus. CNC were usually incorporated in the range of 2.5–10.0 wt% and it was demonstrated to improve the hydrogel properties, in particular mechanical performance, *in vitro* degradation stability, thermal stability, and yielded good *in vitro* osteoblastic cell adhesion and proliferation onto the nanohybrid hydrogels, without affecting their apatite-forming ability (bioactivity) in the simulated body fluid. Researchers found that the obtained hybrid hydrogels exhibit strong potential for further *in vivo* characterization for bone tissue engineering applications [301,302].

Several investigators have suggested the use of cellulose nanostructures in the development of support scaffolds for tissue or bone regeneration [303,304]. The function of these scaffolds is to provide not only a surface for cell growth, but also the mechanical and structural support needed for the original tissue while the new tissue is formed. Pooyan, Tannenbaum, and Garmestani used cellulose acetate propionate and CNC to develop 3D biomaterials for vascular tissue engineering applications [305]. The obtained biomaterial showed excellent mechanical properties when tested in the physiological conditions. These results were correlated to the CNC dispersion in the polymer matrix which permitted obtaining the mechanical stability of the rigid interconnected percolation network within the polymer matrix. Khabibullin et al. developed fluorescent hydrogel based on CNC and graphene quantum dots (GQD), which are used as a cross-linking agent for CNC. Due to the dominant role of hydrogen bonding and hydrophobic interactions between CNC and GQDs, nanofibrillar hydrogels were formed with fluorescence, and birefringence properties. The storage modulus of the hydrogel was tuned from ~50 to ~260 Pa by varying the hydrogel composition. Using 3D printing technology the authors showed the application of this hydrogel as an injectable material (Fig. 11c) [91].

Chen et al. developed a new hydroxyapatite/CNC/silk fibroin scaffold by mixing a solution of silk with hydroxyapatite and CNC nanoparticles, by freeze-drying process [273]. The thermostability and mechanical properties of the scaffolds were significantly better than those of either individual or binary component scaffolds. Additionally, the nanohybrid scaffold exhibited excellent biocompatibility and superior osteoconductivity. Hence, the efficiency of the ternary scaffold was analysed for bone regeneration in the rat calvarial defect model. The results underlined that new-formed bone was revealed after 12 weeks of implantation, and the degradation kinetic of the scaffold was adequate to the bone regeneration rate. Therefore, the new hydroxyapatite/CNC/silk fibroin scaffold is considered to be a strong candidate for the repair of bone defects in bone tissue engineering. The *in vivo* results showed that this scaffold possessed better osteoinductivity, which may have resulted from its promotion of cell proliferation and osteogenic differentiation, and thereby effectively enhanced new bone formation *in vivo* [306].

4.2.3. Antibacterial applications

The use of antibacterial agents is necessary to prevent the microorganism growth and reduce the harmful effects in our life at the same time. Today, inorganic antimicrobial agents are promising such as metal salts, nano-sized metals and metal oxides are promising materials. Metal oxides such as CuO, TiO_2, ZnO, AgO, and Fe_2O_3 are frequently-used as antibacterial agents [307]. CNC extracted from many sources were used to develop nanobiomaterials with antibacterial performance alone or in combination with silver nanoparticles [308]. Singla et al. developed an innovative *in situ* approach for the formation of silver nanoparticles (AgNPs) and their simultaneous impregnation into CNC matrix extracted from Bamboo plants [309]. Results showed a significantly *in vivo* enhancement of skin tissue repair, while a decreasing production of inflammatory cytokines. At the same time the increase fibroblast proliferation, angiogenesis, and finally tissue neo-epithelization and regeneration in less than 14 days by favouring collagen deposition was observed.

Dopamine-modified CNC was used for *in situ* generation and anchoring of AgNPs onto CNC through the reduction of silver ions [308]. The dispersion and stability of silver nanoparticles was significantly improved by the CNC, which is an important parameter to control, since the aggregation of nanoparticles has been shown to reduce the activity of nanomaterials which yield to inferior performance. The high stability of the developed AgNPs-CNC system displayed antimicrobial activity that is four times better than the free AgNP against both Gram-positive and Gram-negative bacteria. In particular TEM analyses (Fig. 11b) indicated that AgNPs may enter the cell and disrupt the cell membrane, while the hybrid only adheres on the surface of the cell due to the adhesive property of polydopamine. CNC was used as an alternative respect to traditional capping agents, in order to develope well-dispersed silver nanoparticles on the surface of CNC.

Many studies have focused on the design, development and antibacterial application of CNC/ZnO nanohybrids [310–313]. In

particular Yang et al. recently, successfully reported flower-like CNC/ZnO nanohybrids using a simple precipitation method, demonstrating good antimicrobial activity for Escherichia coli (E. coli), and Staphylococcus aureus (S. aureus) [312]. A new method for the synthesis of the CNC/ZnO nanohybrids was considered by Abdalkarim et al. [313]. They developed a sheet-like CNC/ZnO nanohybrids by using the hydrothermal method and various morphologies of sheet-like CNC/ZnO with good antimicrobial activity were successfully obtained, and more significantly, the developed CNC/ZnO 5.0 nanohybrid can be recycled three times [313].

Recently we studied the dispersion of metal and metal oxide nanoparticles with different size, shape and chemical characteristics in CNC films. Nanohybrids with CNC and ZnO, TiO_2, or Ag_2O have been successfully obtained through EISA in aqueous solution, showing an effective antimicrobial activity, killing both E. coli RB and S. aureus 8325-4. The antimicrobial results confirm that the incorporation of the tested nanoparticles in CNC films provide an effective antibacterial activity. The direct exposition of E. coli cells to CNC-based films containing Ag_2O or ZnO nanoparticles seems to be effective either at shorter and longer incubation times on both adherent and planktonic cells, more efficient in the case of Ag_2O, respect to ZnO. The antibacterial effect of CNC/TiO_2 was also evident, more marked at longer incubation times for adherent E. coli cells and for S. aureus cells. Interestingly, both types of cells after being in contact with CNC/TiO_2 showed higher survivability suggesting the importance of the direct contact for antibacterial activity [314].

4.2.4. Wound dressing and sutures

One of best known clinical applications of cellulose nanomaterials is as a topical material in wound healing. Burns are very complex injuries, and they cause extensive damage to skin tissue. According to the results of many studies in the field of wound healing, CNC may serve as potential candidates as antibacterial wound dressings for accelerating tissue repair and regeneration [315]. Human skin plays an important role as a physical-chemical barrier and protective layer against environmental aggressions. There are several properties that need to be satisfied in order to develop an “ideal” wound dressing product: non-toxicity and non-allergenic, to maintain a moist environment at the wound surface, have good permeability to gases, have antimicrobial activity, absorb excess exudates and toxins, promote healing preventing further inflammation.

In wound dressing CNC were also used to modulate the mechanical properties of the nano- or micro-metre fibres, alone or in combination with other natural or synthetic polymers. CNC are excellent materials for wound dressing due to their good compaction property and excellent ability to absorb exudates during the dressing process [316]. Besidesthey promote wound recovery by accelerating the contraction via accumulation of external matrix. Nanocellulose has been applied in clinical practice for dressing of deep wound, burn wound and diabetic ulcer [317].

CNC as wound dressing materials was also used in combination with natural or synthetic polymers, mainly in the fibre morphology. Electrospun chitosan fibre mats reinforced with CNC were developed and applied as wound dressing biomaterials. Medical sutures are sterile fibres that play a significant role in early wound-healing stage. The medical textile industry has diversified with new materials and innovative designs. CNC were used to develop bioresorbable fibres with strong and elastic mechanical performance, and a controllable degradation period, in order to prepare novel filaments with good biocompatibility which can meet the demands of surgical sutures.

Most of the CNC based biomaterials for biomedical applications are still on the progress at fundamental level and laboratory work. Only a few reported clinical trial studies have been performed for the *in vitro* treatment. For example, Hakkarainen et al. [318] investigated the potential of nanocellulose wound dressing in a clinical trial on burn patients. Results showed that no allergic reaction or inflammatory response was observed.

Wu et al. developed a novel filament, usable for surgical sutures with good biocompatibility and adequate mechanical performance, by introducing bacterial cellulose nanocrystals (BCNC) in order to reinforce regenerated chitin (RC) fibres to form BCNC/RC filaments (Fig. 11a). The sutures showed good biodegradability, with a rate that can be tuned by varying the concentration of BCNC in the yarn. Biomedical results showed not toxicity both *in vitro*, than *in vivo* studies. In particular *in* vivo experiments on mice demonstrated that suturing with the BCNC/RC yarn can promote wound healing without obvious adverse effects [319].

4.2.5. Drug delivery and cancer therapy

CNC is currently being explored as carriers to develop diverse drug delivery system [274,320,321], by using drugs for treating wounds or illnesses, or dyes to allow for visualizing the trajectory of carriers, as bioactive component. Burt et al. investigated the capability of pure CNC to bind water soluble antibiotics (tetracycline and doxorubicin), and the potential of cationic-CNC to bind non-ionized hydrophobic anticancer agents (docetaxel, paclitaxel and etoposide) [322]. CNC can also be used as co-stabilizer to improve the physicochemical and flow properties of polymeric excipients.

CNC-based drug carriers can be mainly divided into three aspects: microspheres, hydrogels, and membranes. Controlled delivery systems provide an innovative way to modulate bioavailability of therapeutic agents. Here, an active therapeutic is incorporated into a polymeric network structure, and the drug is released from the structure in a predefined manner. Depending on the specific application, the kinetic release can be modulated and the drug release time may be from a few hours to several months. Tong et al. developed curcumin loaded CNC film as antimicrobial drug delivery system in a diabetic wound dressing [317]. Antimicrobial tests suggest the negative effect of the released curcumin on the vitality of the bacteria, while the hair follicle regeneration was significantly improved, due to the curcumin loaded films, showing the ability of curcumin load CNC films to be used for diabetic wound healing applications.

CNC was combined with Fe_3O_4 in order to develop magnetically-triggered drug release and in vitro anti-colon cancer efficacy nanohybrid emulsion containing curcumin (CUR). The drug release rate showed that the exposure of magnetic stabilized emulsion to external magnetic field stimulated the release of bioactive. MTT assay results demonstrated that the CUR-loaded nanomaterials can

effectively inhibit the human colon cancer cell growth down to 18% in the presence of magnetic field. These results suggested that the CNC based materials could be a promising colloidal drug delivery system by using magnetic-triggered release of bioactive and therapeutics [323].

Recent work indicates that biocompatible CNC are promising in constructing gene carriers, due to their rod-shaped morphology and rich hydroxyl groups on the surface for functionalization [324,325]. Nanohybrids of CNC and gold nanoparticles could integrate their individual advantages for multifunctional applications in cancer therapy. Few works focuse on hybrids of CNC-spherical gold nanoparticles (Au NPs), where polymer brushes on the surface of CNC were employed as capping agents and/or reductants [324,326]. Hu et al. reported for the first time, hybrids of CNC and Au nanorods (NRs). Thus, it would be desirable to develop flexible strategies to straightforward fabricate hybrids of CNC and gold nanoparticles with different morphologies. Moreover, more functionality integrated into CNC-Au hybrids would be appealing for the design of new multifunctional cancer therapy device [291]. Multifunctional hetero-nanostructures of CNC-gold nanohybrids were prepared which has been wrapped with low-toxic hydroxyl-rich polycations to integrate versatile functions for effective cancer therapy. Biocompatible CNC with the superior rod-like morphology for high cellular uptake were employed as substrates to flexibly load spherical gold NPs or nanorods *via* gold-thiolate bonds, producing hetero-layered: nanohybrids of CNC-gold NPs or CNC-gold NRs. Previously researchers showed that ethanolamine (EA)-functionalized poly(glycidyl methacrylate) (PGEA) with plentiful flanking secondary amine and hydroxyl groups can produce good gene transfection efficiencies in some cell lines while exhibiting low toxicity [327]. Profound hydroxyl-rich cationic gene carrier, CD-PGEA (comprising β-cyclodextrin cores and ethanolamine-functionalized poly(glycidyl methacrylate) arms), was then assembled onto the surface of CNC-gold nanohybrids via host–guest interaction and gold-thiolate bonds, where PEG was employed as the intermediate and spacer. The resultant CNC-Au-PGEA hetero-nanostructures demonstrated outstanding performances as gene carriers. In addition, CNC-gold nanorod-PGEA comprising gold nanorods showed promising optical absorption characteristics and was validated for photoacoustic imaging and combined photothermal/gene therapy with significant antitumor influences [291]. The development of safe and effective polycationic vectors is of crucial importance for gene therapy [328].

Gonzalez-Domiguez et al. showed the possibility to use CNC as water dispersing agent for SWCNTs and applied them to the colon cancer therapy. They have developed different CNC allomorphs (I and II) by a mercerization-free method consisting only of the acid hydrolysis commonly used to produce nanocellulose from microcellulose. This kind of CNC acquired a great relevance since these nanostructures show very appealing properties and they are used these CNC as enabling enhanced dispersion behaviour in aqueous media. The CNC allomorphs differ not only in shape and morphology but also show significantly different behaviour, leading to a distinct interaction with SWCNTs enabling enhanced dispersion in aqueous media. Further biological tests of the CNC/SWCNT nanohybrids with human intestinal cells reveal that only the one with type-II CNC presents an unprecedented behaviour, with the evidence of the simultaneous effect of colon cancer killing and mitochondrial metabolism enhancement of normal cells, whereas the rest of nanomaterials tested herein display an innocuous trait [289].

5. Environmental impact

The quantification of environmental impact of a product or service, from the initial extraction of raw materials (cradle) through the end-of-life disposal (grave), is generally assessed by using a Life cycle assessment (LCA) methodology, that can be considered as a meaningful and powerful procedure to quantify cumulative environmental attributes of different nanomaterials during the development and final use stage [329,330]. Additionally, LCA can be used to guide emerging fabrication technologies toward reducing environmental impacts and can provide important insights for the large scale industrial production in the absence of industry data and analysis.

In the specific case of cellulose nanocrystals, there are many reports in the literature, that studied, even in a controversial approach, the effects of CNC production and use on climate change potential, water footprint and fossil fuel depletion [331–335], taking into consideration both laboratory and pilot scale fabrication routes [336]. The major outcomes of these studies suggest, however, that cellulose production at the nanoscale requires a number of energy demanding processes and high environmental impact materials such as acids, alternative low impact technologies such as enzymatic extraction methods have the potential to become competitive from an environmental perspective [337]. Some studies also approached the question of acid treatment, reporting on the use of recyclable acids for the hydrolysis of cellulose, making their production process more cost-effective and favourable to the environment [338] and promising economic and environmental opportunities with reduced contamination from acid wastes.

Trying to integrate the results of cellulose nanomaterials extraction with the production of hybrid materials, it is evident that nanohybrid fabrication technologies and their associated material/energy inputs have a pivot role in the overall impact assessment of these materials, being these techniques and procedures costly from the point of view of both materials and energy flows consumption. Additionally, different developing nanofabrication technologies, such as the ones related to the preparation of cellulose nanohybrids, other than being essentially already developed only at lab scale, suffer of lack in data availability, so further research in this field is needed in the development of up-scaling schemes for emerging technologies to overcome these limits [339].

The challenge of developing simple and environmentally friendly methods using solely water in mild conditions to fabricate CNC hybrids by using green synthesis conditions, facile operation and low temperature process is the main requirement now. In this sense, the choice of a renewable starting material is not sufficient to guarantee sustainability, an eco-design approach should bring towards the selection of a cheap and scalable synthetic process, perspective full-scale implementation and low impact end-of life scenarios. Some studies, on the other hand, limited their investigation only to the production stage, from cradle to gate, leaving out the use and end of life stages, mostly due to scarce availability of data regarding the potential release and fate of engineered nanomaterials into

the environment during these stages [340]. Consequently, this approach certainly prevents the valorisation of the typical augmented functionalities improved in the use stage [339], that is actually the strength point of using nanostructured materials.

As an example, CNC are promising material to prepare renewable and biodegradable electronics devices, and became a hot research topic for the development of the next generation 'green' flexible electronics [231] or, as in the case of water remediation, CNC nanohybrids functionalized tailored to specific applications, such as selective adsorption, simultaneous sensing and scavenging, have enormous potential [244], but future research should absolutely focus on development of more efficient methods (able to reduce time and energy for high-volume extraction and high-speed fabrication) and should advance in scalability.

6. Conclusions, perspective and outlook

This review discusses the most recent key developments of using CNC in the field of cellulose nanocrystal based nanohybrids, in terms of CNC properties, nanohybrid preparation by a combination of inorganic or organic nanoparticles and their applications. Due to their multifunctional character, CNC are one of the most interesting nature-based nanomaterials, offering a plethora of outstanding properties, including inherent renewability, biodegradability, commercial availability, flexibility, printability, low density, high porosity, optical transparency as well as extraordinary mechanical, thermal and physicochemical properties.

In this review CNC are analysed in combination with other nanomaterials, as metallic or metal oxide nanoparticles (ZnO, $CoFe_2O_4$, Au, Ag, etc.), carbon nanomaterials (SWCNTs, MWCNTs, fullerenes, graphene, etc.), quantum dots, nanoclays, or other bio-based nanoparticles. The role of nanoparticle type and content is investigated in detail. Furthermore, the main fabrication techniques used to obtain CNC nanohybrids are described as they represent a key aspect towards a proper nanohybrid property modulation. In particular solution casting, filtering, layer-by-layer deposition, soft- and hard-templating, nanoparticle growth onto CNC, sol-gel process, different drying techniques, electrospinning and printing techniques are described.

As discussed in this review paper, in the recent few years, CNC has been successfully conjugated with other nanomaterials for a plenty of different applications, yielding new nanohybrid materials. For example, in energy applications, CNC nanohybrids can be applied to develop supercapacitors, solar cells and batteries. Another important field of application investigated in this review deals with separation technologies and wastewater treatment. Concerning biosensing applications, we mainly focused on electrical and optical biosensing and we foresee that many of the (bio)sensors that are currently based on plastics, glasses or conventional paper platforms will be soon transferred to CNC. We expect that this generation of (bio)sensing platforms could revolutionize the conventional sensing technology. In the biomedical field challenges and future perspectives for cellulose nanocrystals stand out as an indispensable and versatile material to the future for all the practical and innovative applications in tissue engineering and wound repair.

Methods to better control the size and distribution of metal NPs in nanocellulose substrates for a desired application would be a very promising research topic that can result in the development of new functional materials. Also, the combination of diverse metal NPs in cellulosic matrices is an important but less exploited strategy to prepare multifunctional nanohybrids. As the loading limit of different NPs in the nanocellulose matrix may alter their sustainability, therefore research efforts should focus on extending their life or regenerating them thereby making them truly sustainable. In this line, the increasing research into green synthesis and the quest for new products based on CNC will minimize the use of organic solvents which can reduce the release of toxic by-products and waste streams to our environment. As increasing efforts are devoted to the development of cheap and environmentally-friendly materials that will address emerging biomedical and environmental challenges, nanocellulose-based nanohybrids could be a competitive candidate.

Although some progress has been achieved in the preparation, characterization and application of CNC or CNC based nanohybrid materials, from the scientific and technological point of views, there are still some questions to be resolved in order to improve the market.

While several reviews have been written to focus on the synthesis of these materials, little has been done to catalogue the properties and potential applications of CNC-nanohybrids. In this review, we established an up-to-date state-of-the-art in this field, with a special emphasis fabrication, functional properties and application area. We hope that this comprehensive review article will help to increase the interest in further research on the preparation of CNC, their characterization and nanotoxicological evaluation, especially considering the biomedical context.

Numerous existing products could be improved with the addition of cellulose nanomaterials. Countless new products may also be made possible with this novel nanomaterial. Novel products currently being developed in research centres around the world could develop into much larger markets for cellulose nanomaterials, but there are not adequate data to make sound estimations. However, we can conclude that the markets for nanotechnology and nanocellulose will continue to develop and evolve.

Declaration of Competing Interest

The authors declare no competing financial interest.

References

[1] Trache D, Hussin MH, Haafiz MKM, Thakur VK. Recent progress in cellulose nanocrystals: sources and production. Nanoscale 2017;9:1763–86.
[2] Klemm D, Cranston ED, Fischer D, Gama M, Kedzior SA, Kralisch D, et al. Nanocellulose as a natural source for groundbreaking applications in materials science: today's state. Mater Today 2018;21:720–48.

[3] Duran N, Paula Lemes A, B. Seabra A. Review of cellulose nanocrystals patents: preparation, composites and general applications. Recent Pat Nanotechnol 2012;6:16–28.
[4] Klemm D, Kramer F, Moritz S, Lindström T, Ankerfors M, Gray D, et al. Nanocelluloses: A new family of nature-based materials. Angew Chemie - Int Ed 2011;50:5438–66.
[5] Rescignano N, Fortunati E, Montesano S, Emiliani C, Kenny JM, Martino S, et al. PVA bio-nanocomposites: a new take-off using cellulose nanocrystals and PLGA nanoparticles. Carbohydr Polym 2014;99:47–58.
[6] Fortunati E, Mattioli S, Armentano I, Kenny JM. Spin coated cellulose nanocrystal/silver nanoparticle films. Carbohydr Polym 2014;113:394–402.
[7] Lizundia E, Maceiras A, Vilas JL, Martins P, Lanceros-Mendez S. Magnetic cellulose nanocrystal nanocomposites for the development of green functional materials. Carbohydr Polym 2017;175:425–32.
[8] Lizundia E, Nguyen T-D, Vilas JL, Hamad WY, MacLachlan MJ. Chiroptical, morphological and conducting properties of chiral nematic mesoporous cellulose/polypyrrole composite films. J Mater Chem A 2017;5:19184–94.
[9] Jorfi M, Foster EJ. Recent advances in nanocellulose for biomedical applications. J Appl Polym Sci 2015;132.
[10] Yang X, Shi K, Zhitomirsky I, Cranston ED. Cellulose nanocrystal aerogels as universal 3D lightweight substrates for supercapacitor materials. Adv Mater 2015;27:6104–9.
[11] Glatz H, Lizundia E, Pacifico F, Kundu D. An organic cathode based dual-ion aqueous zinc battery enabled by a cellulose membrane. ACS Appl Energy Mater 2019;2:1288–94.
[12] Lizundia E, Delgado-Aguilar M, Mutjé P, Fernandez E, Robles-Hernandez B, Rosario de la Fuente M, et al. Cu-coated cellulose nanopaper for green and low-cost electronics. Cellulose 2016;23:1997–2010.
[13] Chen L, Lai C, Marchewka R, Berry RM, Tam KC. Use of CdS quantum dot-functionalized cellulose nanocrystal films for anti-counterfeiting applications. Nanoscale 2016;8:13288–96.
[14] Hiratani T, Kose O, Hamad WY, MacLachlan MJ. Stable and sensitive stimuli-responsive anisotropic hydrogels for sensing ionic strength and pressure. Mater Horizons 2018;5:1076–81.
[15] Lizundia E, Jimenez M, Altorfer C, Niederberger M, Caseri W. Pt-decorated mesoporous cellulose films for catalytically active free-standing hybrid materials. Cellulose 2019;26:5513–27.
[16] Lucchini M, Lizundia E, Moser S, Niederberger M, Nystrom G. Titania-cellulose hybrid monolith for in-flow purification of water under solar illumination. ACS Appl Mater Interfaces 2018;10:29599–607.
[17] Web of Science database (accessed on June 2019).
[18] Google Patents database. https://patents.google.com/?q=“cellulose+nanocrystal”,nanocellulose, ’“cellulose+nanofi bril”,“cellulose+nanowhisker”, “nanocrystal line+cellulose”&after=19940101&clustered=false (browsed June 2019).
[19] Reid MS, Villalobos M, Cranston ED. Benchmarking cellulose nanocrystals: from the laboratory to industrial production. Langmuir 2017;33:1583–98.
[20] Foster EJ, Moon RJ, Agarwal UP, Bortner MJ, Bras J, Camarero-Espinosa S, et al. Current characterization methods for cellulose nanomaterials. Chem Soc Rev 2018;47:2609–79.
[21] https://fpinnovations.ca (browsed June 2019).
[22] Research M. Nanocrystalline Cellulose - Global Market Outlook (2017-2026).
[23] Markets M and. Nanocellulose Market by Type (Microfibrillated Cellulose, Cellulose Nanocrystals), Application (Pulp& paper, Composites & packaging, Biomedical & pharmaceuticals, Electronics & sensors), and Region (Europe, North America, APAC) - Global Forecast to 2023.
[24] Future Markets. https://www.futuremarketsinc.com/the-nanocellulose-investment-and-pricing-guide (browsed June 2019).
[25] CelluloseLab. https://nanografi.com/nanoparticles/cellulose-nanocrystal-nanocrystalline-cellulose-cnc (browsed June 2019).
[26] Dufresne A. Nanocellulose: a new ageless bionanomaterial. Mater Today 2013;16:220–7.
[27] Marchessault RH, Morehead FF, Walter NM. Liquid crystal systems from fibrillar polysaccharides. Nature 1959;184:632–3.
[28] Revol JF, Bradford H, Giasson J, Marchessault RH, Gray DG. Helicoidal self-ordering of cellulose microfibrils in aqueous suspension. Int J Biol Macromol 1992;14:170–2.
[29] Kamide K. Cellulose and Cellulose Derivatives. 2005. 1st Edition, Elsevier Science, doi:10.1016/B978-0-444-82254-3.X5000-0.
[30] Revol JF, Godbout L, Gray DG. Solid self-assembled films of cellulose with chiral nematic order and opticavly variable properties. J Pulp Pap Sci 1998;24:146–9.
[31] Nguyen TD, Sierra E, Eguiraun H, Lizundia E. Iridescent cellulose nanocrystal films: the link between structural colour and Bragg’s law. Eur J Phys 2018;39:045803.
[32] Sharma V, Crne M, Park JO, Srinivasarao M. Structural origin of circularly polarized iridescence in jeweled beetles. Science 2009;325:449–51.
[33] Nguyen TD, Hamad WY, MacLachlan MJ. Tuning the iridescence of chiral nematic cellulose nanocrystals and mesoporous silica films by substrate variation. Chem Commun 2013;49:11296–8.
[34] Schütz C, Agthe M, Fall AB, Gordeyeva K, Guccini V, Salajková M, et al. Rod packing in chiral nematic cellulose nanocrystal dispersions studied by small-angle X-ray scattering and laser diffraction. Langmuir 2015;31:6507–13.
[35] Kimura F, Kimura T, Tamura M, Hirai A, Ikuno M, Horii F. Magnetic alignment of the chiral nematic phase of a cellulose microfibril suspension. Langmuir 2005;21:2034–7.
[36] Habibi Y, Heim T, Douillard R. AC electric field-assisted assembly and alignment of cellulose nanocrystals. J Polym Sci Part B Polym Phys 2008;46:1430–6.
[37] Dong XM, Gray DG. Effect of counterions on ordered phase formation in suspensions of charged rodlike cellulose crystallites. Langmuir 1997;13:2404–9.
[38] Pan J, Hamad W, Straus SK. Parameters affecting the chiral nematic phase of nanocrystalline cellulose films. Macromolecules 2010;43:3851–8.
[39] Beck S, Bouchard J, Berry R. Controlling the reflection wavelength of iridescent solid films of nanocrystalline cellulose. Biomacromolecules 2011;12:167–72.
[40] Cheung CCY, Giese M, Kelly JA, Hamad WY, MacLachlan MJ. Iridescent chiral nematic cellulose nanocrystal/polymer composites assembled in organic solvents. ACS Macro Lett 2013;2:1016–20.
[41] Peddireddy KR, Capron I, Nicolai T, Benyahia L. Gelation kinetics and network structure of cellulose nanocrystals in aqueous solution. Biomacromolecules 2016;17:3298–304.
[42] Lewis L, Derakhshandeh M, Hatzikiriakos SG, Hamad WY, MacLachlan MJ. Hydrothermal gelation of aqueous cellulose nanocrystal suspensions. Biomacromolecules 2016;17:2747–54.
[43] Beck S, Bouchard J, Chauve G, Berry R. Controlled production of patterns in iridescent solid films of cellulose nanocrystals. Cellulose 2013;20:1401–11.
[44] Tran A, Hamad WY, MacLachlan MJ. Fabrication of cellulose nanocrystal films through differential evaporation for patterned coatings. ACS Appl Nano Mater 2018;1:3098–104.
[45] Park JH, Noh J, Schütz C, Salazar-Alvarez G, Scalia G, Bergström L, et al. Macroscopic control of helix orientation in films dried from cholesteric liquid-crystalline cellulose nanocrystal suspensions. ChemPhysChem 2014;15:1477–84.
[46] Licen M, Majaron B, Noh J, Schutz C, Bergstrom L, Lagerwall J, et al. Correlation between structural properties and iridescent colors of cellulose nanocrystalline films. Cellulose 2016;23:3601–9.
[47] Honorato-Rios C, Lehr C, Schütz C, Sanctuary R, Osipov MA, Baller J, et al. Fractionation of cellulose nanocrystals: enhancing liquid crystal ordering without promoting gelation. NPG Asia Mater 2018;10:455–65.
[48] Tran A, Hamad WY, MacLachlan MJ. Tactoid annealing improves order in self-assembled cellulose nanocrystal films with chiral nematic structures. Langmuir 2018;34:646–52.
[49] Querejeta-Fernández A, Kopera B, Prado KS, Klinkova A, Methot M, Chauve G, et al. Circular dichroism of chiral nematic films of cellulose nanocrystals loaded with plasmonic nanoparticles. ACS Nano 2015;9:10377–85.
[50] Sun J, Zhang C, Yuan Z, Ji X, Fu Y, Li H, et al. Composite films with ordered carbon nanotubes and cellulose nanocrystals. J Phys Chem C 2017;121:8976–81.
[51] Lizundia E, Nguyen TD, Vilas JL, Hamad WY, MacLachlan MJ. Chiroptical luminescent nanostructured cellulose films. Mater Chem Front 2017;1:979–87.
[52] Nguyen TD, Hamad WY, MacLachlan MJ. Near-IR-sensitive upconverting nanostructured photonic cellulose films. Adv Opt Mater 2017;5:1600514.

[53] Xu J, Nguyen TD, Xie K, Hamad WY, MacLachlan MJ. Chiral nematic porous germania and germanium/carbon films. Nanoscale 2015;7:13215–23.
[54] Schlesinger M, Giese M, Blusch LK, Hamad WY, MacLachlan MJ. Chiral nematic cellulose-gold nanoparticle composites from mesoporous photonic cellulose. Chem Commun 2015;51:530–3.
[55] Nguyen TD, Hamad WY, MacLachlan MJ. CdS quantum dots encapsulated in chiral nematic mesoporous silica: New iridescent and luminescent materials. Adv Funct Mater 2014;24:777–83.
[56] Sehaqui H, Liu A, Zhou Q, Berglund LA. Fast preparation procedure for large, flat cellulose and cellulose/inorganic nanopaper structures. Biomacromolecules 2010;11:2195–8.
[57] Henriksson M, Berglund LA, Isaksson P, Lindström T, Nishino T. Cellulose nanopaper structures of high toughness. Biomacromolecules 2008;9:1579–85.
[58] Sehaqui H, Zhou Q, Ikkala O, Berglund LA. Strong and tough cellulose nanopaper with high specific surface area and porosity. Biomacromolecules 2011;12:3638–44.
[59] Moon RJ, Martini A, Nairn J, Simonsen J, Youngblood J. Cellulose nanomaterials review: structure, properties and nanocomposites. Chem Soc Rev 2011;40:3941.
[60] Lizundia E, Urruchi A, Vilas JL, León LM. Increased functional properties and thermal stability of flexible cellulose nanocrystal/ZnO films. Carbohydr Polym 2016;136:250–8.
[61] Nan F, Nagarajan S, Chen Y, Liu P, Duan Y, Men Y, et al. Enhanced toughness and thermal stability of cellulose nanocrystal iridescent films by alkali treatment. ACS Sustain Chem Eng 2017;5:8951–8.
[62] Iler RK. Multilayers of colloidal particles. J Colloid Interface Sci 1966;21:569–94.
[63] Martin C, Barker R, Watkins EB, Dubreuil F, Cranston ED, Heux L, et al. Structural variations in hybrid all-nanoparticle gibbsite nanoplatelet/cellulose nanocrystal multilayered films. Langmuir 2017;33:7896–907.
[64] Tzeng P, Hewson DJ, Vukusic P, Eichhorn SJ, Grunlan JC. Bio-inspired iridescent layer-by-layer assembled cellulose nanocrystal Bragg stacks. J Mater Chem C 2015;3:4260–4.
[65] Xiong R, Hu K, Grant AM, Ma R, Xu W, Lu C, et al. Ultrarobust transparent cellulose nanocrystal-graphene membranes with high electrical conductivity. Adv Mater 2015;28:1501–9.
[66] Trigueiro JPC, Silva GG, Pereira FV, Lavall RL. Layer-by-layer assembled films of multi-walled carbon nanotubes with chitosan and cellulose nanocrystals. J Colloid Interface Sci 2014;432:214–20.
[67] Li L, Ma W, Higaki Y, Kamitani K, Takahara A. Organic-inorganic hybrid thin films fabricated by layer-by-layer assembly of the phosphorylated cellulose nanocrystal and imogolite nanotubes. Langmuir 2018;34:13361–7.
[68] Kresge CT, Leonowicz ME, Roth WJ, Vartuli JC, Beck JS. Ordered mesoporous molecular sieves synthesized by a liquid-crystal template mechanism. Nature 1992;359:710–2.
[69] Giese M, Blusch LK, Khan MK, MacLachlan MJ. Functional materials from cellulose-derived liquid-crystal templates. Angew Chem Int Ed Engl 2015;54:2888–910.
[70] Nguyen TD, Lizundia E, Niederberger M, Hamad WY, MacLachlan MJ. Self-assembly route to TiO_2 and TiC with a liquid crystalline order. Chem Mater 2019;31:2174–81.
[71] Shopsowitz KE, Hamad WY, MacLachlan MJ. Chiral nematic mesoporous carbon derived from nanocrystalline cellulose. Angew Chem Int Ed Engl 2011;50:10991–5.
[72] Dujardin E, Blaseby M, Mann S. Synthesis of mesoporous silica by sol–gel mineralisation of cellulose nanorod nematic suspensions. J Mater Chem 2003;13:696–9.
[73] Shopsowitz KE, Qi H, Hamad WY, Maclachlan MJ. Free-standing mesoporous silica films with tunable chiral nematic structures. Nature 2010;468:422–5.
[74] Giese M, Blusch LK, Khan MK, Hamad WY, Maclachlan MJ. Responsive mesoporous photonic cellulose films by supramolecular cotemplating. Angew Chemie – Int Ed 2014;53:8880–4.
[75] Wu X, Shi Z, Fu S, Chen J, Berry RM, Tam KC. Strategy for synthesizing porous cellulose nanocrystal supported metal nanocatalysts. ACS Sustain Chem Eng 2016;4:5929–35.
[76] Schlesinger M, Hamad WY, MacLachlan MJ. Optically tunable chiral nematic mesoporous cellulose films. Soft Matter 2015;15:4686–94.
[77] Shopsowitz KE, Kelly JA, Hamad WY, MacLachlan MJ. Biopolymer templated glass with a twist: controlling the chirality, porosity, and photonic properties of silica with cellulose nanocrystals. Adv Funct Mater 2014;24:327–38.
[78] Kelly JA, Yu M, Hamad WY, Maclachlan MJ. Large, crack-free freestanding films with chiral nematic structures. Adv Opt Mater 2013;1:295–9.
[79] Kelly JA, Giese M, Shopsowitz KE, Hamad WY, MacLachlan MJ. The development of chiral nematic mesoporous materials. Acc Chem Res 2014;47:1088–96.
[80] Moores MK and A, Audrey. Review: nanocelluloses as versatile supports for metal nanoparticles and their applications in catalysis. Green Chem 2016:622–37.
[81] Awan F, Islam MS, Ma Y, Yang C, Shi Z, Berry RM, et al. Cellulose nanocrystal-ZnO nanohybrids for controlling photocatalytic activity and UV protection in cosmetic formulation. ACS Omega 2018;3:12403–11.
[82] Yan W, Chen C, Wang L, Zhang D, Li A-J, Yao Z, et al. Facile and green synthesis of cellulose nanocrystal-supported gold nanoparticles with superior catalytic activity. Carbohydr Polym 2016;140:66–73.
[83] Eisa WH, Abdelgawad AM, Rojas OJ. Solid-state synthesis of metal nanoparticles supported on cellulose nanocrystals and their catalytic activity. ACS Sustain Chem Eng 2018;6:3974–83.
[84] Lokanathan AR, Uddin KMA, Rojas OJ, Laine J. Cellulose nanocrystal-mediated synthesis of silver nanoparticles: role of sulfate groups in nucleation phenomena. Biomacromolecules 2014;15:373–9.
[85] Annabi N, Tamayol A, Uquillas JA, Akbari M, Bertassoni LE, Cha C, et al. 25th anniversary article: rational design and applications of hydrogels in regenerative medicine. Adv Mater 2014;26:85–124.
[86] Kelly JA, Shukaliak AM, Cheung CCY, Shopsowitz KE, Hamad WY, MacLachlan MJ. Responsive photonic hydrogels based on nanocrystalline cellulose. Angew Chemie – Int Ed 2013;52:8912–6.
[87] Yang X, Bakaic E, Hoare T, Cranston ED. Injectable polysaccharide hydrogels reinforced with cellulose nanocrystals: morphology, rheology, degradation, and cytotoxicity. Biomacromolecules 2013;14:4447–55.
[88] Prince E, Alizadehgiashi M, Campbell M, Khuu N, Albulescu A, De France K, et al. Patterning of structurally anisotropic composite hydrogel sheets. Biomacromolecules 2018;19:1276–84.
[89] You J, Cao J, Zhao Y, Zhang L, Zhou J, Chen Y. Improved mechanical properties and sustained release behavior of cationic cellulose nanocrystals reinforeced cationic cellulose injectable hydrogels. Biomacromolecules 2016;17:2839–48.
[90] Shao C, Wang M, Chang H, Xu F, Yang J. A self-healing cellulose nanocrystal-poly(ethylene glycol) nanocomposite hydrogel via Diels-Alder click reaction. ACS Sustain Chem Eng 2017;5:6167–74.
[91] Khabibullin A, Alizadehgiashi M, Khuu N, Prince E, Tebbe M, Kumacheva E. Injectable shear-thinning fluorescent hydrogel formed by cellulose nanocrystals and graphene quantum dots. Langmuir 2017;33:12344–50.
[92] Ureña-Benavides EE, Ao G, Davis VA, Kitchens CL. Rheology and phase behavior of lyotropic cellulose nanocrystal suspensions. Macromolecules 2011;44:8990–8.
[93] Heath L, Thielemans W. Cellulose nanowhisker aerogels. Green Chem 2010;12:1448–53.
[94] Shafiei-Sabet S, Hamad WY, Hatzikiriakos SG. Ionic strength effects on the microstructure and shear rheology of cellulose nanocrystal suspensions. Cellulose 2014;21:3347–59.
[95] Chau M, Sriskandha SE, Pichugin D, Thérien-Aubin H, Nykypanchuk D, Chauve G, et al. Ion-mediated gelation of aqueous suspensions of cellulose nanocrystals. Biomacromolecules 2015;16:2455–62.
[96] Bertsch P, Isabettini S, Fischer P. Ion-induced hydrogel formation and nematic ordering of nanocrystalline cellulose suspensions. Biomacromolecules 2017;18:4060–6.

[97] Oechsle AL, Lewis L, Hamad WY, Hatzikiriakos SG, MacLachlan MJ. CO_2-switchable cellulose nanocrystal hydrogels. Chem Mater 2018;30:376–85.
[98] Yang X, Cranston ED. Chemically cross-linked cellulose nanocrystal aerogels with shape recovery and superabsorbent properties. Chem Mater 2014;26:6016–25.
[99] Kistler SS. Coherent expanded aerogels and jellies. Nature 1931;127:741.
[100] Pierre AC, Pajonk GM. Chemistry of aerogels and their applications. Chem Rev 2002;102:4243–65.
[101] Baetens R, Jelle BP, Gustavsen A. Aerogel insulation for building applications: a state-of-the-art review. Energy Build 2011;43:761–9.
[102] Pääkkö M, Vapaavuori J, Silvennoinen R, Kosonen H, Ankerfors M, Lindström T, et al. Long and entangled native cellulose I nanofibers allow flexible aerogels and hierarchically porous templates for functionalities. Soft Matter 2008;4:2492.
[103] De France KJ, Hoare T, Cranston ED. Review of hydrogels and aerogels containing nanocellulose. Chem Mater 2017;29:4609–31.
[104] Scherer GW. Drying gels. I. General theory. J Non Cryst Solids 1986;87:199–225.
[105] Lavoine N, Bergström L. Nanocellulose-based foams and aerogels: Processing, properties, and applications. J Mater Chem A 2017;5:16105–17.
[106] Deville S. Freeze-casting of porous biomaterials: Structure, properties and opportunities. Materials 2010;3:1913–27.
[107] Munier P, Gordeyeva K, Bergström L, Fall AB. Directional freezing of nanocellulose dispersions aligns the rod-like particles and produces low-density and robust particle networks. Biomacromolecules 2016;17:1875–81.
[108] Dash R, Li Y, Ragauskas AJ. Cellulose nanowhisker foams by freeze casting. Carbohydr Polym 2012;88:789–92.
[109] Mueller S, Sapkota J, Nicharat A, Zimmermann T, Tingaut P, Weder C, et al. Influence of the nanofiber dimensions on the properties of nanocellulose/poly(vinyl alcohol) aerogels. J Appl Polym Sci 2015;132.
[110] Eyley S, Thielemans W. Imidazolium grafted cellulose nanocrystals for ion exchange applications. Chem Commun 2011;47:4177–9.
[111] Tingaut P, Zimmermann T, Sèbe G. Cellulose nanocrystals and microfibrillated cellulose as building blocks for the design of hierarchical functional materials. J Mater Chem 2012;22:20105–11.
[112] Rosilo H, Kontturi E, Seitsonen J, Kolehmainen E, Ikkala O. Transition to reinforced state by percolating domains of intercalated brush-modified cellulose nanocrystals and poly(butadiene) in cross-linked composites based on thiol-ene click chemistry. Biomacromolecules 2013;14:1547–54.
[113] Shi K, Yang X, Cranston ED, Zhitomirsky I. Efficient lightweight supercapacitor with compression stability. Adv Funct Mater 2016;26:6437–45.
[114] Zhu G, Xu H, Dufresne A, Lin N. High-adsorption, self-extinguishing, thermal, and acoustic-resistance aerogels based on organic and inorganic waste valorization from cellulose nanocrystals and red mud. ACS Sustain Chem Eng 2018;6:7168–80.
[115] Zhu H, Yang X, Cranston ED, Zhu S. Flexible and porous nanocellulose aerogels with high loadings of metal–organic-framework particles for separations applications. Adv Mater 2016;28:7652–7.
[116] Xu YT, Dai Y, Nguyen TD, Hamad WY, MacLachlan MJ. Aerogel materials with periodic structures imprinted with cellulose nanocrystals. Nanoscale 2018;10:3805–12.
[117] Nguyen TD, Hamad WY, MacLachlan MJ. Aerogel templating on functionalized fibers of nanocellulose networks. Mater Chem Front 2018;2:1655–63.
[118] Reneker DH, Yarin AL. Electrospinning jets and polymer nanofibers. Polymer 2008;49:2387–425.
[119] Ahmed FE, Lalia BS, Hashaikeh R. A review on electrospinning for membrane fabrication: challenges and applications. Desalination 2015;356:15–30.
[120] Zhou C, Chu R, Wu R, Wu Q. Electrospun polyethylene oxide/cellulose nanocrystal composite nanofibrous mats with homogeneous and heterogeneous microstructures. Biomacromolecules 2011;12:2617–25.
[121] Ni X, Cheng W, Huan S, Wang D, Han G. Electrospun cellulose nanocrystals/poly(methyl methacrylate) composite nanofibers: morphology, thermal and mechanical properties. Carbohydr Polym 2019;206:29–37.
[122] Murphy SV, Atala A. 3D bioprinting of tissues and organs. Nat Biotechnol 2014;32:773–85.
[123] Studart AR. Additive manufacturing of biologically-inspired materials. Chem Soc Rev 2016;45:359–76.
[124] Compton BG, Lewis JA. 3D-printing of lightweight cellular composites. Adv Mater 2014;26:5930–5.
[125] Schaffner M, Rühs PA, Coulter F, Kilcher S, Studart AR. 3D printing of bacteria into functional complex materials. Sci Adv 2017;3:eaao6804.
[126] Sultan S, Mathew AP. 3D printed scaffolds with gradient porosity based on a cellulose nanocrystal hydrogel. Nanoscale 2018;10:4421–31.
[127] Markstedt K, Mantas A, Tournier I, Martínez Ávila H, Hägg D, Gatenholm P. 3D bioprinting human chondrocytes with nanocellulose-alginate bioink for cartilage tissue engineering applications. Biomacromolecules 2015;16:1489–96.
[128] Martínez Ávila H, Schwarz S, Rotter N, Gatenholm P. 3D bioprinting of human chondrocyte-laden nanocellulose hydrogels for patient-specific auricular cartilage regeneration. Bioprinting 2016;1–2:22–35.
[129] Sydney Gladman A, Matsumoto EA, Nuzzo RG, Mahadevan L, Lewis JA. Biomimetic 4D printing. Nat Mater 2016;15:413–8.
[130] Li VCF, Dunn CK, Zhang Z, Deng Y, Qi HJ. Direct ink write (DIW) 3D printed cellulose nanocrystal aerogel structures. Sci Rep 2017;7:8018.
[131] Wang B, Benitez AJ, Lossada F, Merindol R, Walther A. Bioinspired mechanical gradients in cellulose nanofibril/polymer nanopapers. Angew Chemie – Int Ed 2016;55:5966–70.
[132] Håkansson KMO, Fall AB, Lundell F, Yu S, Krywka C, Roth SV, et al. Hydrodynamic alignment and assembly of nanofibrils resulting in strong cellulose filaments. Nat Commun 2014;5:4018.
[133] Hausmann MK, Rühs PA, Siqueira G, Läuger J, Libanori R, Zimmermann T, et al. Dynamics of cellulose nanocrystal alignment during 3D printing. ACS Nano 2018;12:6926–37.
[134] Yano H, Sasaki S, Shams MI, Abe K, Date T. Wood pulp-based optically transparent film: a paradigm from nanofibers to nanostructured fibers. Adv Opt Mater 2014;2:231–4.
[135] Siqueira G, Kokkinis D, Libanori R, Hausmann MK, Gladman AS, Neels A, et al. Cellulose nanocrystal inks for 3D printing of textured cellular architectures. Adv Funct Mater 2017;27:1604619.
[136] Zhao TH, Parker RM, Williams CA, Lim KTP, Frka-Petesic B, Vignolini S. Printing of responsive photonic cellulose nanocrystal microfilm arrays. Adv Funct Mater 2018:1804531.
[137] Guidetti G, Atifi S, Vignolini S, Hamad WY. Flexible photonic cellulose nanocrystal films. Adv Mater 2016;28:10042–7.
[138] Yao K, Meng Q, Bulone V, Zhou Q. Flexible and responsive chiral nematic cellulose nanocrystal/poly(ethylene glycol) composite films with uniform and tunable structural color. Adv Mater 2017;29:1701323.
[139] Filson P, Dawson-Andoh BE, Schwegler-Berry D. Enzymatic-mediated production of cellulose nanocrystals from recycled pulp. Green Chem 2009;11:1808–14.
[140] Beck-Candanedo S, Roman M, Gray DG. Effect of reaction conditions on the properties and behavior of wood cellulose nanocrystal suspensions. Biomacromolecules 2005;6:1048–54.
[141] Habibi Y, Lucia LA, Rojas OJ. Cellulose nanocrystals: chemistry, self-assembly, and applications. Chem Rev 2010;110:3479–500.
[142] Nishiyama Y, Langan P, Chanzy H. Crystal structure and hydrogen-bonding system in cellulose Iβ from synchrotron X-ray and neutron fiber diffraction. J Am Chem Soc 2002;124:9074–82.
[143] Lin N, Dufresne A. Surface chemistry, morphological analysis and properties of cellulose nanocrystals with gradiented sulfation degrees. Nanoscale 2014;6:5384–93.
[144] Hamad WY, Hu TQ. Structure-process-yield interrelations in nanocrystalline cellulose extraction. Can J Chem Eng 2010;88:392–402.
[145] Gu J, Catchmark JM, Kaiser EQ, Archibald DD. Quantification of cellulose nanowhiskers sulfate esterification levels. Carbohydr Polym 2013;92:1809–16. https://doi.org/10.1016/j.carbpol.2012.10.078.
[146] Lizundia E, Meaurio E, Vilas JL. Chapter 3 – Grafting of Cellulose Nanocrystals. Multifunct. Polym. Nanocomposites Based Cellul. Reinf., 2016, 61–113.
[147] Nishino T, Matsuda I, Hirao K. All-cellulose composite. Macromolecules 2004;37:7683–7.
[148] Lee T-W, Lee S-E, Jeong YG. Highly effective electromagnetic interference shielding materials based on silver nanowire/cellulose papers. ACS Appl Mater Interfaces 2016;8:13123–32.
[149] Diaz JA, Ye Z, Wu X, Moore AL, Moon RJ, Martini A, et al. Thermal conductivity in nanostructured films: from single cellulose nanocrystals to bulk films. Biomacromolecules 2014;15:4096–101.

[150] Lizundia E, Oleaga A, Salazar A, Sarasua JR. Nano- and microstructural effects on thermal properties of poly (l-lactide)/multi-wall carbon nanotube composites. Polymer 2012;53:2412–21.
[151] Csoka L, Hoeger IC, Rojas OJ, Peszlen I, Pawlak JJ, Peralta PN. Piezoelectric effect of cellulose nanocrystals thin films. ACS Macro Lett 2012;1:867–70.
[152] Schütz C, Van Rie J, Eyley S, Gençer A, van Gorp H, Rosenfeldt S, et al. Effect of source on the properties and behavior of cellulose nanocrystal suspensions. ACS Sustain Chem Eng 2018;6:8317–24.
[153] Puglia D, Fortunati E, Santulli C, Kenny JM. Multifunctional ternary polymeric nanocomposites based on cellulosic nanoreinforcements. Nanocellulose Polym Nanocompos Fundam Appl 2014:163–98.
[154] Shuttleworth PS, Matharu A, Clark JH. Polysaccharide-bsed porous materials. Polysacch Build Blocks A Sustain Approach Dev Renew Biomater 2012:271–85.
[155] Pinto RJB. Composites of cellulose and metal nanoparticles. In: Neves MC, editor., Rijeka: IntechOpen; 2012, p. Ch. 4.
[156] Van Rie J, Thielemans W. Cellulose-gold nanoparticle hybrid materials. Nanoscale 2017;9:8525–54.
[157] Majoinen J, Hassinen J, Haataja JS, Rekola HT, Kontturi E, Kostiainen MA, et al. Chiral plasmonics using twisting along cellulose nanocrystals as a template for gold nanoparticles. Adv Mater 2016;28:5262–7.
[158] Chu G, Yin H, Jiang H, Qu D, Shi Y, Ding D, et al. Ultrafast optical modulation of rationally engineered photonic-plasmonic coupling in self-assembled nanocrystalline cellulose/silver hybrid material. J Phys Chem C 2016;120:27541–7.
[159] Chu G, Wang X, Yin H, Shi Y, Jiang H, Chen T, et al. Free-standing pptically switchable chiral plasmonic photonic crystal based on self-assembled cellulose nanorods and gold nanoparticles. ACS Appl Mater Interfaces 2015;7:21797–806.
[160] Campbell MG, Liu Q, Sanders A, Evans JS, Smalyukh II. Preparation of nanocomposite plasmonic films made from cellulose nanocrystals or mesoporous silica decorated with unidirectionally aligned gold nanorods. Materials 2014;7:3021–33.
[161] Liu Q, Campbell MG, Evans JS, Smalyukh II. Orientationally ordered colloidal co-dispersions of gold nanorods and cellulose nanocrystals. Adv Mater 2014;26:7178–84.
[162] Semenikhin NS, Kadasala NR, Moon RJ, Perry JW, Sandhage KH. Individually dispersed gold nanoshell-bearing cellulose nanocrystals with tailorable plasmon resonance. Langmuir 2018;34:4427–36.
[163] Herreros-López A, Hadad C, Yate L, Alshatwi AA, Vicentini N, Carofiglio T, et al. Synthesis and catalytic activity of gold nanoparticles supported on dendrimeric nanocellulose hybrids. Eur J Org Chem 2016;2016:3186–92.
[164] Lukach A, Thérien-Aubin H, Querejeta-Fernández A, Pitch N, Chauve G, Méthot M, et al. Coassembly of gold nanoparticles and cellulose nanocrystals in composite films. Langmuir 2015;31:5033–41.
[165] Querejeta-Fernandez A, Chauve G, Methot M, Bouchard J, Kumacheva E. Chiral plasmonic films formed by gold nanorods and cellulose nanocrystals. J Am Chem Soc 2014;136:4788–93.
[166] Wang Y, Zhang H, Lin X, Chen S, Jiang Z, Wang J, et al. Naked Au nanoparticles monodispersed onto multifunctional cellulose nanocrystal-graphene hybrid sheets: Towards efficient and sustainable heterogeneous catalysts. New J Chem 2018;42:2197–203.
[167] Zhang Z, Sèbe G, Wang X, Tam KC. Gold nanoparticles stabilized by poly(4-vinylpyridine) grafted cellulose nanocrystals as efficient and recyclable catalysts. Carbohydr Polym 2018;182:61–8.
[168] Islam MS, Chen L, Sisler J, Tam KC. Cellulose nanocrystal (CNC)-inorganic hybrid systems: synthesis, properties and applications. J Mater Chem B 2018;6:864–83.
[169] Dawson NJ, Spinella S, Peters KC, Maiorana A, Qian Q, Hepworth V, et al. Optical interactions of silver nanoparticle decorated cellulose nanocrystals created from a one-pot reduction method. J Appl Phys 2017;121.
[170] Kaushik M, Moores A. Review: nanocelluloses as versatile supports for metal nanoparticles and their applications in catalysis. Green Chem 2016;18:622–37.
[171] Elfeky AS, Salem SS, Elzaref AS, Owda ME, Eladawy HA, Saeed AM, et al. Multifunctional cellulose nanocrystal /metal oxide hybrid, photo-degradation, antibacterial and larvicidal activities. Carbohydr Polym 2020;230:115711.
[172] Boury B, Plumejeau S. Metal oxides and polysaccharides: an efficient hybrid association for materials chemistry. Green Chem 2015;17:72–88.
[173] Goikuria U, Larrañaga A, Vilas JL, Lizundia E. Thermal stability increase in metallic nanoparticles-loaded cellulose nanocrystal nanocomposites. Carbohydr Polym 2017;171:193–201.
[174] Wang DC, Yu HY, Song ML, Yang RT, Yao JM. Superfast adsorption-disinfection cryogels decorated with cellulose nanocrystal/zinc oxide nanorod clusters for water-purifying microdevices. ACS Sustain Chem Eng 2017;5:6776–85.
[175] Mashkour M, Kimura T, Kimura F, Mashkour M, Tajvidi M. One-dimensional core-shell cellulose-akaganeite hybrid nanocrystals: synthesis, characterization, and magnetic field induced self-assembly. RSC Adv 2014;4:52542–9.
[176] Nypelö T, Rodriguez-Abreu C, Rivas J, Dickey MD, Rojas OJ. Magneto-responsive hybrid materials based on cellulose nanocrystals. Cellulose 2014;21:2557–66.
[177] Wang Q, Wang Y, Chen L, Cai J, Zhang L. Facile construction of cellulose nanocomposite aerogel containing TiO_2 nanoparticles with high content and small size and their applications. Cellulose 2017;24:2229–40.
[178] Evdokimova O, Svensson F, Agafonov A, Håkansson S, Seisenbaeva G, Kessler V. Hybrid drug delivery patches based on spherical cellulose nanocrystals and colloid titania—synthesis and antibacterial properties. Nanomaterials 2018;8:228.
[179] Xue J, Song F, Yin XW, Zhang ZL, Liu Y, Wang XL, et al. Cellulose nanocrystal-templated synthesis of mesoporous TiO_2 with dominantly exposed (001) facets for efficient catalysis. ACS Sustain Chem Eng 2017;5:3721–5.
[180] Martakov IS, Torlopov MA, Mikhaylov VI, Krivoshapkina EF, Silant'ev VE, Krivoshapkin PV. Interaction of cellulose nanocrystals with titanium dioxide and peculiarities of hybrid structures formation. J Sol-Gel Sci Technol 2018;88:13–21.
[181] Lizundia E, Rincón-Iglesias M, Lanceros-Méndez S. Combining cobalt ferrite and graphite with cellulose nanocrystals for magnetically active and electrically conducting mesoporous nanohybrids. Carbohydr Polym 2020;236:116001.
[182] Mahmoud KA, Lam E, Hrapovic S, Luong JHT. Preparation of well-dispersed gold/magnetite nanoparticles embedded on cellulose nanocrystals for efficient immobilization of papain enzyme. ACS Appl Mater Interfaces 2013;5:4978–85.
[183] Guo J, Filpponen I, Johansson LS, Mohammadi P, Latikka M, Linder MB, et al. Complexes of magnetic nanoparticles with cellulose nanocrystals as regenerable, highly efficient, and selective platform for protein separation. Biomacromolecules 2017;18:898–905.
[184] Ebert LB. Science of fullerenes and carbon nanotubes. Carbon 1997;35:437–8.
[185] Iijima S, Ichihashi T. Single-shell carbon nanotubes of 1-nm diameter. Nature 1993;363:603–5.
[186] Imazu N, Fujigaya T, Nakashima N. Fabrication of flexible transparent conductive films from long double-walled carbon nanotubes. Sci Technol Adv Mater 2014;15.
[187] Geim AK, Novoselov KS. The rise of graphene. Nat Mater 2007;6:183–91.
[188] Zhu Y, Murali S, Cai W, Li X, Suk JW, Potts JR, et al. Graphene and graphene oxide: synthesis, properties, and applications. Adv Mater 2010;22:3906–24.
[189] Kroto HW, Heath JR, O'Brien SC, Curl RF, Smalley RE. C60: buckminsterfullerene. Nature 1985;318:162–3.
[190] Koga H, Saito T, Kitaoka T, Nogi M, Suganuma K, Isogai A. Transparent, conductive, and printable composites consisting of TEMPO-oxidized nanocellulose and carbon nanotube. Biomacromolecules 2013;14:1160–5.
[191] Hamedi MM, Hajian A, Fall AB, Hkansson K, Salajkova M, Lundell F, et al. Highly conducting, strong nanocomposites based on nanocellulose-assisted aqueous dispersions of single-wall carbon nanotubes. ACS Nano 2014;8:2467–76.
[192] Yan C, Wang J, Kang W, Cui M, Wang X, Foo CY, et al. Highly stretchable piezoresistive graphene–nanocellulose nanopaper for strain sensors. Adv Mater 2014;26:2022–7.
[193] Meng Q, Manas-Zloczower I. Carbon nanotubes enhanced cellulose nanocrystals films with tailorable electrical conductivity. Compos Sci Technol 2015;120:1–8.
[194] Wegst UGK, Bai H, Saiz E, Tomsia AP, Ritchie RO. Bioinspired structural materials. Nat Mater 2015;14:23–36.
[195] Podsiadlo P, Kaushik AK, Arruda EM, Waas AM, Shim BS, Xu J, et al. Ultrastrong and stiff layered polymer nanocomposites. Science 2007;318:80–3.
[196] Valentini L, Cardinali M, Fortunati E, Torre L, Kenny JM. A novel method to prepare conductive nanocrystalline cellulose/graphene oxide composite films.

Mater Lett 2013;105:4–7.
[197] Montes S, Etxeberria A, Mocholi V, Rekondo A, Grande H, Labidi J. Effect of combining cellulose nanocrystals and graphene nanoplatelets on the properties of poly(lactic acid) based films. Express Polym Lett 2018;12:543–55.
[198] Zhang X, Liu P, Duan Y, Jiang M, Zhang J. Graphene/cellulose nanocrystals hybrid aerogel with tunable mechanical strength and hydrophilicity fabricated by ambient pressure drying technique. RSC Adv 2017;7:16467–73.
[199] Dhar P, Gaur SS, Kumar A, Katiyar V. Cellulose nanocrystal templated graphene nanoscrolls for high performance supercapacitors and hydrogen storage: an experimental and molecular simulation study. Sci Rep 2018;8:3886.
[200] Fugetsu B, Sano E, Sunada M, Sambongi Y, Shibuya T, Wang X, et al. Electrical conductivity and electromagnetic interference shielding efficiency of carbon nanotube/cellulose composite paper. Carbon 2008;46:1256–8.
[201] Zang X, Wang X, Yang Z, Wang X, Li R, Chen J, et al. Unprecedented sensitivity towards pressure enabled by graphene foam. Nanoscale 2017;9:19346–52.
[202] Zhang Y, Liu G, Yao X, Gao S, Xie J, Xu H, et al. Electrochemical chiral sensor based on cellulose nanocrystals and multiwall carbon nanotubes for discrimination of tryptophan enantiomers. Cellulose 2018;25:3861–71.
[203] Yousefi N, Wong KKW, Hosseinidoust Z, Sørensen HO, Bruns S, Zheng Y, et al. Hierarchically porous, ultra-strong reduced graphene oxide-cellulose nanocrystal sponges for exceptional adsorption of water contaminants. Nanoscale 2018;10:7171–84.
[204] Alivisatos AP. Semiconductor clusters, nanocrystals, and quantum dots. Science 1996;271:933–7.
[205] Bruchez M, Moronne M, Gin P, Weiss S, Alivisatos AP. Semiconductor nanocrystals as fluorescent biological labels. Science 1998;281:2013–6.
[206] Baker SN, Baker GA. Luminescent carbon nanodots: emergent nanolights. Angew Chemie – Int Ed 2010;49:6726–44.
[207] Bao L, Zhang ZL, Tian ZQ, Zhang L, Liu C, Lin Y, et al. Electrochemical tuning of luminescent carbon nanodots: from preparation to luminescence mechanism. Adv Mater 2011;23:5801–6.
[208] Zhang L, Lyu S, Zhang Q, Wu Y, Melcher C, Chmely SC, et al. Dual-emitting film with cellulose nanocrystal-assisted carbon dots grafted $SrAl_2O_4$, Eu^{2+}, Dy^{3+} phosphors for temperature sensing. Carbohydr Polym 2019;206:767–77.
[209] Mohammed N, Baidya A, Murugesan V, Kumar AA, Ganayee MA, Mohanty JS, et al. Diffusion-controlled simultaneous sensing and scavenging of heavy metal ions in water using atomically precise cluster–cellulose nanocrystal composites. ACS Sustain Chem Eng 2016;4:6167–76.
[210] Natarajan G, Mathew A, Negishi Y, Whetten RL, Pradeep T. A Unified framework for understanding the structure and modifications of atomically precise monolayer protected gold clusters. J Phys Chem C 2015;119:27768–85.
[211] Pansare VJ, Hejazi S, Faenza WJ, Prud'homme RK. Review of long-wavelength optical and NIR imaging materials: contrast agents, fluorophores, and multifunctional nano carriers. Chem Mater 2012;24:812–27.
[212] Duong HV, Chau TTL, Dang NTT, Vanterpool F, Salmerón-Sánchez M, Lizundia E, et al. Biocompatible chitosan-functionalized upconverting nanocomposites. ACS Omega 2018;3:86–95.
[213] Fedorov PP, Luginina AA, Kuznetsov SV, Voronov VV, Lyapin AA, Ermakov AS, et al. Composite up-conversion luminescent films containing a nanocellulose and SrF_2: Ho particles. Cellulose 2019;26:2403–23.
[214] Bharath N, W GJ. Bioinspired Bouligand cellulose nanocrystal composites: a review of mechanical properties. Philos Trans R Soc A Math Phys Eng Sci 2018;376:20170050.
[215] Enescu D, Gardrat C, Cramail H, Le Coz C, Sèbe G, Coma V. Bio-inspired films based on chitosan, nanoclays and cellulose nanocrystals: structuring and properties improvement by using water-evaporation-induced self-assembly. Cellulose 2019;26:2389–401.
[216] Okamoto T, Patil JA, Nissinen T, Mann S. Self-assembly of colloidal nanocomposite hydrogels using 1D cellulose nanocrystals and 2D exfoliated organoclay layers. Gels 2017;3:11.
[217] Sheikhi A, Van De Ven TGM. Squishy nanotraps: hybrid cellulose nanocrystal-zirconium metallogels for controlled trapping of biomacromolecules. Chem Commun 2017;53:8747–50.
[218] Carosio F, Kochumalayil J, Fina A, Berglund LA. Extreme thermal shielding effects in nanopaper based on multilayers of aligned clay nanoplatelets in cellulose nanofiber matrix. Adv Mater Interfaces 2016;3:1600551.
[219] He JX, Tan WL, Han QM, Cui SZ, Shao W, Sang F. Fabrication of silk fibroin/cellulose whiskers–chitosan composite porous scaffolds by layer-by-layer assembly for application in bone tissue engineering. J Mater Sci 2016;51:4399–410.
[220] Wang H, Roman M. Formation and properties of chitosan-cellulose nanocrystal polyelectrolyte-macroion complexes for drug delivery applications. Biomacromolecules 2011;12:1585–93.
[221] Wang H, Qian C, Roman M. Effects of pH and salt concentration on the formation and properties of chitosan-cellulose nanocrystal polyelectrolyte-macroion complexes. Biomacromolecules 2011;12:3708–14.
[222] Toivonen MS, Kurki-Suonio S, Schacher FH, Hietala S, Rojas OJ, Ikkala O. Water-resistant, transparent hybrid nanopaper by physical cross-linking with chitosan. Biomacromolecules 2015;16:1062–71.
[223] Akhlaghi SP, Berry RM, Tam KC. Modified cellulose nanocrystal for vitamin C delivery. AAPS PharmSciTech 2015;16:306–14.
[224] Akhlaghi SP, Berry RC, Tam KC. Surface modification of cellulose nanocrystal with chitosan oligosaccharide for drug delivery applications. Cellulose 2013;20:1747–64.
[225] De Mesquita JP, Patrício PS, Donnici CL, Petri DFS, De Oliveira LCA, Pereira FV. Hybrid layer-by-layer assembly based on animal and vegetable structural materials: Multilayered films of collagen and cellulose nanowhiskers. Soft Matter 2011;7:4405–13.
[226] Liu L, Yang X, Yu H, Ma C, Yao J. Biomimicking the structure of silk fibers via cellulose nanocrystal as β-sheet crystallite. RSC Adv 2014;4:14304–13.
[227] Li YY, Wang B, Ma MG, Wang B. Review of recent development on preparation, properties, and applications of cellulose-based functional materials. Int J Polym Sci 2018:8973643.
[228] Pérez-Madrigal MM, Edo MG, Alemán C. Powering the future: Application of cellulose-based materials for supercapacitors. Green Chem 2016;18:5930–56.
[229] Tan KW, Heo SK, Foo ML, Chew IML, Yoo CK. An insight into nanocellulose as soft condensed matter: challenge and future prospective toward environmental sustainability. Sci Total Environ 2019;650:1309–26.
[230] Borghei M, Miettunen K, Greca LG, Poskela A, Lehtonen J, Lepikko S, et al. Biobased aerogels with different surface charge as electrolyte carrier membranes in quantum dot-sensitized solar cell. Cellulose 2018;25:3363–75.
[231] Li S, Lee PS. Development and applications of transparent conductive nanocellulose paper. Sci Technol Adv Mater 2017;18:620–33.
[232] Zhou Y, Fuentes-Hernandez C, Khan TM, Liu JC, Hsu J, Shim JW, et al. Recyclable organic solar cells on cellulose nanocrystal substrates. Sci Rep 2013;3:1536.
[233] Kritzer P, Cook JA. Nonwovens as separators for alkaline batteries. J Electrochem Soc 2007;154:A481.
[234] Schmidt M, Heider U, Kuehner A, Oesten R, Jungnitz M, Ignat'ev N, et al. Lithium fluoroalkylphosphates: a new class of conducting salts for electrolytes for high energy lithium-ion batteries. J. Power Sources 2001;97–98:557–60.
[235] Kuribayashi I. Characterization of composite cellulosic separators for rechargeable lithium-ion batteries. J Power Sources 1996;63:87–91.
[236] Zhang J, Yue L, Kong Q, Liu Z, Zhou X, Zhang C, et al. Sustainable, heat-resistant and flame-retardant cellulose-based composite separator for high-performance lithium ion battery. Sci Rep 2014;4:3935.
[237] Jiang F, Yin L, Yu Q, Zhong C, Zhang J. Bacterial cellulose nanofibrous membrane as thermal stable separator for lithium-ion batteries. J Power Sources 2015;279:21–7.
[238] Lee SY, Chun SJ, Kang IA, Park JY. Preparation of cellulose nanofibrils by high-pressure homogenizer and cellulose-based composite films. J Ind Eng Chem 2009;15:50–5.
[239] Gonçalves R, Lizundia E, Silva MM, Costa CM, Lanceros SM. Mesoporous cellulose nanocrystal membranes as battery separators for environmentally safer lithium-ion batteries. ACS Appl Mater Interfaces 2019;2:3749–61.
[240] Hänsel C, Lizundia E, Kundu D. A single Li-ion conductor based on cellulose. ACS Appl Energy Mater 2019;2:5686–91.
[241] Karim Z, Mathew AP, Grahn M, Mouzon J, Oksman K. Nanoporous membranes with cellulose nanocrystals as functional entity in chitosan: Removal of dyes from water. Carbohydr Polym 2014;112:668–76.

[242] Voisin H, Bergström L, Liu P, Mathew A. Nanocellulose-based materials for water purification. Nanomaterials 2017;7:57.
[243] Carpenter AW, De Lannoy CF, Wiesner MR. Cellulose nanomaterials in water treatment technologies. Environ Sci Technol 2015;49:5277–87.
[244] Mohammed N, Grishkewich N, Tam KC. Cellulose nanomaterials: promising sustainable nanomaterials for application in water/wastewater treatment processes. Environ Sci Nano 2018;5:623–58.
[245] Yu X, Tong S, Ge M, Wu L, Zuo J, Cao C, et al. Adsorption of heavy metal ions from aqueous solution by carboxylated cellulose nanocrystals. J Environ Sci 2013;25:933–43.
[246] Korhonen JT, Kettunen M, Ras RHA, Ikkala O. Hydrophobic nanocellulose aerogels as floating, sustainable, reusable, and recyclable oil absorbents. ACS Appl Mater Interfaces 2011;3:1813–6.
[247] Zhu C, Liu P, Mathew AP. Self-assembled TEMPO cellulose nanofibers: graphene oxide-based biohybrids for water purification. ACS Appl Mater Interfaces 2017;9:21048–58.
[248] Yao Q, Fan B, Xiong Y, Jin C, Sun Q, Sheng C. 3D assembly based on 2D structure of cellulose nanofibril/graphene oxide hybrid aerogel for adsorptive removal of antibiotics in water. Sci Rep 2017;7:45914.
[249] Rafieian F, Hosseini M, Jonoobi M, Yu Q. Development of hydrophobic nanocellulose-based aerogel via chemical vapor deposition for oil separation for water treatment. Cellulose 2018;25:4695–710.
[250] Pan K, Wang W-X. Trace metal contamination in estuarine and coastal environments in China. Sci Total Environ 2012;421–422:3–16.
[251] Steffen W, Richardson K, Rockstrom J, Cornell SE, Fetzer I, Bennett EM, et al. Planetary boundaries: Guiding human development on a changing planet. Supplementary Material. Science (80-) 2015;347:1259855–1259855.
[252] Grzelczak M, Vermant J, Furst EM, Liz-Marzán LM. Directed self-assembly of nanoparticles. ACS Nano 2010;4:3591–605.
[253] Li Z, Yao C, Yu Y, Cai Z, Wang X. Highly efficient capillary photoelectrochemical water splitting using cellulose nanofiber-templated TiO_2 photoanodes. Adv Mater 2014;26:2262–7.
[254] Wu X, Lu C, Zhang W, Yuan G, Xiong R, Zhang X. A novel reagentless approach for synthesizing cellulose nanocrystal-supported palladium nanoparticles with enhanced catalytic performance. J Mater Chem A 2013;1:8645–52.
[255] An X, Long Y, Ni Y. Cellulose nanocrystal/hexadecyltrimethylammonium bromide/silver nanoparticle composite as a catalyst for reduction of 4-nitrophenol. Carbohydr Polym 2017;156:253–8.
[256] Zhan Y, Meng Y, Li W, Chen Z, Yan N, Li Y, et al. Magnetic recoverable $MnFe_2O_4$/cellulose nanocrystal composites as an efficient catalyst for decomposition of methylene blue. Ind Crops Prod 2018;122:422–9.
[257] Kaushik M, Basu K, Benoit C, Cirtiu CM, Vali H, Moores A. Cellulose nanocrystals as chiral inducers: enantioselective catalysis and transmission electron microscopy 3D characterization. J Am Chem Soc 2015;137:6124–7.
[258] Mahmoud KA, Male KB, Hrapovic S, Luong JHT. Cellulose nanocrystal/gold nanoparticle composite as a matrix for enzyme immobilization. ACS Appl Mater Interfaces 2009;1:1383–6.
[259] Golmohammadi H, Morales-Narváez E, Naghdi T, Merkoçi A. Nanocellulose in sensing and biosensing. Chem Mater 2017;29:5426–46.
[260] Kafy A, Akther A, Shishir MIR, Kim HC, Yun Y, Kim J. Cellulose nanocrystal/graphene oxide composite film as humidity sensor. Sens Actuat A Phys 2016;247:221–6.
[261] Mun S, Chen Y, Kim J. Cellulose–titanium dioxide–multiwalled carbon nanotube hybrid nanocomposite and its ammonia gas sensing properties at room temperature. Sens Actuat B Chem 2012;171–172:1186–91.
[262] Sadasivuni KK, Ponnamma D, Ko H-U, Kim HC, Zhai L, Kim J. Flexible NO_2 sensors from renewable cellulose nanocrystals/iron oxide composites. Sens Actuat B Chem 2016;233:633–8.
[263] Sadasivuni KK, Kafy A, Zhai L, Ko H-U, Mun S, Kim J. Transparent and flexible cellulose nanocrystal/reduced graphene oxide film for proximity sensing. Small 2015;11:994–1002.
[264] Zhu S, Meng Q, Wang L, Zhang J, Song Y, Jin H, et al. Highly photoluminescent carbon dots for multicolor patterning, sensors, and bioimaging. Angew Chemie - Int Ed 2013;52:3953–7.
[265] Zhao Y, Gao G, Liu D, Tian D, Zhu Y, Chang Y. Vapor sensing with color-tunable multilayered coatings of cellulose nanocrystals. Carbohydr Polym 2017;174:39–47.
[266] Nielsen LJ, Eyley S, Thielemans W, Aylott JW. Dual fluorescent labelling of cellulose nanocrystals for pH sensing. Chem Commun 2010;46:8929–31.
[267] Chauhan P, Hadad C, López AH, Silvestrini S, La Parola V, Frison E, et al. A nanocellulose–dye conjugate for multi-format optical pH-sensing. Chem Commun 2014;50:9493–6.
[268] Wu W, Song R, Xu Z, Jing Y, Dai H, Fang G. Fluorescent cellulose nanocrystals with responsiveness to solvent polarity and ionic strength. Sens Actuat B Chem 2018;275:490–8.
[269] Murphy WL, McDevitt TC, Engler AJ. Materials as stem cell regulators. Nat Mater 2014;13:547–57.
[270] Morena F, Armentano I, Montanucci P, Argentati C, Fortunati E, Montesano S, et al. Design of a nanocomposite substrate inducing adult stem cell assembly and progression toward an Epiblast-like or Primitive Endoderm-like phenotype via mechanotransduction. Biomaterials 2017;144:211–29.
[271] Trujillo S, Lizundia E, Vilas JL, Salmeron-Sanchez M. PLLA/ZnO nanocomposites: Dynamic surfaces to harness cell differentiation. Colloids Surfaces B Biointerfaces 2016;144:152–60.
[272] Argentati C, Morena F, Montanucci P, Rallini M, Basta G, Calabrese N, et al. Surface hydrophilicity of poly(L-lactide) acid polymer film changes the human adult adipose stem cell architecture. Polymers 2018;10:140.
[273] Smyth M, Fournier C, Driemeier C, Picart C, Foster EJ, Bras J. Tunable structural and mechanical properties of cellulose nanofiber substrates in aqueous conditions for stem cell culture. Biomacromolecules 2017;18:2034–44.
[274] Lin N, Dufresne A. Nanocellulose in biomedicine: current status and future prospect. Eur Polym J 2014;59:302–25.
[275] Modulevsky DJ, Lefebvre C, Haase K, Al-Rekabi Z, Pelling AE. Apple derived cellulose scaffolds for 3D mammalian cell culture. PLoS ONE 2014;9:e97835.
[276] Sannino A, Demitri C, Madaghiele M. Biodegradable cellulose-based hydrogels: design and applications. Materials 2009;2:353–73.
[277] Miyamoto T, Takahashi S -i, Ito H, Inagaki H, Noishiki Y. Tissue biocompatibility of cellulose and its derivatives. J Biomed Mater Res 1989;23:125–33.
[278] Entcheva E, Bien H, Yin L, Chung CY, Farrell M, Kostov Y. Functional cardiac cell constructs on cellulose-based scaffolding. Biomaterials 2004;25:5753–62.
[279] Sultan S, Siqueira G, Zimmermann T, Mathew AP. 3D printing of nano-cellulosic biomaterials for medical applications. Curr Opin Biomed Eng 2017;2:29–34.
[280] Sannino A, Madaghiele M, Conversano F, Mele G, Maffezzoli A, Netti PA, et al. Cellulose derivative-hyaluronic acid-based microporous hydrogels cross-linked through divinyl sulfone (DVS) to modulate equilibrium sorption capacity and network stability. Biomacromolecules 2004;5:92–6.
[281] Sannino A, Pappadà S, Madaghiele M, Maffezzoli A, Ambrosio L, Nicolais L. Crosslinking of cellulose derivatives and hyaluronic acid with water-soluble carbodiimide. Polymer 2005;46:11206–12.
[282] Roman M. Toxicity of cellulose nanocrystals: a review. Ind Biotechnol 2015;11:25–33.
[283] Clift MJD, Foster EJ, Vanhecke D, Studer D, Wick P, Gehr P, et al. Investigating the interaction of cellulose nanofibers derived from cotton with a sophisticated 3D human lung cell coculture. Biomacromolecules 2011;12:3666–73.
[284] Hanif Z, Ahmed FR, Shin SW, Kim Y-K, Um SH. Size- and dose-dependent toxicity of cellulose nanocrystals (CNC) on human fibroblasts and colon adenocarcinoma. Colloids Surfaces B Biointerfaces 2014;119:162–5.
[285] Mahmoud KA, Mena JA, Male KB, Hrapovic S, Kamen A, Luong JHT. Effect of surface charge on the cellular uptake and cytotoxicity of fluorescent labeled cellulose nanocrystals. ACS Appl Mater Interfaces 2010;2:2924–32.
[286] Catalán J, Ilves M, Järventaus H, Hannukainen K-S, Kontturi E, Vanhala E, et al. Genotoxic and immunotoxic effects of cellulose nanocrystals in vitro. Environ Mol Mutagen 2015;56:171–82.
[287] Yanamala N, Farcas MT, Hatfield MK, Kisin ER, Kagan VE, Geraci CL, et al. In vivo evaluation of the pulmonary toxicity of cellulose nanocrystals: a renewable and sustainable nanomaterial of the future. ACS Sustain Chem Eng 2014;2:1691–8.
[288] Herreros-López A, Carini M, Da Ros T, Carofiglio T, Marega C, La Parola V, et al. Nanocrystalline cellulose-fullerene: novel conjugates. Carbohydr Polym

2017;164:92–101.
[289] González-Domínguez JM, Ansón-Casaos A, Grasa L, Abenia L, Salvador A, Colom E, et al. Unique properties and behavior of nonmercerized type-II cellulose nanocrystals as carbon nanotube biocompatible dispersants. Biomacromolecules 2019;20:3147–60.
[290] Javanbakht S, Namazi H. Doxorubicin loaded carboxymethyl cellulose/graphene quantum dot nanocomposite hydrogel films as a potential anticancer drug delivery system. Mater Sci Eng C 2018;87:50–9.
[291] Hu Y, Wen C, Song L, Zhao N, Xu F-J. Multifunctional hetero-nanostructures of hydroxyl-rich polycation wrapped cellulose-gold hybrids for combined cancer therapy. J Control Release 2017;255:154–63.
[292] Domingues RMA, Gomes ME, Reis RL. The potential of cellulose nanocrystals in tissue engineering strategies. Biomacromolecules 2014;15:2327–46.
[293] Chau M, De France KJ, Kopera B, Machado VR, Rosenfeldt S, Reyes L, et al. Composite hydrogels with tunable anisotropic morphologies and mechanical properties. Chem Mater 2016;28:3406–15.
[294] Dugan JM, Gough JE, Eichhorn SJ. Bacterial cellulose scaffolds and cellulose nanowhiskers for tissue engineering. Nanomedicine 2013;8:287–98.
[295] Courtenay JC, Johns MA, Galembeck F, Deneke C, Lanzoni EM, Costa CA, et al. Surface modified cellulose scaffolds for tissue engineering. Cellulose 2017;24:253–67.
[296] Wang X, Wen J, Jiang L, Li Y, Zhang L, Gong M. Preparation and properties of nano-hydroxyapatite/chitosan/carboxymethyl cellulose composite scaffold. Carbohydr Polym 2008;74:680–4.
[297] Torres-Rendon JG, Femmer T, De Laporte L, Tigges T, Rahimi K, Gremse F, et al. Bioactive gyroid scaffolds formed by sacrificial templating of nanocellulose and nanochitin hydrogels as instructive platforms for biomimetic tissue engineering. Adv Mater 2015;27:2989–95.
[298] Syverud K, Pettersen SR, Draget K, Chinga-Carrasco G. Controlling the elastic modulus of cellulose nanofibril hydrogels-scaffolds with potential in tissue engineering. Cellulose 2015;22:473–81.
[299] Courtenay JC, Deneke C, Lanzoni EM, Costa CA, Bae Y, Scott JL, et al. Modulating cell response on cellulose surfaces; tunable attachment and scaffold mechanics. Cellulose 2018;25:925–40.
[300] Du H, Liu W, Zhang M, Si C, Zhang X, Li B. Cellulose nanocrystals and cellulose nanofibrils based hydrogels for biomedical applications. Carbohydr Polym 2019;209:130–44.
[301] Kumar A, Rao KM, Han SS. Synthesis of mechanically stiff and bioactive hybrid hydrogels for bone tissue engineering applications. Chem Eng J 2017;317:119–31.
[302] De France KJ, Chan KJW, Cranston ED, Hoare T. Enhanced mechanical properties in cellulose nanocrystal-poly(oligoethylene glycol methacrylate) injectable nanocomposite hydrogels through control of physical and chemical cross-linking. Biomacromolecules 2016;17:649–60.
[303] Liang D, Hsiao BS, Chu B. Functional electrospun nanofibrous scaffolds for biomedical applications. Adv Drug Deliv Rev 2007;59:1392–412.
[304] Wan YZ, Huang Y, Yuan CD, Raman S, Zhu Y, Jiang HJ, et al. Biomimetic synthesis of hydroxyapatite/bacterial cellulose nanocomposites for biomedical applications. Mater Sci Eng C 2007;27:855–64.
[305] Pooyan P, Tannenbaum R, Garmestani H. Mechanical behavior of a cellulose-reinforced scaffold in vascular tissue engineering. J Mech Behav Biomed Mater 2012;7:50–9.
[306] Chen X, Zhou R, Chen B, Chen J. Nanohydroxyapatite/cellulose nanocrystals/silk fibroin ternary scaffolds for rat calvarial defect regeneration. RSC Adv 2016;6:35684–91.
[307] Hajipour MJ, Fromm KM, Akbar Ashkarran A, Jimenez de Aberasturi D, Larramendi IR de, Rojo T, et al. Antibacterial properties of nanoparticles. Trends Biotechnol 2012;30:499–511.
[308] Shi Z, Tang J, Chen L, Yan C, Tanvir S, Anderson WA, et al. Enhanced colloidal stability and antibacterial performance of silver nanoparticles/cellulose nanocrystal hybrids. J Mater Chem B 2015;3:603–11.
[309] Singla R, Soni S, Kulurkar PM, Kumari A, S. M, Patial V, et al. In situ functionalized nanobiocomposites dressings of bamboo cellulose nanocrystals and silver nanoparticles for accelerated wound healing. Carbohydr Polym 2017;155:152–62.
[310] Yu HY, Chen GY, Wang YB, Yao JM. A facile one-pot route for preparing cellulose nanocrystal/zinc oxide nanohybrids with high antibacterial and photocatalytic activity. Cellulose 2015;22:261–73.
[311] Lefatshe K, Muiva CM, Kebaabetswe LP. Extraction of nanocellulose and in-situ casting of ZnO/cellulose nanocomposite with enhanced photocatalytic and antibacterial activity. Carbohydr Polym 2017;164:301–8.
[312] Yang R-T, Yu H-Y, Song M-L, Zhou Y-W, Yao J-M. Flower-like zinc oxide nanorod clusters grown on spherical cellulose nanocrystals via simple chemical precipitation method. Cellulose 2016;23:1871–84.
[313] Abdalkarim SYH, Yu H-Y, Wang C, Huang L-X, Yao J. Green synthesis of sheet-like cellulose nanocrystal–zinc oxide nanohybrids with multifunctional performance through one-step hydrothermal method. Cellulose 2018;25:6433–46.
[314] Lizundia E, Goikuria U, Vilas JL, Cristofaro F, Bruni G, Fortunati E, et al. Metal nanoparticles embedded in cellulose nanocrystal based films: material properties and post-use analysis. Biomacromolecules 2018;19:2618–28.
[315] Singla R, Soni S, Patial V, Kulurkar PM, Kumari A, S. M, et al. Cytocompatible anti-microbial dressings of syzygium cumini cellulose nanocrystals decorated with silver nanoparticles accelerate acute and diabetic wound healing. Sci Rep 2017;7:10457.
[316] Moritz S, Wiegand C, Wesarg F, Hessler N, Müller FA, Kralisch D, et al. Active wound dressings based on bacterial nanocellulose as drug delivery system for octenidine. Int J Pharm 2014;471:45–55.
[317] Tong WY, bin Abdullah AYK, binti Rozman NAS, bin Wahid MIA, Hossain MS, Ring LC, et al. Antimicrobial wound dressing film utilizing cellulose nanocrystal as drug delivery system for curcumin. Cellulose 2018;25:631–8.
[318] Hakkarainen T, Koivuniemi R, Kosonen M, Escobedo-Lucea C, Sanz-Garcia A, Vuola J, et al. Nanofibrillar cellulose wound dressing in skin graft donor site treatment. J Control Release 2016;244:292–301.
[319] Wu H, Williams GR, Wu J, Wu J, Niu S, Li H, et al. Regenerated chitin fibers reinforced with bacterial cellulose nanocrystals as suture biomaterials. Carbohydr Polym 2018;180:304–13.
[320] Plackett D, Letchford K, Jackson J, Burt H. A review of nanocellulose as a novel vehicle for drug delivery. Nord Pulp Pap Res J 2014;29:105–18.
[321] Seabra AB, Bernardes JS, Fávaro WJ, Paula AJ, Durán N. Cellulose nanocrystals as carriers in medicine and their toxicities: a review. Carbohydr Polym 2018;181:514–27.
[322] Jackson JK, Letchford K, Wasserman BZ, Ye L, Hamad WY, Burt HM. The use of nanocrystalline cellulose for the binding and controlled release of drugs. Int J Nanomed 2011;6:321–30.
[323] Low LE, Tan LT-H, Goh B-H, Tey BT, Ong BH, Tang SY. Magnetic cellulose nanocrystal stabilized Pickering emulsions for enhanced bioactive release and human colon cancer therapy. Int J Biol Macromol 2019;127:76–84.
[324] Hu H, Hou X-J, Wang X-C, Nie J-J, Cai Q, Xu F-J. Gold nanoparticle-conjugated heterogeneous polymer brush-wrapped cellulose nanocrystals prepared by combining different controllable polymerization techniques for theranostic applications. Polym Chem 2016;7:3107–16.
[325] Hu H, Yuan W, Liu F-S, Cheng G, Xu F-J, Ma J. Redox-responsive polycation-functionalized cotton cellulose nanocrystals for effective cancer treatment. ACS Appl Mater Interfaces 2015;7:8942–51.
[326] Lam E, Hrapovic S, Majid E, Chong JH, Luong JHT. Catalysis using gold nanoparticles decorated on nanocrystalline cellulose. Nanoscale 2012;4:997–1002.
[327] Hu Y, Chai MY, Yang WT, Xu FJ. Supramolecular host–guest pseudocomb conjugates composed of multiple star polycations tied tunably with a linear polycation backbone for gene transfection. Bioconjug Chem 2013;24:1049–56.
[328] Bacakova L, Pajorova J, Tomkova M, Matejka R, Broz A, Stepanovska J, et al. Applications of nanocellulose/nanocarbon composites: focus on biotechnology and medicine. Nanomaterials 2020;10:196.
[329] Hellweg S, Milà i Canals L. Emerging approaches, challenges and opportunities in life cycle assessment. Science 2014;344:1109–13.
[330] Guinée JB, Heijungs R, Huppes G, Zamagni A, Masoni P, Buonamici R, et al. Life cycle assessment: past, present, and future. Environ Sci Technol 2011;45:90–6.
[331] Shatkin JA, Kim B. Environmental health and safety of cellulose nanomaterials and composites. Handb Nanocellulose Cellul Nanocomposites 2017:683–729.

[332] de Figueirêdo MCB, Rosa M de F, Ugaya CML, Souza Filho M de SM de, Silva Braid ACC da, Melo LFL de. Life cycle assessment of cellulose nanowhiskers. J Clean Prod 2012;35:130–9.
[333] Shatkin JA, Kim B. Cellulose nanomaterials: life cycle risk assessment, and environmental health and safety roadmap. Environ Sci Nano 2015;2:477–99.
[334] Li Q, McGinnis S, Sydnor C, Wong A, Renneckar S. Nanocellulose life cycle assessment. ACS Sustain Chem Eng 2013;1:919–28.
[335] Leão RM, Miléo PC, Maia JMLL, Luz SM. Environmental and technical feasibility of cellulose nanocrystal manufacturing from sugarcane bagasse. Carbohydr Polym 2017;175:518–29.
[336] Piccinno F, Hischier R, Seeger S, Som C. Predicting the environmental impact of a future nanocellulose production at industrial scale: Application of the life cycle assessment scale-up framework. J Clean Prod 2018;174:283–95.
[337] Ribeiro RSA, Pohlmann BC, Calado V, Bojorge N, Pereira N. Production of nanocellulose by enzymatic hydrolysis: trends and challenges. Eng Life Sci 2019;19:279–91.
[338] Yu H, Abdalkarim SYH, Zhang H, Wang C, Tam KC. Simple process to produce high-yield cellulose nanocrystals using recyclable citric/hydrochloric acids. ACS Sustain Chem Eng 2019;7:4912–23.
[339] Thonemann N, Schulte A, Maga D. How to conduct prospective life cycle assessment for emerging technologies? A systematic review and methodological guidance. Sustain 2020;12:1192.
[340] Tan L, Mandley SJ, Peijnenburg W, Waaijers-van der Loop SL, Giesen D, Legradi JB, et al. Combining ex-ante LCA and EHS screening to assist green design: A case study of cellulose nanocrystal foam. Sustain 2018;178:494–506.

Erlantz Lizundia Erlantz Lizundia completed his PhD in Advanced Materials Engineering in 2011 at the University of the Basque Country (UPV/EHU), which was recognized with the Extraordinary Doctoral Award (award limited to the Top 10 percent). During the 2012-2013 he moved into the private industry to focus on the industrial application of biopolymers. From 2014 he has been combining teaching and research at the UPV/EHU. He joined Mark MacLachlan group at the University of the British Columbia (Canada) as a visiting scientist for 6 months in January 2016, and The Laboratory for Multifunctional Materials (Prof. Dr. Markus Niederberger) at ETH Zurich (Switzerland) as an Academic Guest for further 6 months in January 2018. In September 2016 he was appointed Associate Professor at the Bilbao School of Engineering (UPV/EHU). His current research deals with the development of cellulose nanocrystal-based nanohybrids for packaging, biomedicine, bioimaging, sensing, energy storage, catalytic and water purification applications. He has over 50 published works in international peer reviewed journals in the fields of materials science, applied chemistry, nanomaterials, green chemistry and biomedicine. https://scholar.google.es/citations?user=fDlHA4YAAAAJ&hl=es.

Debora Puglia received her PhD in Industrial Engineering at the Material Science and Technology Lab of the University of Perugia in 2003. Her research interests are related to the study of biodegradable polymeric composites and nanocomposites reinforced with biobased reinforcements (vegetable macrofibers, crops, cellulose and lignin based nanoparticles), nanocomposites reinforced with silica and carbon nanostructures. She is author of 20 book chapters and 170 scientific peer reviewed papers (h index= 41, Scopus database). She currently has a position as Associate Professor at the University of Perugia. https://scholar.google.it/citations?user=pPws5pQAAAAJ&hl=it&oi=ao.

Thanh-Dinh Nguyen Thanh-Dinh Nguyen received his PhD from the Department of Chemical Engineering at Laval University in 2011. He later joined the MacLachlan group at The University of British Columbia as a Postdoctoral researcher, where he awarded a NSERC Postdoctoral Fellow. In 2016, he was appointed Research Associate at the same University. His research spans the area of materials chemistry including inorganic materials and polymer materials. His current research activity is centered on the inspiration of new structural forms from the supramolecular self-assembly, biomimicry, and cluster evolution to develop hierarchical materials at micro- and nano-size scales. He has published over 50 research and review papers and book chapters in international peer-reviewed journals in the fields of chemistry of materials and applied science of materials. https://scholar.google.es/citations?user=oZS-uwIAAAAJ&hl=es.

Ilaria Armentano Ilaria Armentano is actually (2016-present) an Assistant Professor in Applied Physics at Tuscia University. She was a post-doc researcher in the Material Science and Technology group at the University of Perugia, in the Engineering Department. She has a long experience in the nanomaterial field in terms of materials synthesis, characterization, and surface properties. She was researcher at the Italian Interuniversitary Consortium on Materials Science and Technology (INSTM), at the NIPLAB laboratory on nanocomposites and multifunctional polymeric hybrid materials. She obtained her PhD in 2006 at the Universty of Perugia on carbon nanotubes. Now she worked mainly on two important subjects: nanocomposite scaffolds for biomedical applications based on biodegradable polymers, and surface modification method in terms of film deposition and plasma surface treatments. She was involved in National and International research projects (NANOFUN-POLY; NANOFIRE, NANOBIOCOM, POCO, SAMSUNG). In the National research programme she was involved in the T.A.U.T project, on Artificial transplantable human tissues. She was involved in the teaching activities at the University of Perugia, in the Material Science and Biotechology fields, at the Master Courses and at the undergraduate Courses, for different academic years. She was supervisor of 8 MSc degrees and 5 Ph.D thesis. She attended more than 30 International Conferences in the material science and biotechnology field with oral and presentation. She is author of more than 100 articles on revised journals and book chapter, reviewer for international journals and she is the guest Editor of “Silver Nanoparticles: Synthesis, Uses and Health Concerns”, 2013, Nova Science Publishers. She has the National teaching qualification for Associate Professorship, Disciplinary Sector ING-IND/22- Science and Technology of Materials (01/2014). https://scholar.google.it/citations?user=7TbOFPoAAAAJ&hl=it&oi=ao.